Durham E-Theses

An assessment of the use of airborne LiDAR for estimating growth of Sitka spruce (Picea sitchensis) plantation forestry at Kielder Forest, UK

Woodget, Amy Sara

An Assessment of the Use of Airborne LiDAR for Estimating Growth of Sitka Spruce (*Picea sitchensis*) Plantation Forestry at Kielder Forest, UK

By

Amy Sara Woodget

A thesis presented for the degree of Master of Science

University of Durham
Department of Geography

2007

ACKNOWLEDGEMENTS

ABSTRACT

A growing need exists for the collection of accurate and up-to-date information on forest growth rates for management purposes. Recent studies indicate that airborne laser scanning (ALS) offers a quicker and more cost-effective approach than the traditional methods of forest inventorying and may have the potential not only to revolutionise forest management but also provide key data concerning world carbon stocks.

This study aims to assess the potential of ALS to estimate forest growth rates of the temperate Sitka spruce plantation forests using canopy height distribution models at Kielder Forest, Northumberland. ALS data from 2003 and 2006 provides an excellent, unique opportunity to contribute to existing work which has so far been limited in focus, looking primarily at individual tree growth in the less densely stocked, slow-growing, cold climate forests of Scandinavia.

ALS point cloud data from first and last pulse returns are filtered and classified. Ground returns are used to create digital elevation models (DEM), and first returns used to create digital canopy height models (DCHM). Key ALS variables are then extracted and summarised. Processed ALS data from both years are compared to estimate forest growth. The results are compared with ground truth data. Height correlations are strong and positive. Growth is detected at all plot locations but correlations with ground truth data are weak and mostly negative. Potential explanations for the lack of correlation are presented and discussed, including; data misalignment, inherent error within the ground truth data and the set-up of the LiDAR systems. Further study is necessary to quantify and eliminate systematic and random error within both the LiDAR and ground truth data before ALS may be used routinely for forest management purposes.

KEYWORDS

LiDAR, Forestry, Growth, Kielder.

CONTENTS

FIGURES

TABLES

1 INTRODUCTION

1.1 GENERAL INTRODUCTION

Airborne laser scanning (ALS) or LiDAR provides significant advantages over more traditional techniques such as photogrammetry, aerial photography and optical imagery for surface profiling. There is a larger time window for data capture as LiDAR systems are not hampered by sun angle, time of day, weather conditions or seasonality. Data are automatically georeferenced from the moment of acquisition so that lengthy geocorrectional processes are not necessary. LiDAR systems can also be used successfully on steep or shadowed slopes (Hollaus *et al.*, 2006). Indeed, LiDAR offers unique potential for terrain and forest monitoring within inhospitable and inaccessible regions. If this technique can be tested and honed in less extreme environments then ALS may be able to provide the essential tools necessary for management and planning in remote areas. Furthermore, numerous studies have reported that airborne laser scanning provides a cheaper, quicker alternative to more established methods of data collection (Nelson *et al.*, 1988; Hyyppä *et al.*, 2000; Næsset 2002; Næsset and Økland 2002; Popescu *et al.*, 2002; Suarez *et al.*, 2005; Watt 2005; Watt and Donoghue 2005). Penetration of low level vegetation and the opportunity for non-monoscopic three-dimensional analysis are some of the benefits offered. Indeed, Watt (2005) argues that the accuracy and value of LiDAR data is undisputable.

To date, the majority of LiDAR data obtained for forestry has been used to estimate canopy heights and other variables such as biomass and volume. Few studies have attempted to quantify forest growth and the work of Yu *et al.*, (2004; 2006) suggests this is a

complicated task with the potential for large error. Very few studies detail their exact methodology and it seems there is a need to hone and develop the algorithms used for LiDAR processing in order to obtain a greater level of maturity (Dubayah *et al.*, 2000). The majority of current growth studies have looked solely at the slow-growing, cold climate forests of Scandinavia. However, the 2003 and 2006 LiDAR datasets available for the Kielder region provide an excellent opportunity for extending the study of growth to the temperate, faster growing forests of north east England. Indeed, the high tree densities, simple silvicultural regimes and short forest rotations make British forests particularly suitable for the study of growth over short time periods.

The few studies of forest growth using ALS that have been published to date have found errors associated with growth estimation to be large (Yu *et al.*, 2004). As a result it is highly necessary that the collection of ground truth data within this project, and further afield, is as accurate and precise as possible. It is evident that much effort has been channelled into accurately locating the ground truth data for precise spatial comparison with the LiDAR transects (Means *et al.*, 1999; Popescu *et al.*, 2002; Næsset 2002; Næsset and Økland 2002; Donoghue *et al.*, 2004; Watt 2005; Watt and Donoghue 2005; Yu *et al.*, 2006). Whilst this is important and worthwhile, little attention has been paid to the accuracy and precision of the instruments and equipment used to collect other forest variable data, such as height, which is key for growth estimation. The Vertex hypsometer, Suunto clinometer and height poles have been used extensively for height measurements, yet an exhaustive assessment and comparison of these techniques remains long overdue. Consequently, it is a specific aim of this project to perform an evaluation of various height-measuring instruments as well as to assess the level of error introduced to height

measurements by the user. This will permit a better estimation of forest growth and thereby allow more reliable conclusions to be drawn.

To date, the widespread use of remote sensing in forestry has been hindered somewhat by mistrust and misunderstanding amongst foresters (Suarez *et al.*, 2005; Watt 2005). Indeed, it seems that there remains a gap between research and forestry which needs to be bridged by proving the value of remote sensing. Limited experience of most forms of remote sensing, with the exception of aerial photography, compounds an inertia amongst foresters to acquire new and valuable skills. Yet ALS has the potential to provide accurate and repeatable measurements of solid wood quantities and for predicting the commercial value of standing timber stocks (Næsset 2002; Næsset and Økland 2002; Suarez *et al.*, 2005). Thus, this project aims to build on earlier work undertaken as part of the ForestSAFE project, with a view to emphasise the value of remote sensing, and particularly ALS, for forest growth monitoring whilst working alongside the Forestry Commission at Kielder Forest. As of yet, no study has looked solely at airborne LiDAR data for Kielder for establishing forest growth rates and it is here that this project endeavours to contribute.

The wider contributions of this research also need consideration. Indeed, LiDAR data can provide essential information for improving our understanding of the role of forests in the carbon and nutrients cycles (Henning and Radtke 2006). The need for such an understanding is becoming ever more acute in an age of severe climate change. LiDAR data may be used as a non-invasive technique to better our estimations of carbon stocks and thereby help facilitate the international decision making process concerning carbon policy and global climate change (Drake *et al.*, 2002; Gobakken and Næsset 2004; Watt 2005; Yu

et al., 2006). Furthermore, for the first time ALS provides the ability to monitor and model terrain beneath forestry, thereby enabling advanced hydrographic surveillance in tropical regions prone to landsliding and volcanic activity. Thus, LiDAR may also have a wider role to play in disaster management and mitigation (Blair *et al.,* 1999).

1.2 BACKGROUND

1.2.1 LiDAR

1.2.1.1 The Theory of Airborne Laser Scanning

LiDAR is an active form of remote sensing capable of providing information in three dimensions at high spatial resolutions and vertical accuracies. The term 'LiDAR' is synonymous with 'laser altimetry' and 'airborne laser scanning' (ALS). All terms refer to a light detection and ranging system which determines distance using time and the speed of light (Lim *et al.* 2003). A pulse of energy is emitted from the sensor, usually of a green or near-infrared wavelength, and the time it takes to return is used to quantify the distance to the reflecting object or surface (Dubayah and Drake 2000). As the scanning system is flown over an area, a 3D representation of the surface below is assimilated into a laser point cloud. Onboard GPS and inertial navigation systems (INS) (Fig.1.1) allow the exact location and orientation of the aircraft to be known so that each point within the cloud can be accurately positioned (Goodwin *et al.*, 2006; Kraus 2002). The sampling pattern of these points is largely predetermined by the design of the specific laser scanner and is highly dependent on platform altitude, scan angle and pulse repetition rate (Ackermann 1999).
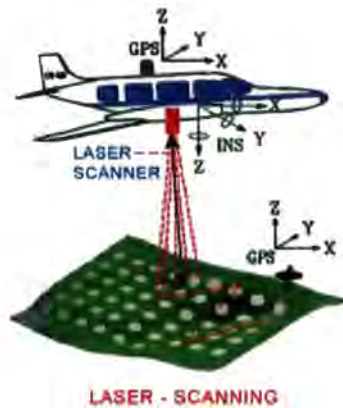
Figure 1.1 LiDAR system including onboard dGPS and ground base station, and inertial navigation system. (Source: www.gis.gov.ae accessed 15.01.07)

Currently two types of airborne laser scanner are available, differing in the way they record the reflected energy pulse (Fig.1.2). Discrete return systems record a set number of laser returns per pulse. Usually only the first and last returns are recorded; however some sensors are capable of collecting as many as five returns per pulse (Popescu *et al.* 2002). Such systems are currently more common than the alternative full waveform sensors (Lim *et al.* 2003). The latter are able to monitor the entire return signal of the emitted pulse so that a full waveform profile may be observed. This is often useful for measuring forest structural attributes. However, full waveform sensors are presently more expensive and less widely available and therefore are used less frequently.
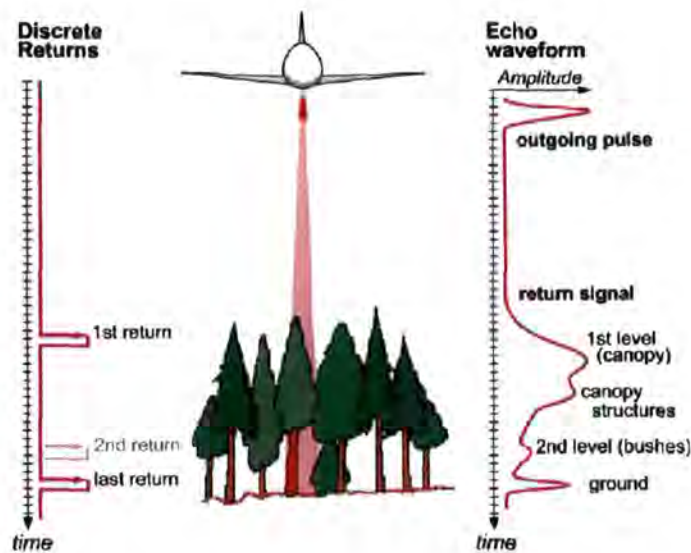
Figure 1.2. Schematic representation of discrete and waveform LiDAR systems.
(Source: www.riegl.com accessed 15.01.07)

Discrete return systems have been most extensively used within forestry to date, and their use for the purposes of this project is appropriate. They work on the principle that the reflectance of the laser pulse is Lambertian in character (Goodwin *et al.*, 2006; Friess *pers comm.* 2007; Kobler *et al.*, 2007). Therefore, depending on the nature of the surface only a portion of the emitted pulse is expected to return to the sensor. Then, only if the intensity of this reflected pulse exceeds a certain threshold is the elapsed time recorded and distance calculated. Below this predetermined threshold, reflected energy is impossible to differentiate from random noise. Consequently, any reduction in reflection intensity may lead to the recording of fewer returns. This may result from rough targets which produce complex scattering patterns, the reflection from each small surface then being naturally lower in intensity. Larger distances between the sensor and reflecting surface also cause intensity reduction, as dictated by Newton's Inverse Distance Law[1]. Thus, greater platform

---

[1] Newton's Inverse Distance Law can be applied to light and all wavelengths of electromagnetic radiation. It states that the intensity of light radiating from a given source (in this case, the LiDAR sensor) will be

altitudes often incur lower density returns (Goodwin *et al.,* 2006). Furthermore, the range of scan angles of the LiDAR system also determines the nature of the interaction between emitted pulse and reflecting surface. Again given Lambertian type reflectance, the intensity of the returned pulse is directly proportional to the cosine of the incident angle as stated by Lambert's Cosine Law. Thus, when the incident angle of emitted radiation is normal to the reflecting surface the maximum intensity of reflectance is observed. In relating this to airborne laser scanning, we find that greater scan angles give returns of lower intensity. Therefore, at the very edges of scan lines where incident angles are greatest there is also greatest likelihood that very low intensities of reflectance fall below the preset energy threshold and thus are unrecorded. Furthermore, greater scan angles induce heavier shadowing leading to gaps in the resulting dataset (Yu *et al.,* 2004). As a consequence, recommended scan angles for discrete return systems should be below $\pm 10^{\circ}$ and certainly should not exceed $\pm 20^{\circ}$ (Ackermann 1999; Yu *et al.,* 2004).

1.2.1.2 *The Development of LiDAR*

Laser scanning is still a fairly new and emerging active remote sensing technology. However, it has experienced significant development since its early beginnings in the 1970's and 80's in North America (Table 1.1), where initial research was led by NASA (Ackermann 1999). In Europe, it was first used in oceanographic applications for bathymetry mapping and depth sounding, often by defence research agencies (Nilsson 1996; Yu *et al.,* 2004). Initial problems with georeferencing and aircraft movement distortion hindered the early development of laser scanning systems. However, the advent

---

inversely proportional to the square of the distance between the source and target surface or object. Hence the reduction in intensity with distance.

of differential GPS and aircraft inertial navigation systems (INS) has now largely solved such serious positioning problems. Indeed, the investigations of researchers at the University of Stuttgart in the early 1990's demonstrated the potential of laser scanning systems for high geometric accuracy, especially in the generation of digital elevation models (DEMs) (Ackermann 1999). Today LiDAR data is used frequently to create DEMs of terrain surfaces with high levels of spatial resolution (10 hits per m^2) and vertical accuracy (15cm) (Lim *et al.*, 2003; Yu *et al.*, 2004). Such DEMs have been used widely and in a variety of applications ranging from road planning to archaeology (Perreira and Jansen 1999). Indeed, since its early development LiDAR has migrated into many other fields, satisfying the needs of both scientific and commercial communities. Today, the airborne laser scanner is an easily obtainable and highly reliable instrument for commercial surveying (Kraus and Pfeifer 1998).

Characteristics	*1993*	*2007*
Laser Pulse Frequency	2 kHz	170 kHz
Max Height A.G.L	1000 m	4500 m
Nature of Returns	First or last	Multiple returns to full waveform
Point Spacing	4-5 m	<1 m

Table 1.1 The development of laser scanner instrument technical specifications.

(Source: Friess 2007 *pers. comm.*)

1.2.1.3 The Potential of LiDAR for Forestry

Despite not being initially developed for forest applications, the potential of LiDAR in this field has become increasingly evident. Indeed, the unique ability of ALS to penetrate through gaps in foliage to the underlying terrain makes it a breakthrough technology for estimating forest canopy parameters and generating DEMs in forested regions (Ackermann

1999; Rieger *et al.,* 1999; Dubayah *et al.,* 2000; Hollaus *et al.,* 2006). This is especially useful for steep and otherwise difficult to access areas, and offers an alternative to traditional forest inventorying practices. In mountainous areas there is a growing trend for planting mixed aged stands due to the inherent dangers of clear cutting large areas of same age forest. The characteristics of mixed age stands are difficult to estimate using traditional methods so this is where LiDAR offers an advantage (Rieger *et al.,* 1999). In less extreme environments too, ALS can supply coverage of large areas much more quickly and cost effectively than the labour intensive field data collection methods, providing estimates of canopy height, volume, basal area, stem diameter and biomass (Drake *et al.,* 2002; Lim *et al.,* 2003).

There remains, however, a lack of experience in the use of LiDAR amongst forest practitioners. Thus, its great potential goes somewhat overlooked and unexploited (Dubayah *et al.,* 2000). Furthermore, there is a lack of maturity in the algorithms used to process laser data (although some recent work has aided progression: Sithole and Vosselman 2004; Zaksek and Pfeifer 2006; Kobler *et al.,* 2007). This emphasises the need to demonstrate the potential of ALS for forestry through active experimentation and the integration of field data with analysis (Dubayah *et al.,* 2000). The following sections explore how ALS has been used for forest applications to date and then introduce the specific aims and objectives of the use of ALS for forestry within this project.

1.2.2   LiDAR for Forestry

1.2.2.1   Initial Findings

Early work by Schreier *et al.* (1984) looked at terrain profiling in Canada using airborne laser scanning. They noted that dense vegetation cover introduced an element of noise into profiles which led them to suggest the use of laser profiling for assessing vegetation canopies. In the same year, Nelson *et al.* (1984) used laser altimetry to demonstrate the detection of changing canopy density conditions. They showed that LiDAR data could be used to estimate mean tree height to within 60cm of that predicted by photogrammetric methods. Aldred and Bonner (1985) also demonstrated the use of LiDAR for measuring stand heights but estimated a lower accuracy of laser-derived heights within 4.1m of photogrammetric measures at the 95% confidence level. They also found that laser heights constantly underestimated those taken by ground-truthing. Further work by Schreier *et al.* (1985) reported that the use of laser beams of near-infrared wavelength was advantageous for accurate tree height measurement.

Following these initial experiments, the work of Nelson *et al.* (1988) began a series of studies using small-footprint LiDAR to assess various forest canopy characteristics. Nelson *et al.* (1988) collected data concerning canopy heights over a pine forest in southwest Georgia, USA. Using this data they were able to predict total tree volume and mean biomass to within 2.6% and 2.0% of ground-truth values respectively. Like Aldred and Bonner (1985) however, they too found laser height measurements consistently underestimated true heights. It was suggested that this was due to the majority of laser pulses falling on the 'shoulders' of the dominant trees rather than their peaks. This has

11

since been reported by a number of studies (Nilsson 1996; Næsset 1997; Dubayah *et al.*, 2000; Næsset 2002; Popescu *et al.*, 2002; Suarez *et al.*, 2005; Yu *et al.*, 2004).

At this early stage in the history of the use of LiDAR for forestry applications, problems with georeferencing were a major source of error. Nelson *et al.* (1988) used balloons and tarpaulins as navigational aids for the pilots and determined the LiDAR transect positions using clearly identifiable ground features. In his study of forests in Ålö, Sweden, Nilsson (1996) placed large white plastic squares on the terrain as ground control points for locating the LiDAR transects. In addition, up until the year 2000 GPS measurements of these locations were hampered by selective availability (SA)[2], meaning that the total locational error was greater than 35m. This lead Nilsson (1996) to conclude that:

"if airborne laser data could be given both height and planimetric co-ordinates with high accuracy, single trees or groups of trees could be identified and detailed terrain models could be generated. This would be of great importance in many different situations, for example, choosing a forest regeneration method, planning and constructing forest roads etc. " (Nilsson 1996 p.6)

Over the following few years the development of differential GPS (dGPS) and the switching off of SA means that it is now possible to locate specific points or trees with sub-meter accuracy (5-15cm).

---

[2] Selective Availability (SA) was the term used for the intentional error introduced by the United States Department of Defence. Noise was introduced to the signal and satellites given erroneous orbital data in order to prevent the GPS system being used against the USA by enemy forces. This caused significant reduction in accuracy of measurements until it was switched off in the year 2000 (Hurn 1993).

Within the last decade, the work of Næsset in southeast Norway has been central in testing the ability of small footprint laser scanning for determining tree heights and other canopy characteristics. Næsset and Bjerknes (2001) derived mean heights for young stands (<6m tall) in Våler and found that regression analyses accounted for 83% of the variability between laser- and ground-measured values. Similarly, work with Økland in 2002 over a boreal nature reserve in Østmarka showed how regressions accounted for 75% of the variation in mean height values from LiDAR and ground-truthing. Indeed, the correlation between these variables is high with an R^2 of 0.91 (Næsset and Økland 2002). They note that LiDAR height estimates are of equal if not better accuracy than more typical methods of forest inventorying. Many other papers have found similarly good correlations between small footprint, discrete return LiDAR data and field derived height metrics (Rieger *et al.,* 1999; St-Onge 1999; Means *et al.,* 2000; Næsset 2002; Popescu *et al.,* 2002; Donoghue and Watt 2006). Yet many also note that mean errors frequently fall within the range of 1-2m (Rieger *et al.,* 1999; St-Onge 1999; Næsset 2002). As a result, Næsset and Økland suggest that in order to make best use of such data, the ground truth sampling must be accurate, precise and extensive, as must the post-processing of laser data. Indeed, there is much focus today on developing superior processing techniques and improving processing software (Sithole and Vosselman 2004; Zaksek and Pfeifer 2006; Kobler *et al.,* 2007). This has been driven, in part, by a shift from technology-driven to applications-driven development. Yet it is also due to a growing trend of multi-temporal surveying aimed at quantifying change rather than just measuring static forest characteristics. Herein lies the study of forest growth, and the theme for this project.

1.2.2.2 LiDAR for Forest Growth

It was Yu *et al.* (2004) who first studied the use of multi-temporal, small footprint, high density LiDAR (10 points/m^2) surveys for change detection in the forests of Kalkkinen, Finland, between 1998 and 2000. Tree-to-tree matching algorithms were used in an object-orientated approach to estimate growth and detect individual harvested trees. A method based on the algorithm of Ruppert *et al.,* (2000) was used to create a DEM with an expected accuracy of about 14cm (Ahokas *et al.,* 2002). A digital surface model (DSM) was generated from the highest laser values falling within each 0.5m pixel. The difference between this DSM and the DEM was then taken as the canopy height model (CHM).

Change detection was next performed using difference imaging, where each pixel value in the 2000 CHM was subtracted from the equivalent pixel in the 1998 CHM. Areas of high positive differences were highlighted using a certain threshold value and then subjected to a segmentation procedure to enable the identification of individual harvested trees. Of a total of 83 harvested trees identified in the field, 61 were successfully detected and these were mostly the more mature trees at the time of the first laser survey acquisition. For growth estimation, trees present at the time of both laser acquisitions were delineated for each CHM using a segmentation procedure as defined in Hyyppä *et al.,* (2001a). Local maxima filters followed by a watershed based procedure then allowed single tree crowns to be identified. Growth estimation then required matching of individual trees in both CHMs, which is where a threshold distance of 0.5m was introduced in Yu *et al.,*'s (2004) tree-to-tree matching algorithm.

Verification of height and growth estimates was carried out by comparison with field-measured values. Like many before them, Yu *et al.* (2004) noted that individual tree height, and as a result growth, was systematically underestimated, in this case by as much as 67cm. This corresponds to about 2-3 years growth in the Norway spruce and Scots pine trees present in the region of Kalkkinen, and means that errors associated with growth estimation are actually larger than the estimated growth itself. Yu *et al.,* (2004) found that discrepancies between the two DEMs were largely responsible for this underestimation. Following DEM compensation to remove such errors agreement with field data was much improved- the precision of growth estimates was approximated to 5cm at stand level and 10-15cm at plot level. This led to the suggestion that the lack of laser pulses hitting the tree tops was an unlikely explanation of LiDAR height underestimation and instead that it may be caused in part by errors in the DEM. This highlights a serious issue and substantiates the need for further study of forest growth using airborne laser scanning.

In 2006, Yu *et al.,* produced a follow up paper, again attempting to quantify forest growth in the Kalkkinen region, using high density LiDAR data from 1998 and 2003. They introduced a new algorithm for individual tree matching, based on the concept of the Hausdorff distance technique, which produced growth values of a more acceptable accuracy. The best correlation between laser- and ground truth-derived growth values was reported at $R^2 = 0.68$ for maximum pixel heights. However, correlation for growth variables remain below those reported elsewhere for height, which are consistently above 0.8 (Rieger *et al.,* 1999; St-Onge 1999; Næsset and Bjerknes 2001; Næsset 2002; Næsset and Økland 2002; Popescu *et al.,* 2002; Donoghue and Watt 2006). Yu *et al.,* (2006) anticipate that this is largely due to errors incurred by the difficulty of measuring mature trees in the field, yet

15

it may also result from wind displacement of treetops and the different viewing geometries of the two surveys. Thus they give two key recommendations; firstly, the same flight plan should be used for all multi-temporal surveys to eliminate problems associated with different points of view and; secondly, *a priori* information concerning expected growth patterns should be observed when measuring mature trees. Ultimately, the work of Yu *et al.,* has demonstrated that it is possible to measure individual tree growth using multiple ALS surveys (Yu *et al.,* 2004; Yu *et al.,* 2005; Yu *et al.,* 2006). This said, it is also important to remain aware of the limitations of these current methods.

Recent papers of Næsset and Gobakken have taken a slightly different approach to make an important contribution to studies of forest growth using ALS. Using laser data collected in 1999 and 2001 over the Våler region of southeast Norway they took a statistical approach to test whether forest growth could be detected (Gobakken and Næsset 2004; Næsset and Gobakken 2005). Pulse densities were much lower than those obtained by Yu *et al.,* (2004; 2005; 2006) and thus an object oriented method was unfeasible. It was argued that a lower density, larger area approach is more viable in terms of economic cost and processing demands. A DEM was created for each dataset using last pulse returns only generated into a TIN[3]. A height accuracy of 25cm was expected for the TIN model. First returns were spatially aligned with the TIN and the height of each point calculated as a difference from the terrain surface. Various height metrics were next computed for each field plot based on the heights of all laser points falling within their boundaries. It was found that all metrics differed significantly between the two years thus confirming the ability of ALS to detect forest growth. However, on comparison with field derived data it was found that the

---

[3] TIN stands for triangulated irregular network and is discussed in more detail in Chapter 4 – Methodology.

accuracy and precision of laser growth metrics was low. Næsset and Gobakken (2005) suggest that this may be due to inherent errors within the ground truth data and the well-known problems associated with the co-registration of multi-temporal same area datasets. Little attention is paid to the accuracy of ground truth measurements in the wider literature concerning ALS for forestry and perhaps represents an area for further study. In order that co-registration is as accurate as possible, Næsset and Gobakken recommend that multi-temporal data acquisition routines are as robust and as similar as possible. The work of Wulder *et al.*, (2007) endorses the combination of optical imagery with LiDAR surveys in order to ameliorate inevitable positioning discrepancies. It also seems that the choice of an appropriate ground reference level is key for growth estimation. As found by Yu *et al.*, (2004) discrepancies in the DEMs account for large amounts of error. Indeed, St-Onge and Vepakomma (2004) suggest that use of exactly the same terrain surface for each year is imperative if height and growth estimates are to be relied upon. There is also some discussion that a two year period is not sufficient to detect growth given the noise incurred by error. Normal forest inventorying practices would not expect to analyse growth over much less than a five year period (Gobakken and Næsset 2004). Yu *et al.*, (2005) found correlations between laser and field variables improved significantly for a five year timescale ($R^2 = 0.66$) as compared to two years ($R^2 = 0.29$). Thus, it is concluded that further study is necessary to determine how short timescales can be used to provide more reliable growth estimations.

Having examined much of the existing work concerning the use of ALS for forest height and growth studies, it is evident that a number of key issues recur frequently and deserve further note here;

- Only the dominant tree layer is detected by ALS (St-Onge 1999; Næsset and Bjerknes 2001; Popescu *et al.*, 2002; Maltamo *et al.*, 2004).

- The tops of trees are often missed with the majority of laser pulses falling on the shoulders of dominant trees. This frequently leads to underestimation of 'true' height by the LiDAR system (Nilsson 1996; Næsset 1997; Dubayah *et al.*, 2000; Næsset 2002; Popescu *et al.*, 2002; Suarez *et al.*, 2005; Yu *et al.*, 2004).

- ALS offers a real alternative to expensive and time-consuming traditional forest inventorying practices carried out in the field (Hyyppä *et al.*, 2000; Næsset 2002; Næsset and Økland 2002; Popescu *et al.*, 2002; Watt 2005; Watt and Donoghue 2005).

- Inaccurate and imprecise LiDAR growth estimates may result, in part, from inaccuracies within the reference (ground truth) data (St-Onge 1999; Næsset and Gobakken 2005).

- Areas for future development include: improving the accuracy of DEM, multi-temporal dataset co-registration and spatial data fusion (Pereira and Janssen 1999; St-Onge 1999; Lim *et al.*, 2003; Romano *et al.*, 2004; Yu *et al.*, 2004; Næsset and Gobakken 2005; Donoghue and Watt 2006; Yu *et al.*, 2006; Wulder *et al.*, 2007).

1.3 AIMS AND OBJECTIVES

The aim of this research is to investigate the potential of multi-temporal, small footprint, discrete return LiDAR surveys for estimating growth at plot level, over a three year period, of coniferous plantation forestry in Northern England.

Key research questions:

1. Can multi-temporal ALS detect forest growth over a three year period?

2. If so, how accurately is this growth predicted?

3. Can this tell us anything about:

    a. the robustness of our LiDAR processing and;

    b. the accuracy, precision and reliability of our methods used to test the LiDAR data?

In answering these questions, this project will attempt to:

1. Quantify the heights and amount of growth exhibited by Sitka spruce plantations of different ages between 2003 and 2006 using airborne LiDAR data from Kielder Forest;

2. Verify these height and growth estimations made by ALS data using ground based observations and;

3. Assess the accuracy of ground truth equipment and data.

In order to address the research questions the project has the following objectives:

1. Develop a method of summarising and extracting LiDAR height variables from the laser point cloud data with a view to estimate growth.

2. Design and execute a suitable method of ground truth data collection.

3. Design and execute a trial-based assessment of the error associated with ground truth data collection.

4. Compare LiDAR and ground-truth derived metrics at a specified scale, considering associated errors, to estimate tree growth at Kielder.

5. Identify and investigate potential sources of error in height and growth estimation.

2 METHODOLOGY

2.1 STUDY SITE

The 6km^2 research area studied here is located within the wider district of Kielder Forest, located in Northumberland, England (Fig.2.1). It is owned and managed by the UK Forestry Commission and is the largest forest in the UK covering approximately 62,000 hectares. Kielder is a plantation forest comprised primarily of Sitka spruce trees (*Picea sitchensis* (Bong.) Carr.). It lies at a mean altitude of 270m and has a mean slope angle of 6°. It was established in 1926 by the Commission principally for timber production. Today the forest plays an important role in the tourism industry of Northern England and continues to produce a commercial crop of up to 1300 tonnes of timber daily (www.kielder.org accessed 18.10.06). Annual British timber production is set to rise from 11 to 15 million m^3/ha by the year 2020 (Watt 2005) and as a consequence, efficient forest management is paramount. Precise, accurate, up-to-date information concerning forest resources is a growing necessity, particularly considering the short forest rotations and fast growth rates of trees at Kielder. This is where remote sensing, and more specifically LiDAR, may be of value for both local and national forest management.
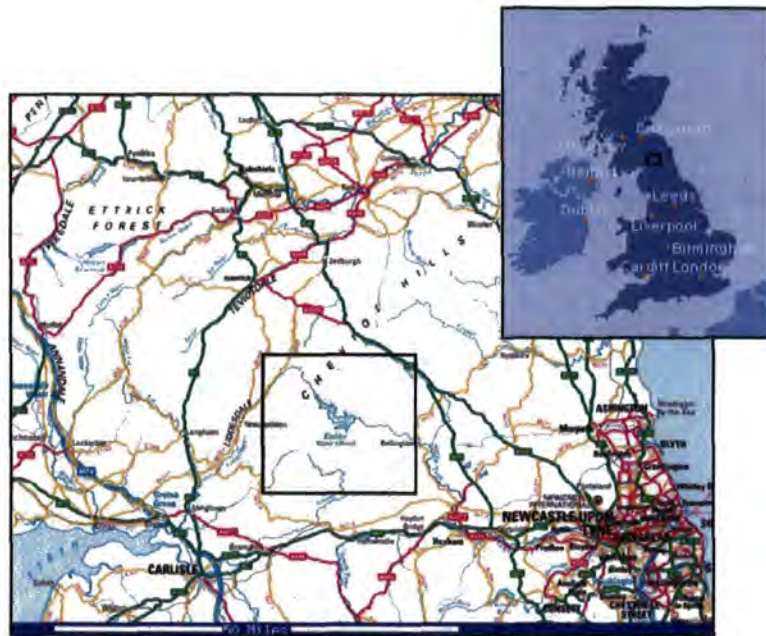
Figure 2.1 Location map for Kielder Forest.
(Source: www.multimap.co.uk accessed 15.01.07)

There is a growing literature highlighting the value of new remote sensing technologies for forest applications. At the local level at Kielder, the remote sensing work carried out during the EU ForestSAFE project has been fundamental. Watt (2005) evaluated the potential of LiDAR, as well as IKONOS and Landsat ETM+ for providing data concerning forest structure. A key aim here was to evaluate the usefulness of techniques other than aerial photography for assessing forest characteristics. Watt and Donoghue (2005) published a study investigating the use of terrestrial laser scanning systems at Kielder. Their results suggest that forest canopy structural characteristics can be accurately quantified using this method and that it offers significant advantages over traditional field survey methods. Further work in 2006 reinforces the mounting evidence from elsewhere in the scientific literature, highlighting the potential of high resolution airborne LiDAR data for accurate and thorough forest resource estimation (Donoghue and Watt 2006).
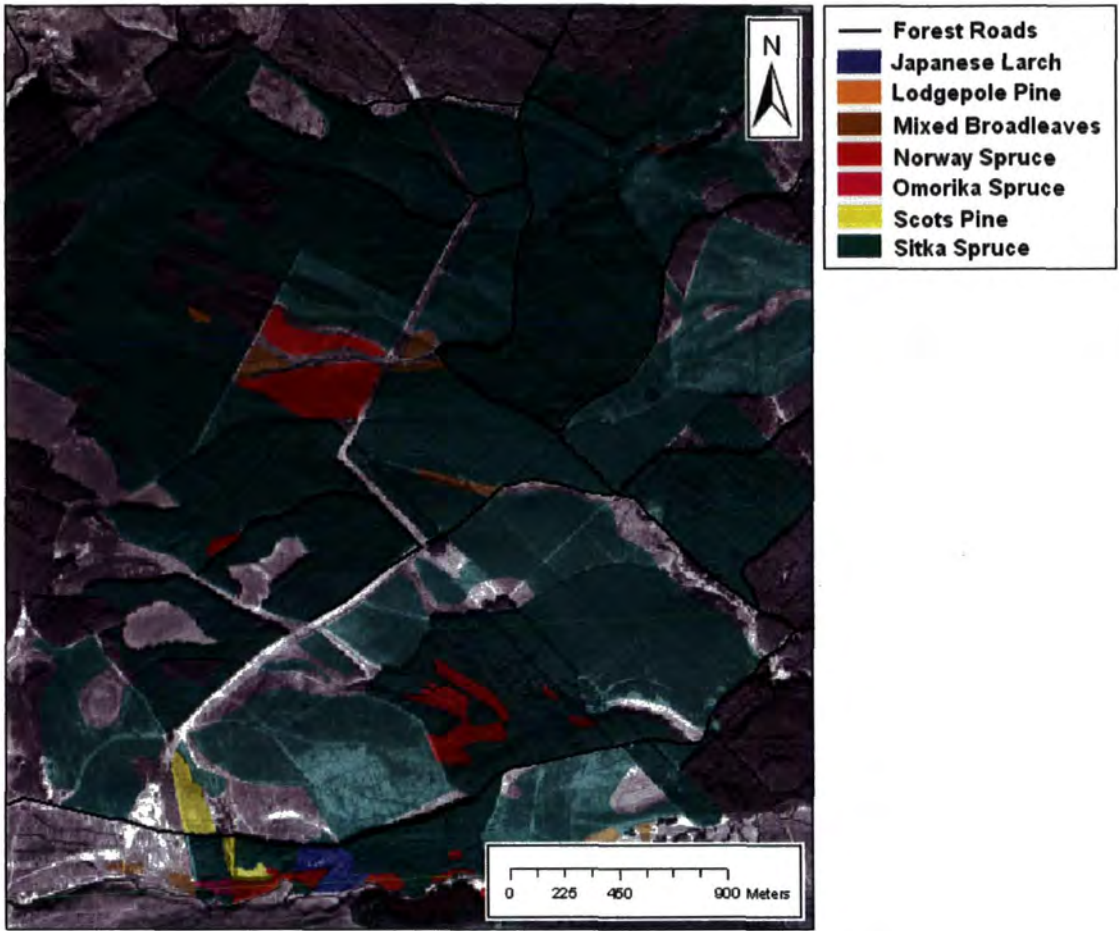
Figure 2.2 The study area (IKONOS panchromatic imagery underlies GIS data).

2.2   LiDAR DATA AND SENSORS

The multi-temporal laser data was collected during the summers of 2003 and 2006. In 2003 an Optech 2033 laser scanner was flown by the Environment Agency on behalf of the Forestry Commission. In 2006 an Optech 3033 laser scanner was flown by the NERC Airborne Research and Survey Facility (ARSF) in conjunction with Cambridge Unit for Landscape Modeling onboard their Dornier 228-101 aircraft.

These are both small footprint, discrete return systems which recorded first and last pulses and intensity. Both systems operated in the near-infrared region of the electromagnetic spectrum to collect swaths of data, covering the $6km^2$ test area (Fig 2.4). The 2003 dataset is the same as that used by Watt (2005) in his study of Kielder Forest.

Figure 2.3 The Optech ALTM 3033 laser scanner and associated data collection equipment.

Sensor	Optech ALTM 2033	Optech ALTM 3033
Date of Survey	26.03.03	05.05.06
Scan Angle	10°	16.5°
Pulse Density	$2/m^2$	$4/m^2$
Flying Altitude	950m	1750m

Table 2.1 Technical Specifications of LiDAR Systems.
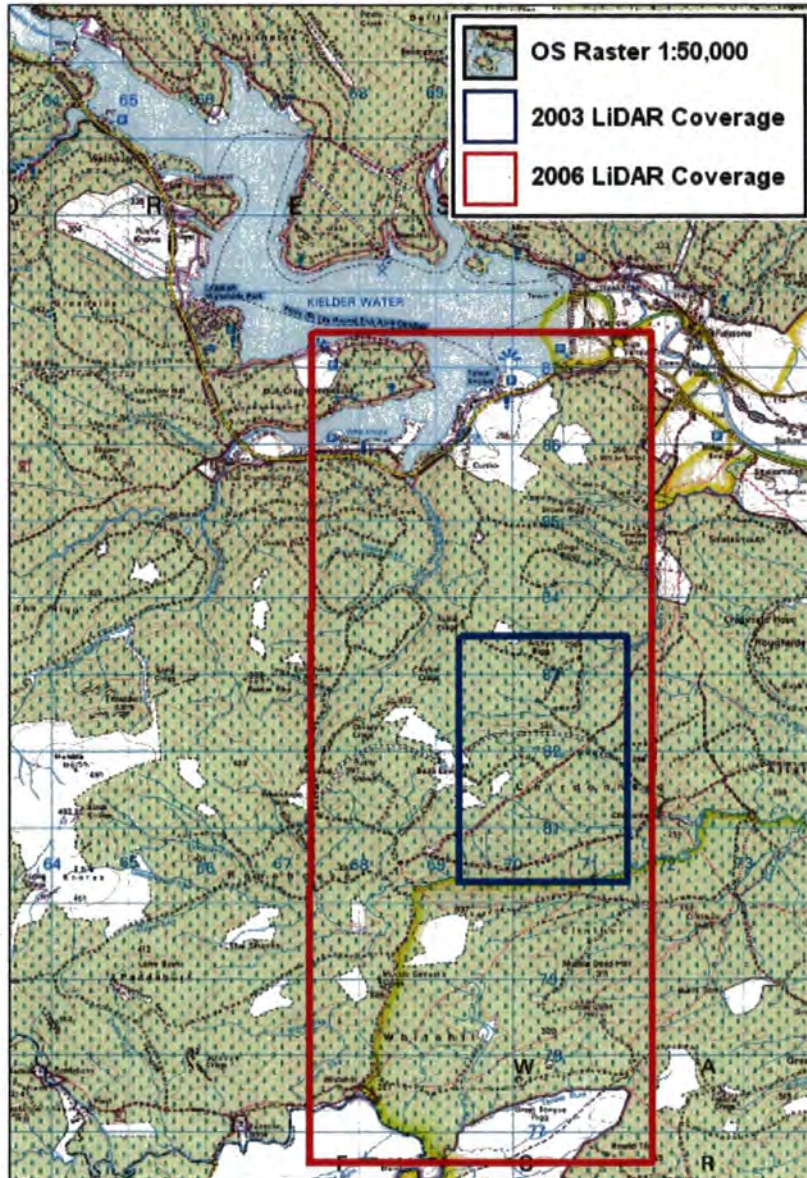
Figure 2.4 Coverage of the LiDAR datasets.

2.3 LIDAR PROCESSING

2.3.1 Raw laser points

Both sets of LiDAR point cloud data were provided in *ASCII* format, having been corrected for geometric distortions by the data providers. The 2003 data was delivered in two files which had been separated into first and last returns, each containing four columns of data: easting (x), northing (y), elevation (z) and intensity (i). Each file was then halved so that it contained around 7,000,000 points, to improve the manageability of the data. The 2006 data was provided in separate time-of-flight order swaths. Each swath was represented by one file containing all data from both returns in eight distinct columns. These swaths each contained approximately 9,000,000 points but were small enough to process individually so that further file splitting was unnecessary. In order to estimate canopy heights and growth rates it is first necessary to create a Digital Elevation Model (DEM) of the ground surface and a Digital Surface Model (DSM) of the vegetation canopy.

2.3.2 Filtering

For each dataset, all points were loaded into the LiDAR processing package TerraScan (www.terrasolid.fi). This is a dedicated software program for filtering and classification of laser points, as well as digital surface generation. The process functions embedded within TerraScan are highly automated yet also allow the user to define point classes, to modify classification parameters and to delete erroneous returns. It also provides a good platform for point cloud interpolation and consequent digital surface visualisation.

Filtering of the returns is the first step in the creation of a DEM or DSM. The main aim of filtering is to remove erroneous returns which do not represent the true ground or canopy surface. Viewing the point clouds in TerraScan from individual flight strips and smaller files allowed obviously erroneous returns to be identified and removed. Such points fall above or below the main cloud and thus are easily isolated. These errors may be caused by recording inaccuracies in the Time Measurement Unit (TMU) or due to possible multiple paths followed by some of the return pulses. This occurs when the laser pulse is reflected between a number of surfaces before it is returned to the sensor. This causes a time delay, which then means an inaccurate range distance is calculated (Hurn 1993; Watt 2005). Thus it is highly important that such returns are removed from the dataset before further processing is implemented.

2.3.3 Classification of LPs

Following the filtering, it is next necessary to classify points into the categories of 'ground' or 'canopy' to then create the DEMs and DSMs. Ground classification was undertaken first using local neighbourhood filters based on a predetermined set of discontinuity thresholds to create the DEMs. Last returns only were used in this process. There has been some suggestion that a combination of first and last returns is helpful for DEM creation (Zaksek and Pfeifer 2006), however this has been found in areas of very dense canopy and steep terrain, where the FPs help to identify a terrain gradient and thus aid in terrain modelling. This approach assumes that the gradient of vegetation cover and the underlying ground are parallel which of course may not always be true. Furthermore, such an approach is most helpful when employing a slope based filtering technique. Given that a TIN densification

algorithm is used here and that the study area is relatively flat, the decision was made to use last returns only. This also helps to reduce processing speeds.

Certain software packages are already equipped with algorithms for filtering and are able to perform DEM generations almost instantaneously. Here, the progressive TIN[4] densification algorithm developed by Axelsson (2000) and embedded within the TerraScan software was employed. This is an iterative algorithm which combines filtering and thresholding. It works by passing a moving window of user defined size (defaulted at 60m x 60m) over the data to select neighbourhood minima. A number of explicit assumptions are made at this stage in the processing. Firstly, it is assumed that the lowest returns within the dataset do in fact represent the ground surface and secondly; that there is at least one laser return per window.
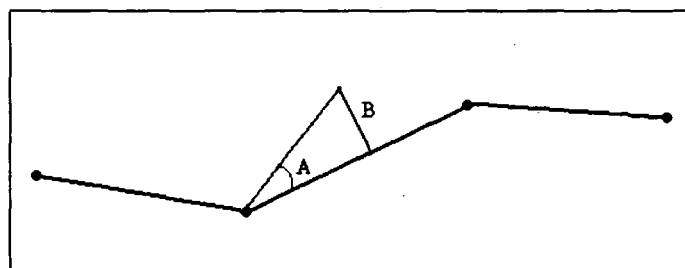
Figure 2.5 Creation of a TIN: A = iteration angle, B = distance.

Following the selection of local minima, further points are added to the TIN with each iteration of the algorithm, provided that they conform to predetermined iteration angle and distance thresholds (Fig.2.5). These thresholds set the largest acceptable angle between

---

[4] A 'Triangulated Irregular Network' or TIN is a network of triangles formed between the data points.

28

points and the TIN facet (A) and the smallest allowable distance to each triangle node (B), respectively. The higher the value of A and B then the higher the elevations of points added to the TIN. When no points remain below the defined boundary the iterative process finishes and selected points are interpolated to form the DEM.

Watt (2005), in his study of Kielder Forest, found that the initial default settings of a window size of 60m x 60m and iteration distance of 1.4m did not produce a satisfactory DEM. Consequently, window size was changed to 100m x 100m and the threshold distance was reduced from 1.4m to 0.5m. This helped to reduce errors within the DEM and better defined the ground surface.
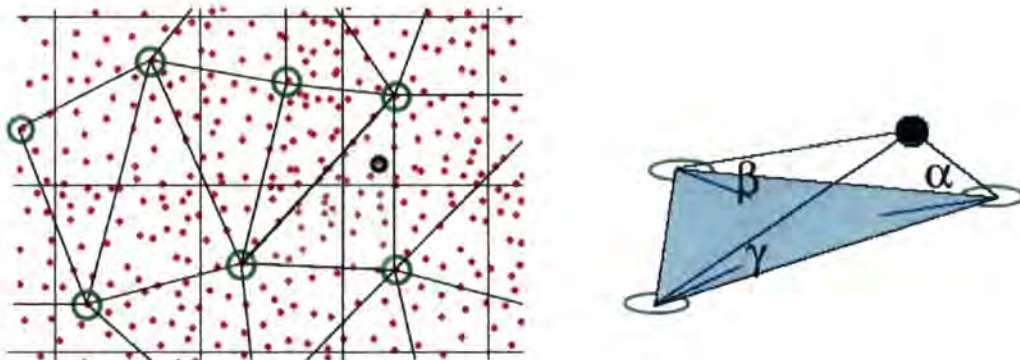
Figure 2.6 3D representation of the progressive TIN densification technique. Local neighbourhood minima are located (green circles) and triangulated. New points (black circle) are considered for joining to the TIN based on predetermined threshold iteration angle and distance. (Source: Pfeifer 2007).

In this study, the ground classification parameters were experimented with to test their suitability for creating a DEM. Initially, the window size was set at 60m x 60m. As found by Watt (2005) however, the resultant DEM was not acceptable. It appeared to feature a number of holes where interpolation seemed not to have occurred. On closer interrogation it emerged that these holes corresponded with areas of very dense canopy. In fact, such was

the density of the canopy in these areas that no ground hits were found within the 60m x 60m window. If the ground height cannot be determined then there is no reference point from which to estimate tree height and growth, which also gives errors in the canopy model. Figure 2.7 demonstrates this problem. Scenario 1 represents the use of a smaller window size. Here, sufficient ground returns in window A in box (i) allows creation of the DEM successfully, as displayed in box (ii). However, the lack of ground hits in window B (box i) causes a hole in the resultant DEM in box (ii).

As a result, the window size was adjusted to 200m x 200m in an attempt to help the algorithm interpolate over these problem areas. This is represented by the increased window size in scenario 2 of Figure 2.7. This allows the DEM from window A to be successfully generated again. Furthermore, the wider window now covers ground hits at the edges of window B. As a result, the DEM can also be created for this area. In this respect, the change was successful and the gaps were eliminated. However, the extended width of the search window also allowed points to be falsely classified as 'ground'. This is evident in Figure 4.2c in Chapter 4 where the structure and location of the stands has become evident on the DEM. This results from LPs which actually fall on low vegetation or in the canopy being classified as 'ground'. This may also introduce problems elsewhere in the DEM leading to an overestimation of the terrain surface. This highlights a well known problem of producing high accuracy DEMs in heavily wooded areas where the amount of penetration to the ground is low (Kraus and Pfeifer 1998; Zaksek and Pfeifer 2006; Hyyppä et al., 2005; Hollaus et al., 2006). Indeed, a number of studies have found percentages of last returns that reach the ground to be as low as 25% (Flood and Gutelius 1997; Kraus and Pfeifer 1998; Popescu et al., 2002).

As a consequence of such problems, Watt's (2005) recommended window size of 100m x 100m was tested. This helped to reduce the DEM gap problem somewhat yet also did not compromise the quality of the rest of the DEM. Thus it was carried forward and used with an iteration angle of 8° and an iteration distance of 0.5m. Such parameters consider the compromise of window size and make allowances for the mean slope angle of 6° in this region. Some DEM gaps did remain however. Others have used Delaunay triangulation and linear interpolation to remove such problem areas (Yu *et al.*, 2006), yet interpolation to cover missing pixels was not performed here. Such gaps help identify areas of very dense canopy where the ALS systems run into difficulties. This highlights the current limits of ALS and helps to define a problem which deserves further research. Furthermore, it was found that none of the key ground truth validation plots fell within these problem areas, therefore leaving the gaps caused no further problems for assessing the relationship between LiDAR and ground truth derived variables.
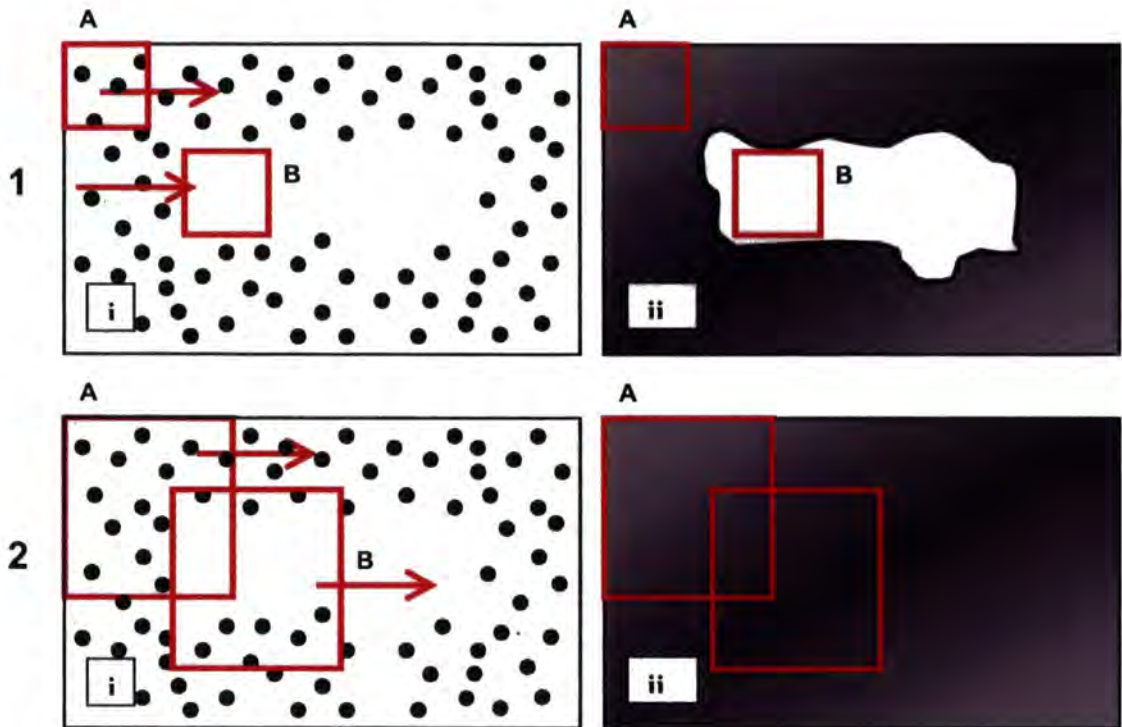
Figure 2.7 The effects of varying window size on DEM creation.

The indication from elsewhere in the literature suggests that the accuracy of DEMs created in this manner lies in the region of 20-25cm (Næsset 1997; Næsset and Bjerknes 2001; Næsset and Økland 2002; Yu *et al.*, 2006). However, no direct check on the accuracy of the DEMs was carried out by this study. Instead, the accuracy is inferred indirectly by the estimation of tree heights and growth values for reference data plots. Furthermore, a comparison of the DEMs from the different survey datasets provides a secondary insight into the quality of the terrain model. This was achieved by exporting all points classified as 'ground' out of TerraScan at this point. Sections 2.3.6 to 2.3.8 describe in greater detail the processes which followed to compare the multi-temporal DEMs.

2.3.4 Classification of FPs and remaining LPs

Following the filtering of erroneous points and classification of the ground surface, the next step is to classify points as 'canopy'. This was achieved by selecting all remaining hits, whether first or last returns, which fell between 2m and 45m above the ground surface. These are then assumed to represent the tree canopy layer. Those hits with a height of less than 2m above the ground were excluded to eliminate the effects of small shrubs and other low lying material. This is a commonly used approach, used to help improve the quality of canopy height metric estimations (Næsset 1997; Næsset and Bjerknes 2001; Næsset and Økland 2002; Yu et al., 2004). The upper limit of 45m was set using *a priori* information concerning maximum tree heights reached within this geographical area. The classified laser point clouds were re-checked visually after canopy classification to ensure that no misclassifications had occurred.

2.3.5 Creation of digital canopy height model

At this stage in the processing, the canopy points still hold an elevation value above the OSGB 1936 Newlyn Datum. Consequently, the next necessary step for height and growth estimation is to give these points a height above the ground surface. This was achieved in TerraScan by setting the ground surface model to act as a geoid to which canopy points could then be adjusted. This has exactly the same effect as subtracting the heights of canopy points from the DEM. Thus canopy points were given a height above the ground, and the points within the DEM were set at 0m.

2.3.6 Extraction of height metrics to a 5m x 5m grid

The following step involved exporting all ground and canopy points out of TerraScan in *ASCII* format. Each point exported was characterised by x (easting), y (northing), z (height above ground), i (intensity) and c (class) values. At this stage, the point data remained separated into smaller files (2003 data) and time-of-flight swaths (2006 data). Each of these files was then imported into the statistical software package STATA and processed separately.

The choice of an appropriate grid resolution was key at this stage in the processing. The resolution of the laser data determines the lower limit of grid size which can sensibly be used. For example, for a pulse density of 1 hit per m^2 a grid size of more than 1m x 1m is necessary so as to prevent bias in the output. Furthermore, if the grid size becomes too large then spatial subtleties within the data are lost. A compromise was reached with a 5m x 5m grid resolution. This allowed height and growth to be assessed fairly at both the plot and stand level.

It is possible to process canopy height and ground data in TerraScan, however this software only allows the output of a single height measure at one time. Conversely, the use of a specially developed routine in STATA permitted a much wider variety of height metrics to be computed. These included mean, maximum, a number of height percentiles, standard deviation, covariance and number of hits per square. Each one of these metrics was computed for all laser hits falling within every 5m x 5m square of the entire area of coverage (Fig.2.8). The output data was then exported as an ASCII file.
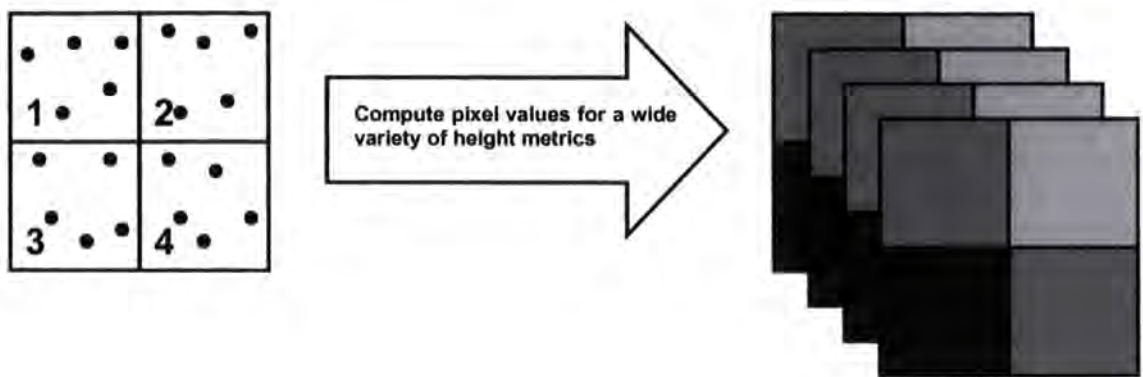
Figure 2.8 Schematic representation of the purpose of the STATA processing routine.

The output *ASCII* file for each metric of each separate file was next loaded into ArcGIS and processed into raster format. The 2006 time-of-flight order swaths featured some overlapping areas for all metrics and for the DEMs. Difference imaging was performed for the areas of overlap of the DEMs to check for consistency between the files. Some large discrepancies were revealed which are presented and discussed in Chapters 4 and 5. The separate smaller (2003) and time-of-flight (2006) files were next merged together using the mosaicking tool. In areas of overlap the mean value of overlying pixels was taken. The now whole 2003 and 2006 datasets were next clipped to the extent of roughly 6km^2 area of interest. This allowed comparison both within (in terms of different statistics) and between the multi-temporal datasets.

2.3.7 Co-registration of datasets

The use of any multi-temporal data requires special consideration in terms of geo-registration. If the datasets do not overlay accurately then the accuracy of any subsequent analyses will be jeopardised. Theoretically, the integrated GPS within the airborne laser scanning system means that all data are accurately and automatically georeferenced from

the moment of acquisition. However, investigations with the Kielder datasets found the 2006 data to be offset by about 5m in a northerly direction. This was determined by highlighting clearly identifiable features on both images and measuring the shift in their location. Careful assessment indicated that the same, seemingly systematic shift was true for all different metric files. When difference imaging was performed, the offset incurred edge effects. Given the simple linear nature of the shift between datasets, the process of correction was fairly straightforward. All 2006 files were exported into the image processing software package 'ERDAS Imagine'. This program enabled the 2006 datasets to be moved south by 5m, so that on re-importation into ArcMap they were aligned properly with the 2003 data and the edge effects were removed (Fig.4.12b). The reason for this shift remains unclear and time constraints prevented reprocessing the initial raw point clouds by the data providers.

2.3.8   Difference Imaging

Having computed a variety of height metrics and adjusted files for geo-registration issues, the next step for extraction of growth values is to perform difference imaging. This simply involves the spatial subtraction of 2006 data from 2003 data in ArcMap, for any given metric. Taking the resulting image as a whole allows visual assessment of growth for the entire study area. For example, Figure 4.12b shows the spatial subtraction for mean height following geospatial adjustments.

2.3.9 Extraction of LiDAR Plot Data

The ground truth validation plots and the trees within them were next added on top of the height and difference imagery in ArcMap (Fig.2.9). The exact location and dimensions of each plot and each tree were recorded using a Leica series 300 differential GPS which resulted in accurate positioning over the LiDAR datasets. This allowed a spatial extraction tool to be used to determine the LiDAR pixel height or growth value at the location of every tree in every plot. This data was exported into the statistics package STATA for comparison with ground truth data.
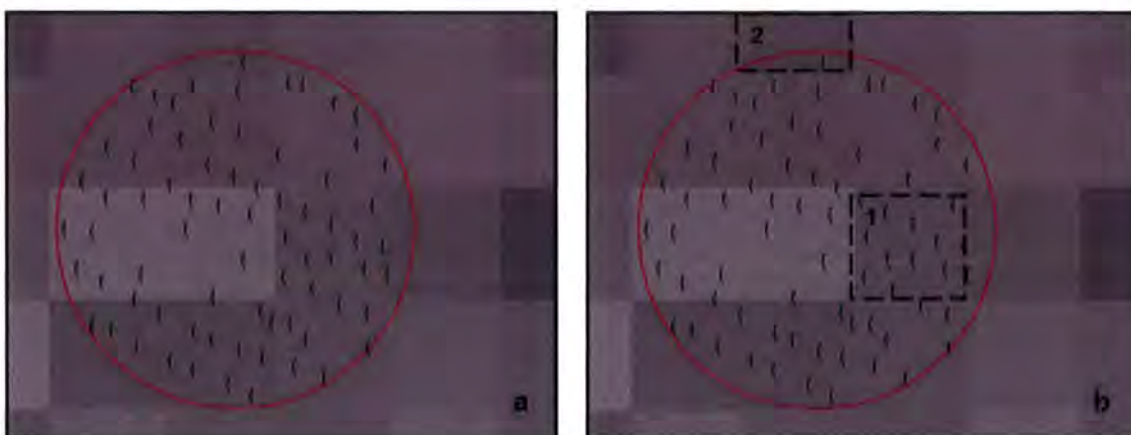
Figure 2.9 (a) Example of overlaying plot and tree locations on mean height growth LiDAR data. (b) Highlighted pixels 1 and 2 demonstrate high and low numbers of trees- important in terms of generating weighted LiDAR plot values.

Furthermore, two averaging methods were also deployed for extraction of LiDAR values at the plot level, ready for comparison with ground truth reference data. The first of these weighted all pixel values falling within the boundaries of each plot by the number of trees falling within that pixel. For example, Figure 2.9b highlights two different pixels. Pixel 1 contains many more trees that pixel 2 and therefore the LiDAR value for that pixel will be weighted much more heavily that that of pixel 2 when computing an average value per plot.

It was anticipated that this may provide an average plot value which better represented the distribution of trees within the plot and thus would correlate better when regressed against height and growth measures obtained in the field. This method is summarised by Equation 1 where t represents the number of trees within the plot and p the pixel value.

$$h_w = \sum_i \frac{t_i p_i}{\sum_i t_i}$$
Equation 1

The second averaging method took the unweighted mean of all pixels falling within the plot area. Pixel values were considered in the calculation of mean plot height or growth regardless of whether the entire pixel fell within the plot boundary or not. In this case, the LiDAR values of pixels 1 and 2 in Figure 2.9 would be considered with equal weight. Plot averages obtained by both these approaches were also inputted into STATA for comparison with ground truth data.

A summary of the LiDAR processing methodology is displayed in Figure 2.10.

```
┌─────────────────────────────────────────────────────────────────────────┐
│                         ┌─────────────────────┐                           │
│                         │   Raw laser points  │                           │
│                         └─────────────────────┘                           │
│                                    │                                       │
│              ┌─────────────────────────────────────────────┐              │
│              │ Filtering of erroneously high and low points │             │
│              └─────────────────────────────────────────────┘              │
│                                    │                                       │
│     ┌───────────────────────────────────────────────────────────────┐     │
│     │ Last returns classified as ground by preset ground classification │  │
│     │  parameters using the embedded TIN densification algorithm      │    │
│     │                      (Axelsson 2000)                            │    │
│     └───────────────────────────────────────────────────────────────┘     │
│                                    │                                       │
│     ┌───────────────────────────────────────────────────────────────┐     │
│     │  Remaining last and first returns lying more than 2m above the  │    │
│     │                 ground are classified as canopy hits            │    │
│     └───────────────────────────────────────────────────────────────┘     │
│                                    │                                       │
│     ┌───────────────────────────────────────────────────────────────┐     │
│     │  Ground surface (DEM) is subtracted from canopy surface (DSM)   │    │
│     │    to give canopy hits a height above ground level (DCHM)       │    │
│     └───────────────────────────────────────────────────────────────┘     │
│                                    │                                       │
│      ┌─────────────────────────────────────────────────────────────┐      │
│      │ Various height metrics extracted from point clouds to a 5m grid │   │
│      └─────────────────────────────────────────────────────────────┘      │
│                                    │                                       │
│            ┌─────────────────────────────────────────────┐                │
│            │  Co-registration of multi-temporal datasets  │               │
│            └─────────────────────────────────────────────┘                │
│                                    │                                       │
│            ┌─────────────────────────────────────────────┐                │
│            │   Difference imaging to obtain growth data    │               │
│            └─────────────────────────────────────────────┘                │
│                                    │                                       │
│     ┌───────────────────────────────────────────────────────────────┐     │
│     │  Extraction of plot and tree-wise LiDAR data: weighted and     │     │
│     │          unweighted variables computed at plot level           │     │
│     └───────────────────────────────────────────────────────────────┘     │
│                                    │                                       │
│     ┌───────────────────────────────────────────────────────────────┐     │
│     │   LiDAR height and growth variables regressed against ground    │    │
│     │                         truth data                              │    │
│     └───────────────────────────────────────────────────────────────┘     │
└─────────────────────────────────────────────────────────────────────────┘
```

Figure 2.10 Summary of the LiDAR processing chain.

2.4   GROUND TRUTHING

The collection of ground truth data is an imperative part of any LiDAR based investigation. When forest mensuration data can be collected and matched accurately to the exact location of each individual tree it can provide a check on the quality of the laser data. Within the literature, many different approaches have been taken to collecting biophysical validation data. Within them all lies a common thread; the strive for accuracy and precision.

A sub-compartment database, supplied by the Forestry Commission, provided data concerning stand ages, species types and yield classes[5]. These data were used in combination with previously acquired forest survey data at known plot and tree locations in Kielder Forest (Watt 2005). Such reference plots are used routinely to sample of trees believed to be representative of the forest structure in any one given forest stand.

The Forestry Commission recommends that in order to be truly representative of forest structure, plot sizes should not be less than 0.01ha. For safety reasons slope angles should not be too great and plots should be easily accessible from forest roads. Furthermore, plots should be spread over a range of different sub-compartments in order that they fully sample the range of age classes and site conditions within the forest.

The ForestSAFE project established and recorded biophysical data for a total of 60 ground reference plots within the 6km[2] study area at Kielder in 2003. These data were used to validate the 2003 LiDAR dataset and set the standard recording procedure for collection of

---

[5] The yield class for any given stand provides a measure of the expected productivity of that stand, given consistent age and species type. Yield classes are derived from empirical models and range from 6 (lowest expected productivity) to 14 (higher expected productivity) for the plots at Kielder assessed here.

ground truth data in 2006. Of the 60 plots measured by the ForestSAFE team in 2003, 22 were re-visited in 2006 (Fig.2.11), of which 11 were again re-surveyed in early 2007 (before the next growing season began). The 22 plots then provided sufficient data from which to quantify growth over the 3 year period. The 11 plots surveyed again in 2007 formed part of this study which will look into ground truth measurement error and is discussed further in Chapter 3.
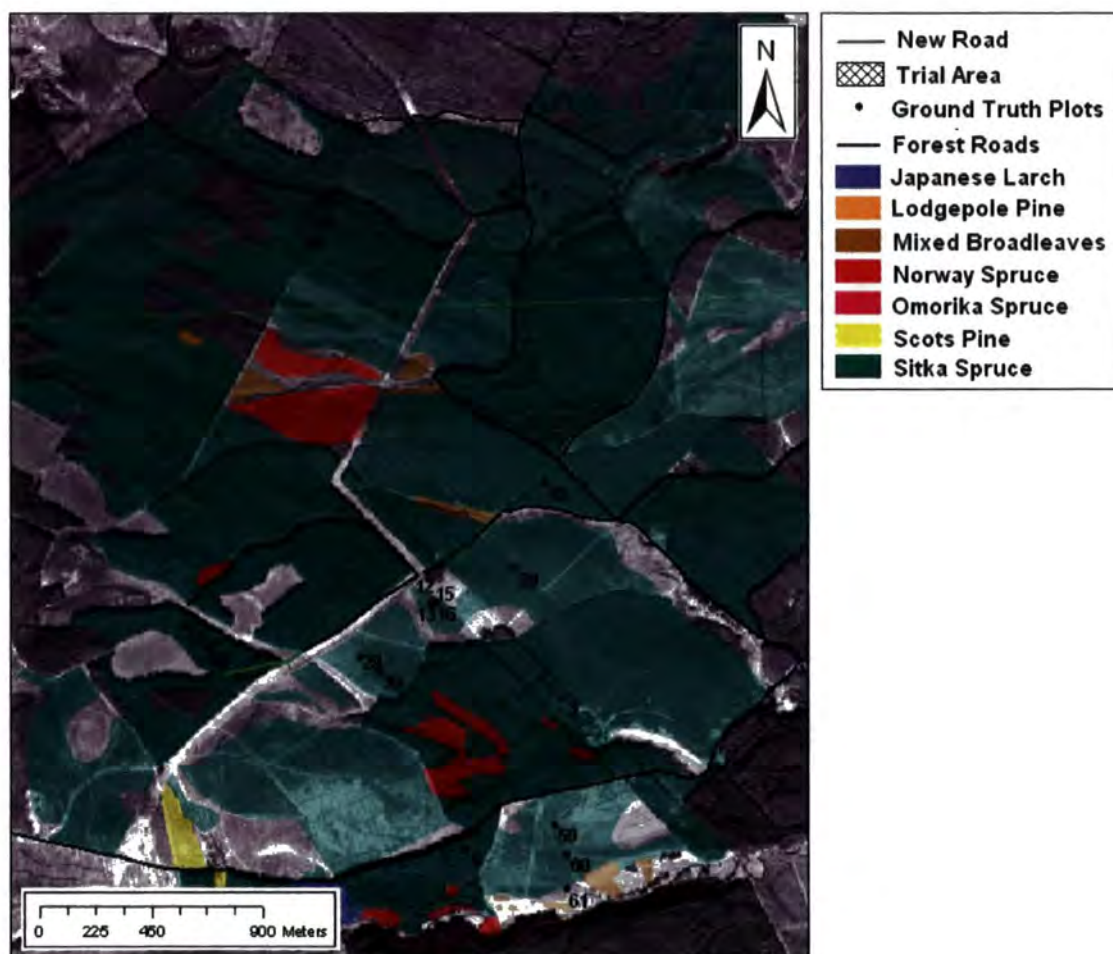
Figure 2.11 The location of the 22 ground validation plots.

The majority of the 22 ground validation plots were 0.02ha in size and followed the conventional circular layout (Fig 2.12a). The plot centre was located with a wooden stake and its location surveyed using a Leica 300 series dGPS. The plot boundary was then determined as 7.98m from this central stake using a Vertex hypsometer as a digital distance measuring device. A couple of plots were set out not as circles but as squares covering 0.01ha (Fig 2.12b). Here each plot corner was marked with a wooden stake and surveyed using the Leica 300 series dGPS. These plots were previously established by Watt (2005) as part of larger 0.16ha squares intended for comparison with the coarser spatial resolution of Landsat data (Watt 2005). Obviously such large plot sizes were not needed here given the finer resolution of LiDAR data. However, given the existence of ground reference data for these square plots from 2003 and 2006 it seemed appropriate to exploit these plots for their height and growth measurements.

All trees which fell within plot boundaries were numbered and marked using plastic clips (for younger trees) or by spraying the trunk with orange paint. The position of each tree was also determined using dGPS. When view of the sky was too heavily obstructed by dense canopies to enable a signal to be obtained, the principles of trigonometry and Pythagoras's theorem were employed using a compass and bearing to locate the tree in relation to the centre of the plot. The positional accuracy of plot centres is expected to be ± 0.05m given a clear view of the sky. However, for trees located using trigonometric measures, a locational accuracy of ± 0.70m is anticipated.
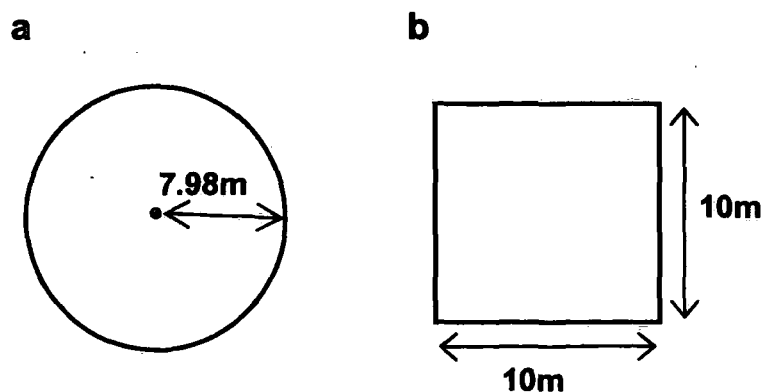
Figure 2.12 Plot layouts: (a) the conventional circular 0.02ha plot and (b) the square 0.01ha plot.

For each plot, a set of biophysical measurements were made and recorded in 2003 (by the ForestSAFE project), 2006 (by a team from Durham University) and in 2007 (by this study). This included the height, diameter, basal area and level of dominance of every tree within the plot boundary.

Under standard forest inventorying procedures only a sample of the entire plot is measured for height however here it was considered necessary that each tree should be surveyed and positioned for comparison with the LiDAR data. All trees taller than 1.37m were measured using a Vertex III hypsometer (Haglöf, Sweden) and those smaller than 1.37m with a tape measure. For those measurements taken under this study special attention was paid to locating the top of very tall trees in dense canopies.

Diameter at breast height[6] (dbh) was also recorded for each tree, using a diameter tape. Measurements were rounded to the nearest half centimetre. Standard practise in measuring dbh dictates that where the ground is sloping, the 1.37m should be measured from the up-

---

[6] Diameter at breast height or dbh is the girth of the tree at 1.37m above the ground.

slope side of the tree. Similarly, when the tree itself is leaning, the measurement should be made from the underside of the tree (Fig.2.13).
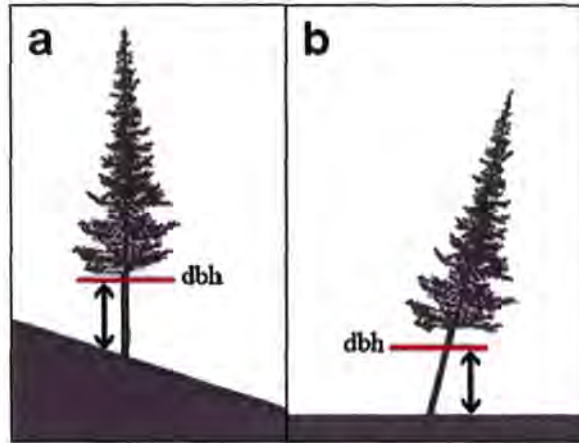
Figure 2.13 Rules of dbh measurement: a) where the tree lies on sloping ground, dbh is measured on the upslope side of the tree; b) where the tree is leaning, dbh is measured on the underside of tree.

Dbh measures were then used as detailed in Equation 2 to calculate tree basal area (m^2).

$$G = \pi \left(\frac{dbh}{200} \right)^2 \qquad\qquad\text{Equation 2}$$

Basal area (G) can then be used to compute Lorey's Mean Height (LMH). This is a plot height average which weights each tree by basal area. The calculation of LMH is displayed in Equation 3, where g is basal area (m^2) and h is tree height (m). It has previously been shown as a useful plot averaging technique for comparison with LiDAR plot averages and thus was calculated for the each of the 22 plots in this study (Næsset 2002; Næsset and Gobakken 2005).

$$h_L = \frac{\sum(gh)}{\sum g}$$

<div style="text-align:right">Equation 3</div>

Tree dominance was also recorded for each tree during ground truthing. This uses a classification scheme developed to categorise trees based on their proximity to the surrounding trees, their crown size and crown light exposure (Bechtold 2003). In this case, five key classes were used as detailed below (Watt 2005). These classes have been represented as a cartoon in Figure 2.14.

A. Dominant: Tree crown sits above height of other tree crowns so that it is exposed to light from above and from the side.

B. Co-Dominant: Tree crown sits at the level of the main canopy, receiving the majority of light from above

C. Sub-Dominant: Tree crown extends into the main canopy, but tree is shorter than dominant and co-dominant trees, receiving very little light from above.

D. Suppressed: Tree crown sits well below height of main canopy therefore receiving no direct light from above or the side.

E. Dead: Tree crown is not live.

Finally, the position of each tree and all its associated data were coded in GIS format. This was necessary for the extraction of LiDAR data at the location of each tree.
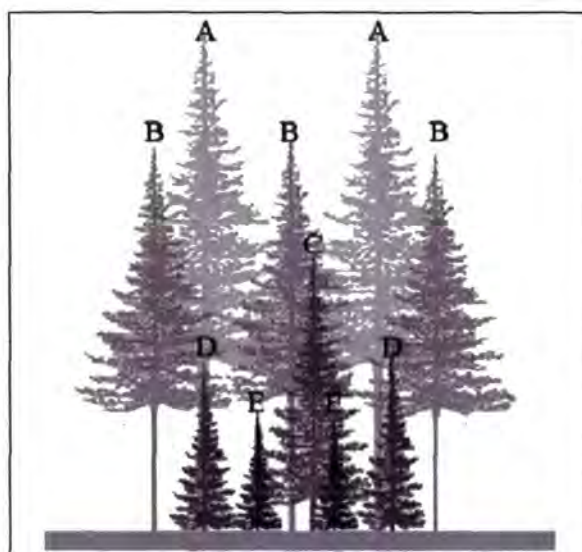
Figure 2.14 Schematic representation of the five levels of tree dominance.

2.5 SUMMARY

This chapter has introduced the study area and LiDAR datasets. The LiDAR processing chain and ground truth data collection were also detailed. The assessment of ground truth error is presented in the following chapter, the results are presented in Chapter 4, analysed in the Chapter 5 and drawn together in the discussion presented in Chapter 6.

3   ASSESSMENT OF GROUND TRUTH ERROR

3.1   AIMS

To date, the reported errors associated with estimating forest growth from LiDAR data have been large (Yu *et al.,* 2004; Yu *et al.,* 2006). Yet the source of this error (LiDAR or ground truth) cannot be determined with any certainty. As a result, much effort has been channelled into developing superior processing techniques and into co-registering the LiDAR and ground truth data as accurately as possible (Means *et al.,* 1999; Pfeifer *et al.,* 1999; Popescu *et al.,* 2002; Naesset 2002; Naesset and Økland 2002; Donoghue *et al.,* 2004; Sithole and Vosselman 2004; Zaksek and Pfeifer 2006; Hyyppä *et al.,* 2005; Watt 2005; Watt and Donoghue 2005; Hollaus *et al.,* 2006; Yu *et al.,* 2006; Kobler *et al.,* 2007; Pfeifer 2007 *pers. comm.*). Very few studies have attempted to quantify precision or bias in ground-based observation. A study by Barron (2001) compared a number of tree height measuring instruments and found the Vertex III to produce precise and unbiased results. However, this study is one of very few and so further assessment remains long overdue. Indeed, St-Onge (1999) acknowledges that in many studies of ALS for tree height estimation, the 'true' height of the trees remains unknown and that *"the accuracy of the laser-predicted heights is evaluated from error ridden ground truth data"* (p.5).

This chapter details the design, implementation and results of an evaluation of a range of height measuring devices undertaken within this project. It is anticipated that this assessment will allow an estimation of the errors associated with ground truthing thereby enabling better estimates of forest growth to be obtained.

3.2   ASSESSMENT DESIGN

The location of the test site for this study was chosen following consultation with the Forestry Commission due to its easy accessibility and because the trees were already scheduled for felling (Woodhouse, *pers. comm.*). Indeed, it was important that the trees could be felled to determine their true height without causing problems for areas of high commercial or environmental value. The study area runs alongside a new forest road as seen in Fig.3.1, sits within the area of ground truth plots and is covered by both LiDAR surveys. The stand has a yield class of 10 and was planted in 1956 with a tree spacing of 1.7m.

Figure 3.1 Close up of the new road and trial area.

A total of fifteen trees were selected to cover a range of different heights and levels of dominance. As a result, the trees were not located in a cluster like they might be in a normal plot layout but were scattered over an area of approximately $250m^2$. Each tree was numbered and marked with orange spray paint. The height at which dbh is measured (1.37m) was also marked in orange as a ring around the trunk (Fig 3.2). This was to enable faster and more consistent measurements of dbh. Each tree was then measured for height

and dbh by nine different people, with varying levels of experience, using three different

height measuring instruments and from two different angles

Figure 3.2 Photograph of the forest and new road, the test site for assessment of ground truth error. The trees surveyed are situated to the left of the road (Photo: A.Woodget 05.06.07).

Figure 3.3 The trial area showing how the tree number and dbh was marked in orange. Field assistant using a tape measure as part of the technique of measuring tree height with a Suunto clinometer (Photo: A. Woodget 05.06.07).

3.2.1 Instrument Effect

In order to assess the effect of error associated with ground truth height measurements devices, three different instruments were compared. These were the Vertex III hypsometer, a Suunto clinometer and tape measure and the LaserAce hypsometer (Fig 3.4). The technical specifications of all these instruments are presented in Table 3.1.

Figure 3.4 The three height measuring devices: (a) Vertex III Hypsometer, (b) LaserAce Hypsometer and (c) Suunto Clinometer.

The Vertex III (Fig 3.4a), manufactured by the Swedish company Haglöf, is widely used for forest mensuration applications. The handset works using ultrasonic communication with an associated T3 transponder unit. The transponder unit is placed at a height of 1.37m on the tree trunk. The user then stands in a position where they can see both transponder and tree top. The vertex is next used to measure the distance between user and transponder with ultrasound (distance d on Fig.3.5). The angles of inclination to the tip of the tree and the transponder are then measured by the embedded digital inclinometer (angle b on Fig 3.5). The height of the tree to the nearest 0.1m is then calculated internally (Equation 4) and the result shown on the handset's digital display.

Vertex Tree Height (m)   Equation 4
$$H_v = 1.37 + h_1 + h_2$$

Where $h_1 = d(\tan a)$

$h_2 = d(\tan b)$

It should also be stressed that it is vital to calibrate the vertex before survey work commences. Humidity, air pressure and temperature have a distorting effect on the range and extension of the ultrasound signal. If calibration using the incorporated temperature sensor is performed regularly then problems incurred by changing atmospheric conditions are minimised. The measurement inaccuracy resulting from a lack of calibration is estimated at 2cm per ^{o}C (www.haglofsweden.com).
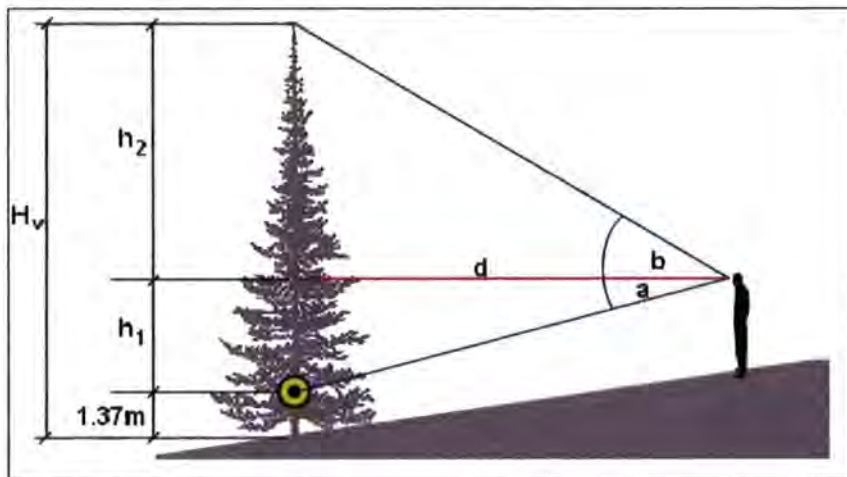
Figure 3.5 The tree height measurement principles of the Vertex III hypsometer. The yellow and black circular device represents the transponder.

The LaserAce hypsometer device (Fig 3.4b) is manufactured by MDL Laser Systems (www.laserace.com) and has been less commonly used than the Vertex III. It uses a laser rangefinder and an inbuilt accelerometer inclinometer to determine distance and angle from

the user's position to both the base and tip of the tree (Fig 3.6). The unit then calculates tree height to the nearest 0.01m and displays the result on the LCD screen. In order to work properly the rangefinder must have a clear line of sight to the tree base and top. If not, the laser will rebound from a closer object (such as branches and stems), causing an incorrect range to be recorded and thus an inaccurate height to be calculated. The LaserAce can measure ranges and calculate tree heights from a distance of up to 150m without using reflective targets. It can also be used to calculate tree diameter and lean angle, however the height measuring function was the only one employed within this study.
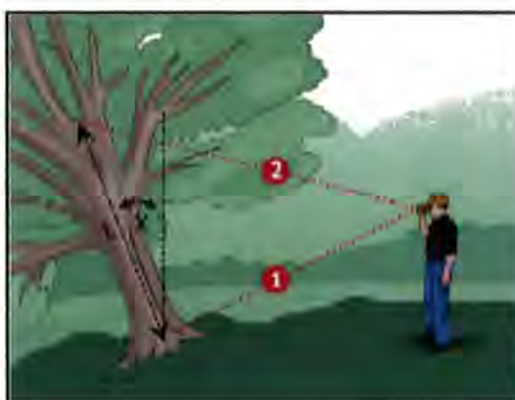
Figure 3.6 The use of the LaserAce Hypsometer. Distances 1 and 2 are determined in order to measure the height or length (L) of the tree (Source: www.laserace.com).

The clinometer (Fig.3.4c) is a widely used instrument, manufactured by the Finnish company Suunto. It can be used not only for measuring the height of distant objects, but also angles and slopes. Unlike the Vertex III and LaserAce, the Suunto clinometer does not feature a rangefinder device and therefore must be used with a tape measure to determine range to the tree. The instrument is first held horizontally. It is then tilted down to the base of the tree at which point the angle of inclination is recorded by the user. It is then tilted upwards to the top of the tree, and the inclination angle also recorded (Fig.3.7). Once these

two angles and the range to the tree is known, tree height may then be calculated in a similar fashion to that employed by the Vertex III (Equation 5).

	Vertex III Hypsometer	LaserAce Hypsometer	Suunto Clinometer
Operating temperature	-15 to +45 °C	-10 to +45 °C	Unknown
Height resolution	0.1m	0.01m	1/40 of the range
Angle range	-60° to +94°	-70° to +70°	-90° to +90°
Angle resolution	0.1°	0.1°	1°

Table 3.1 Technical specifications of height measuring instruments.

Suunto Clinometer Tree Height (m)   Equation 5
$$H_s = h_1 + h_2$$

Where $h_1 = d(\text{Tan } a)$

$h_2 = d(\text{Tan } b)$
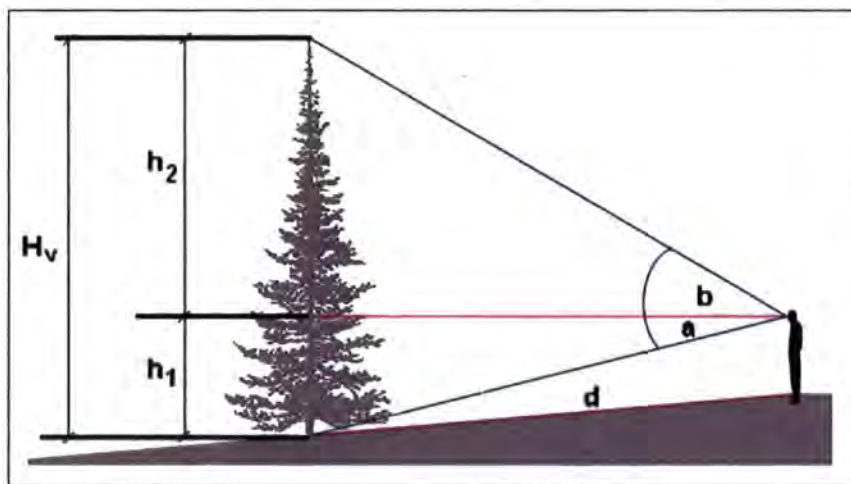
Figure 3.7 The use of the Suunto clinometer for measuring tree height.

3.2.2 Instrument User Effect

The second part of this study aimed to assess what variability can be expected within ground truth measurements due to different users. To achieve this, each person from a total of nine, was asked to survey the height of each of the 15 trees using each of the height measuring devices. The users had varying levels of experience with the devices and of working in forest conditions. They ranged from the totally inexperienced to regular users.

3.2.3 Viewing Angle Effect

The final part of the trial aimed to assess whether an increased amount of error in ground truth measurements could be observed due to viewing angle. The set-up of the study site was well suited to investigate this. Each user was asked to make two height measurements of each tree; one from the new road and one from within the forest itself (Fig. 3.8). The line of sight to the top of the tree was much clearer from the road edge thus allowing a straight forward assessment of instrument and user error. However, those measurements taken from within the forest better simulated normal ground truth plot conditions. As a result, this allowed an assessment of error incurred under normal, operational constraints.
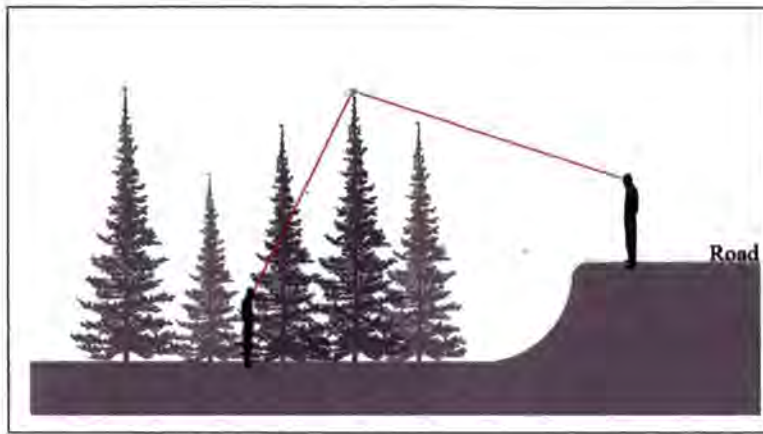
Figure 3.8 Cartoon demonstrating the difference between viewing tree tops from the road (clear line of sight) and from within the forest (sight obstructed by forest foliage).

3.2.4 Plot 3

Further to this trial study, data was also collected from Plot 3 for the purposes of assessing the errors of ground truth validation (See Figure 2.11 for location). This is a pure Sitka spruce plot, planted in 1975 with a yield class of 14 and an average spacing of 2.0m. It is located on a steep slope with an average slope angle of 13.9°. Dominant trees make up 44.8% of the total tree count.

This plot was surveyed during both LiDAR flights and ground data was collected in 2003 and 2006. The stand in which the plot is located was scheduled for felling in spring 2007. Consequently the plot was resurveyed using ground truthing methods in 2007, a week before the felling took place. Once felled, all trees were measured using a tape measure. These datasets provide a unique opportunity to compare LiDAR and ground truth height measures with the felled tree heights. The data from this part of the study is presented in section 3.3.

3.2.5   The 2007 Revisits

Of the 22 plots visited for ground validation purposes in 2003 and 2006, 11 were revisited in 2007. The ground truth data from 2003 and 2006 was taken into the field in 2007. All trees were resurveyed for height using the Vertex and diameter using the diameter tape. The purpose of these revisits was to investigate any tree growth values which seemed dubious from the previous datasets as a means of assessing the accuracy and precision of the ground truth data.

Trees exhibiting anomalous growth were carefully assessed during re-measurement, any peculiarities noted and a dataset of adjusted measurements was created. Peculiarities included broken off stems, tree tops that were very hard to see, species other than Sitka and double and multiple leaders. For example, a tree was recorded as being 14m in 2003, then 11m in 2006 and then 14.2m in 2007. In this scenario it seems obvious that an error was made in the 2006 measurement and thus the new dataset is corrected to display 14.2m for 2006. Despite the fact that a 2007 measurement has been used for 2006 and thus the value is not entirely accurate, it provides a better estimate of the true tree height than the previous measure. In another scenario, when reassessed in 2007 the tree recorded at 14m in 2003 and then 11m in 2006 is found to have a broken stem and is thus again recorded at 11m. In this case, what first seemed a strange negative growth value is logically explained by the tree's condition. Therefore the 2006 value is left at 11m in the new dataset. In a third scenario, a different tree is found to be 17m in 2003 and 21m in 2006. A 4m growth in three years is highly unlikely and thus the tree is resurveyed in 2007 and is found to be 19m. This too seems unusually high so again the tree is surveyed. This time the height is recorded as 22m. The conclusion of this scenario is that the top of the tree is very difficult to identify and

thus measure accurately. This detail is noted and the 2006 measure is left at 21m in the new database.

So for the 11 plots revisited in 2007, two ground truth height datasets are available; first, those values recorded in 2003 and 2006 and second, an adjusted set of values reflecting the findings of the 2007 revisits. Only the first of these datasets is used extensively in comparison with the LiDAR data in the following chapters as it provides full coverage of the 22 ground validation plots. The results of the second dataset are presented in Chapter 3.3 in order make some conclusions concerning the accuracy and precision of ground validation data collected routinely for forest inventorying purposes.

3.3 RESULTS

This subsection presents the results from the investigations into the accuracy and precision of ground truth data collection. Firstly it looks at data collected during the instrument trial near the new forest road. Then it presents the results from felled plot number 3 and finally it looks at the outcome of the revisits to the 11 plots during spring 2007.

3.3.1 Instrument Assessment

This section presents the data collected during the trial study near the new road section at Kielder Forest. For comparing the different instruments, an average tree height was calculated from the 9 different user measurements for each viewing angle. The average values taken from the road are displayed in Table 3.2 and compared graphically in Figure 3.9. The average values taken from the forest are displayed in Table 3.3 and compared graphically in Figure 3.10. From this point onwards, the term 'height error' or h_ε will be used to describe the mean difference between the measured tree height and the felled tree height.

Tree Number	Felled Height	Vertex	Clinometer	LaserAce
1	22.80	21.2	21.6	22.1
2	11.13	12.1	12.6	9.6
3	21.02	19.6	21.2	15.7
4	21.48	21.4	20.6	17.6
5	21.78	21.6	21.4	16.2
6	17.43	17.4	16.9	16.6
7	20.70	20.4	20.3	19.4
8	19.45	19.3	19.0	16.2
9	17.70	17.4	16.7	15.8
10	17.58	17.1	17.3	16.8
11	18.52	18.5	18.3	16.0
12	14.15	13.6	15.4	11.2
13	15.43	15.1	15.4	12.2
14	17.66	17.5	17.8	16.2
15	17.50	16.7	16.6	16.8

Table 3.2 Heights recorded by different instruments as viewed from the road, and felled height.

It can be seen in Figure 3.9 (road viewing angle) that the Vertex and Clinometer measurements sit closer to the x = y line than the LaserAce does, indicating a better measure of felled height. The height errors for the Vertex and Clinometer are as great as about 1.5m, however most of the data points sit within ±1m of the x = y line. In contrast to this, the LaserAce consistently underestimates the true height of the trees, with height error in the range of -0.7 to -5.5m. There appears to be a trend amongst all the instruments to underestimate true height. Indeed, only a small number of data point sit above the x = y line. These observations are reflected in the statistics presented in Table 3.4.
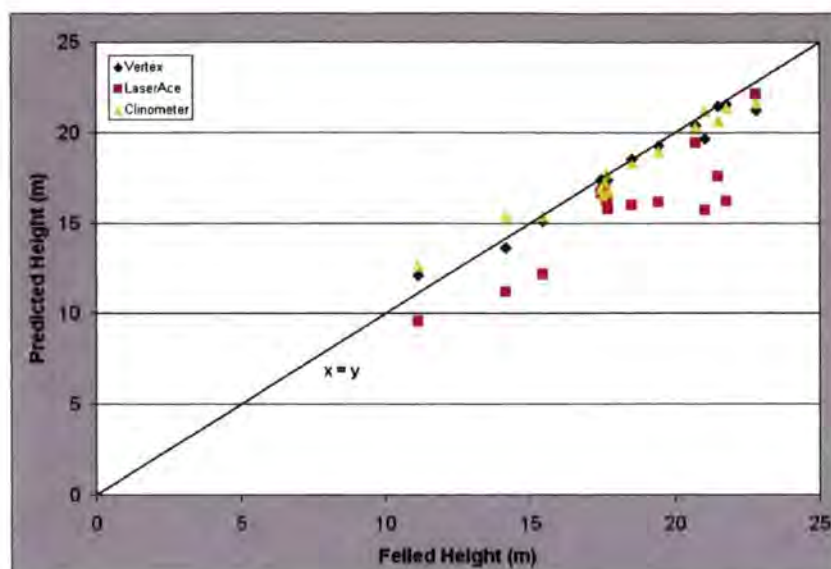
Figure 3.9 Comparison of Average Instrument Tree Heights from the Road.

Tree Number	Felled Height	Vertex	Clinometer	LaserAce
1	22.8	20.9	22.0	11.6
2	11.1	11.4	11.0	9.3
3	21.0	21.4	21.2	12.3
4	21.5	21.0	21.6	11.5
5	21.8	21.8	19.5	13.7
6	17.4	16.7	17.1	10.3
7	20.7	20.4	21.2	10.6
8	19.5	19.1	18.4	10.6
9	17.7	18.1	19.0	10.1
10	17.6	17.9	17.0	9.2
11	18.5	18.1	18.5	8.4
12	14.2	14.5	14.9	7.1
13	15.4	15.6	15.5	8.4
14	17.7	17.8	19.0	8.7
15	17.5	17.3	18.5	10.0

Table 3.3 Heights recorded by different instruments as viewed from the forest, and felled height.

In comparison to this, Figure 3.10 gives the felled height versus predicted heights from the three instruments from the forest viewing angle. It initially seems that data points are more widely spread from the x = y line than for the road viewing angle, especially for the LaserAce. This time, the height error is as great as 1.9m for the Vertex, 2.3m for the

Clinometer and 11.2m for the LaserAce. Thus, it is also evident that the patterns observed

from the road viewing angle remain. The Vertex and Clinometer measurements sit much

closer to the felled height than the LaserAce, as indicated by the mean difference figures in

Table 3.4. The LaserAce continues to underestimate true tree height, but to a much greater

extent than from the road viewing angle. The best height estimates from the LaserAce are

still almost 2m from the true height. Table 3.4 indicates that the strongest association with

felled height data is with the Vertex measurements. The clinometer appears to show least

systematic height error (indicated by the mean differences) but the Vertex consistently

shows the least random error (indicated by the standard deviations) of the three instruments.
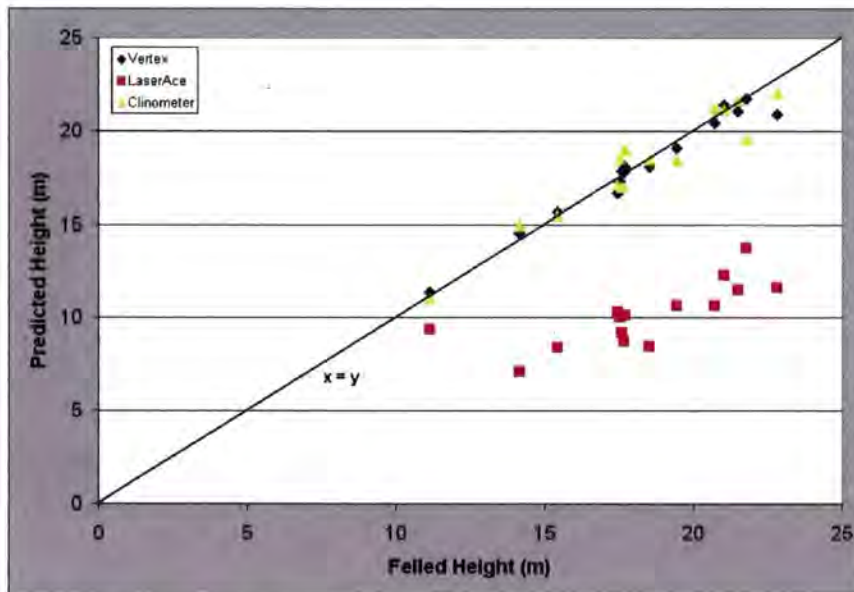
Figure 3.10 Comparison of Average Instrument Tree Heights from the Forest.

Viewing Angle	Instrument	R^2	Equation	Mean difference	Standard Deviation
Road	Vertex	0.971	y = 0.89x + 1.70	-0.4	1.0
	LaserAce	0.745	y = 0.85x + 0.32	-2.4	1.3
	Clinometer	0.959	y = 0.82x + 3.00	-0.2	1.2
Forest	Vertex	0.967	y = 0.90x + 1.72	-0.2	1.4
	LaserAce	0.551	y = 0.40x + 2.72	-8.2	2.0
	Clinometer	0.906	y = 0.90x + 1.99	0.0	1.7

Table 3.4 Statistics for the regression between felled height and Vertex, LaserAce and Clinometer measured heights of trees studied by the trial.

Figure 3.11 takes the Vertex measurements from the road viewing angle and compares the results from the nine different users. The users were separated into three categories depending on their level of experience with the equipment. All experienced users were able to measure tree heights using the Vertex to within 2m of the true height, with most results falling within 1m of the true height. This is indicated by the red triangles which sit close to the x = y line. Users with some experience, shown by the blue squares in Figure 3.11, also mostly managed to measure tree height to within 2m of the true height, with one anomaly. The scatter of points for inexperienced users is greater, with differences from the true tree heights being as great as -5.1m. However, the majority of all measurements fell within 1.5m of true height, regardless of level of experience.
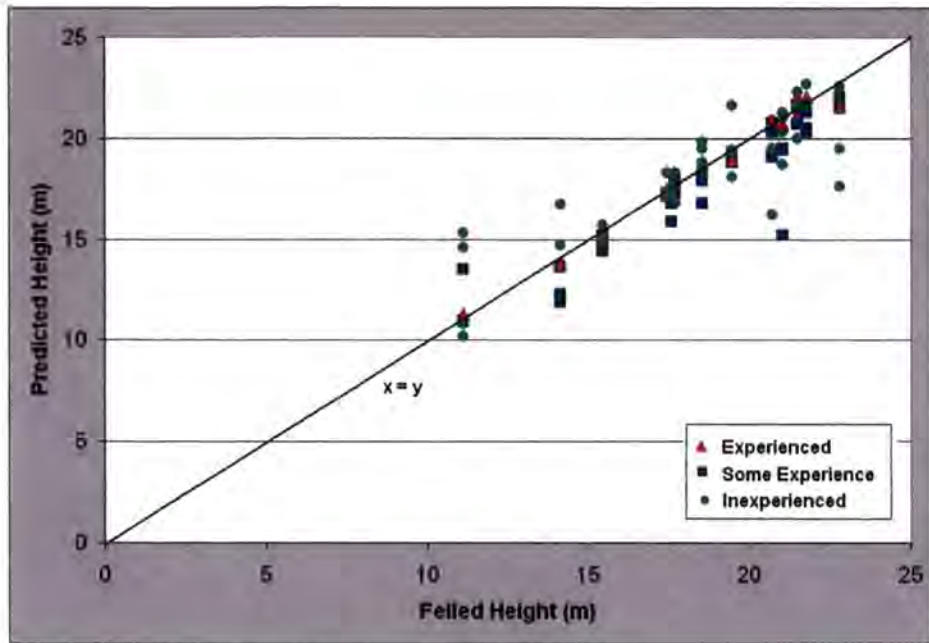
Figure 3.11 Vertex measurements by tree taken from the road view. Users colour coded by level of experience.

Figure 3.12 takes Vertex measurements to compare results from the different users from the forest viewing angle. All experienced users, again indicated by the red triangles, measured all of the trees to within 2m of true height which results in the data points sitting closer to the x = y line than the those for the other users. The measurements taken by users with some experience (blue squares) ranged up to 3.5m from the true height, yet most points fell within 2m. Most measurements by inexperienced users were within 4m of the x = y line but some ranged as much as 6.8m from the felled tree height. Comparing Figure 3.12 with Figure 3.11 it is evident that the measurements taken from forest viewing angle have a greater spread from the x = y line than those taken from the road viewing angle. This visual assessment is consolidated by an average standard deviation figure. This was calculated by computing the standard deviation of the difference from true height measurements for each tree, and then averaging these values. This resulted in a mean standard deviation of 1.0m for the road viewing angle and 1.4m for the forest. The same is also true for the clinometer

and LaserAce, for which the standard deviation values for the road are 1.2m and 1.3m, and for the forest are 1.7m and 2.0m respectively (Table 3.4). This also serves to show that the precision of the Vertex instrument is greater than the clinometer, which is also greater than the LaserAce.
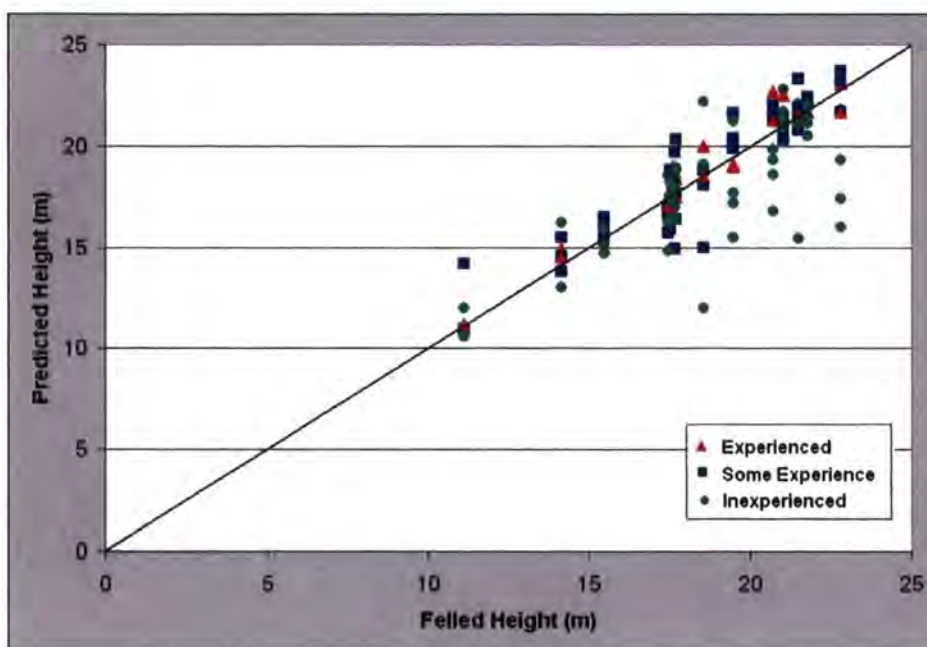
Figure 3.12 Vertex measurements by tree taken from the forest view. Users colour coded by level of experience.

3.3.2 Plot 3 Data

This section presents the 2007 ground truth, 2006 LiDAR and 2007 felled height data collected at plot 3. Figure 3.13 shows the LiDAR and ground truth measures plotted against the measured 2007 felled height. The blue crosses of the 2007 ground truth data better mirror the x = y line than the red points of the 2006 LiDAR data. This indicates that the ground truth data is better able to predict the felled height of the trees within this plot. This is reflected by a co-efficient of determination of $R^2 = 0.87$ for the regression between

ground truth and felled height data. A number of red LiDAR points do fall near the x = y

line, however most fall well below it. This is shown by the mean values displayed in Table

3.5. The R^2 value of 0.001 for the regression between LiDAR and felled height data also

demonstrates the lack of a relationship here. The spread of LiDAR points is greater, with

the height error (difference from the felled height) ranging from -6.1m to 5.5m. In contrast

the height error of ground truth points ranges only from -2.55 to 1.3m. This is also reflected

in the standard deviations for the two datasets, as displayed in Table 3.5.

	Height Error (m)	
	Ground Truth	LiDAR
Max.	1.3	5.5
Min.	-2.55	1.3
Mean	-0.4	-2.5
St. Dev.	0.9	2.5

Table 3.5 Statistics for ground truth and LiDAR differences from felled heights for plot 3.
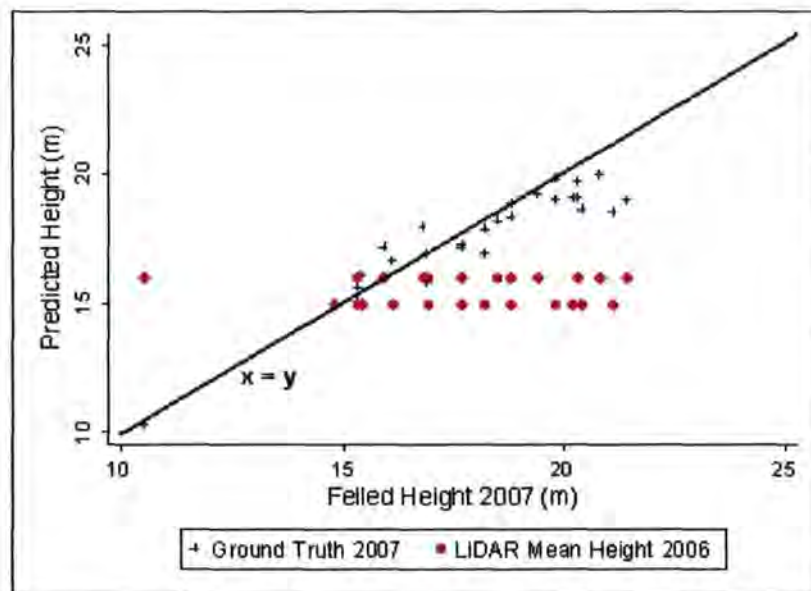
Figure 3.13 Plot 3: 2006 LiDAR and 2007 ground validation data plotted against felled height 2007.

Both the ground truth and LiDAR datasets show an increasing underestimation of felled

height as felled height increases (Fig.3.13). For the ground truth data this demonstrates the

difficulty of measuring taller trees in the field, reflecting the findings of the trial study. For the LiDAR data, this may be a result of the nature of summarising the data into 5m by 5m pixels. Two horizontal lines of data can be clearly observed, reflecting the values of the pixels that fall within the plot boundary. This suggests that this approach may not be a very fair way of comparing the LiDAR with the ground truth and felled height data. The latter two datasets are available at the scale of the individual tree yet the LiDAR data has been summarised into coarser scale pixels. The data might be better compared if the LiDAR data was processed to the single tree level or if data from more plots were available so that plot averages could then be computed and compared. It was not within the scope of this project to delineate single trees and the constraints of working within an operational forest environment meant that felled height data could not be obtained for other plots.

3.3.3 The 2007 Revisits

This section presents the data from the 2007 revisits, where 11 of the 22 ground validation plots were resurveyed and checked for errors. The 11 plots contained a total of 536 trees, of which the heights of only 44 trees were considered to need adjustment for the new dataset. Of these 44 trees, 10 adjustments were made due to obscured tree top effects and 15 due the inaccuracies caused by the presence of double or multiple leaders. The remaining trees were adjusted simply due to recording or measuring inaccuracies in the previous datasets (it is impossible to distinguish which).

Figure 3.14 displays the data organised by type of recording inaccuracy and planting year. The bars represent the percentage of trees planted in a given year which were adjusted due

to some kind of inaccuracy. Note that if one tree height needed adjustment for both an obscured top and double/multiple leader status it was counted twice, as it is not possible to say for certain which was the cause of the recorded inaccuracy.
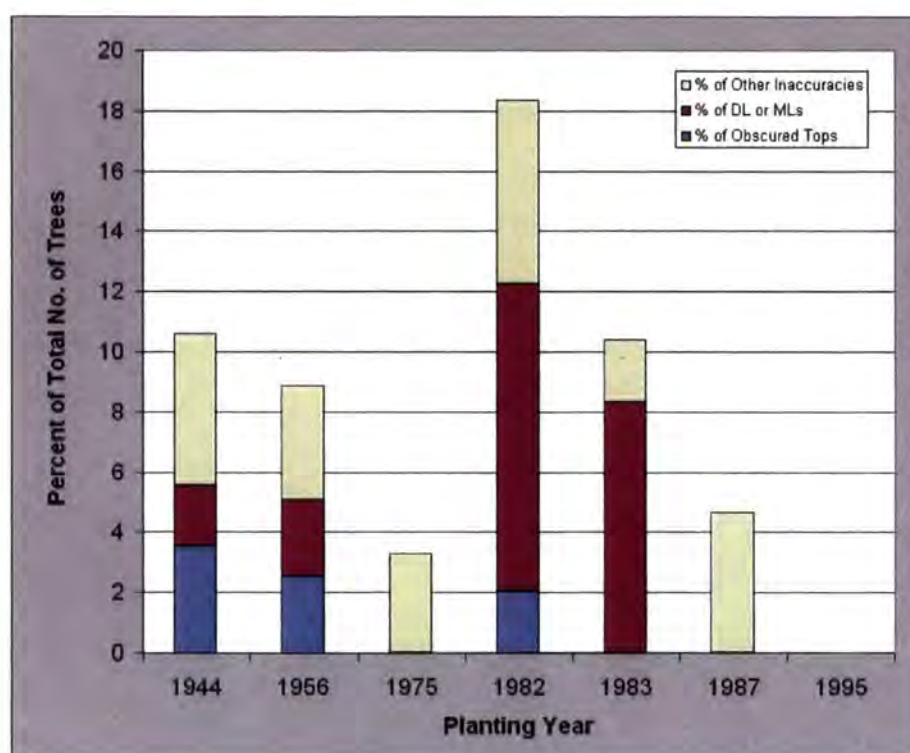
Figure 3.14 A stacked column chart showing the percentage of adjustments made to tree height measurements by type for each planting year (DL and ML refer to double and multiple leaders).

Planting Year	Plots	Total No. of Trees	No. of Adjusted Trees	% of Adjusted Trees	No. of Obscured Tops	% of Obscured Tops	No. of DL or MLs	% of DL or MLs	No. of Other Errors	% of Other Errors
1944	62, 63, 64	198	19	9.60	7	3.54	4	2.02	10	5.05
1956	52, 53	79	7	8.86	2	2.53	2	2.53	3	3.80
1975	3, 4	61	2	3.28	0	0.00	0	0.00	2	3.28
1982	2	49	8	16.33	1	2.04	5	10.20	3	6.12
1983	54	48	5	10.42	0	0.00	4	8.33	1	2.08
1987	10	43	2	4.65	0	0.00	0	0.00	2	4.65
1995	29	58	0	0.00	0	0.00	0	0.00	0	0.00

Table 3.6 Numbers and percentages of trees adjusted under the 2007 revisits, by planting year.

The greatest number of adjustments were made to those trees planted in 1944 (Table 3.6- fourth column from left) and the least of those planted in 1995. However, when looked at as percentages of the total tree count, the greatest percentage of adjustments were made to trees planted in 1982 and the least to those planted in 1995. There does not appear to be a trend of percent of adjustments made with planting year. Although, the percentage of trees adjusted due to obscured tops does seem to decrease with planting year. However there is no trend observed for adjustments made due to double or multiple leaders or other inaccuracies.

Many of the trees revisited in 2007 had obscured tops or were double or multiple leaders and yet their heights did not need adjusting. Given this, as well as the fairly low percentages displayed in Figure 3.14 it is concluded that the 2007 revisits indicate few problems with the ground truth data, or at least that any measuring issues are consistent.

3.4   SUMMARY

This chapter has detailed the approach to the assessment of ground truth error and has presented the resulting data. This included data from plot 3 and the 2007 revisits. These results are analysed and discussed further in Chapters 5 and 6.

4 RESULTS

This chapter presents results from the LiDAR processing and ground truthing. Interpretation and analysis of the results are presented in Chapter 5 and drawn together in the discussion presented in Chapter 6.

4.1 LiDAR

Within this subsection results are presented from the LiDAR processing. This includes the DEMs and associated issues, height and growth maps and the LiDAR data extracted at the ground validation plot locations.

4.1.1 Digital Elevation Models

4.1.1.1 The DEM Gaps

The ground classification procedure used to create the DEMs from the laser point cloud initially tested a window size of 60m x 60m and an iteration distance of 1.4m. The resultant DEM from these parameters is shown in Figure 4.1c. Figure 4.1a is a panchromatic IKONOS image to give context to this small subset of the data. Figure 4.1b presents the count of ground returns for the same area. The black areas on the DEM (Fig.4.1c) indicate areas of no data and occur as a result of a lack of ground returns. This then also causes a gap in the canopy height map for this area, as displayed in Figure 4.2a and 4.2b.
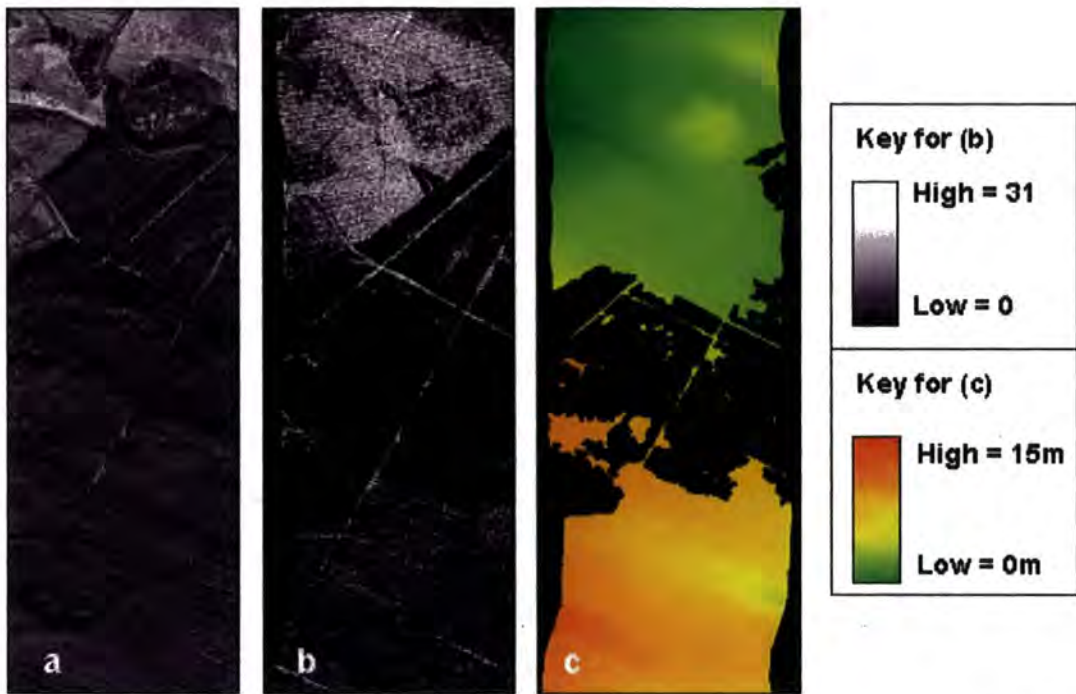
Figure 4.1 The DEM hole issue displayed using 2006 LiDAR data. Image a is a panchromatic IKONOS image. Image b shows the ground return count. Image c shows the resultant DEM.

In order to address this, a window size of 200m x 200m was tested which resulted in the DEM shown in Figure 4.2c and the canopy height map shown in 4.2d. It is evident that this larger window size allowed the holes to be interpolated over, as described in Chapter 2.3.3. However, this also leads to some points being falsely classified as ground. This is evident in Figure 4.2c where elements of the canopy structure appear visible in the DEM.
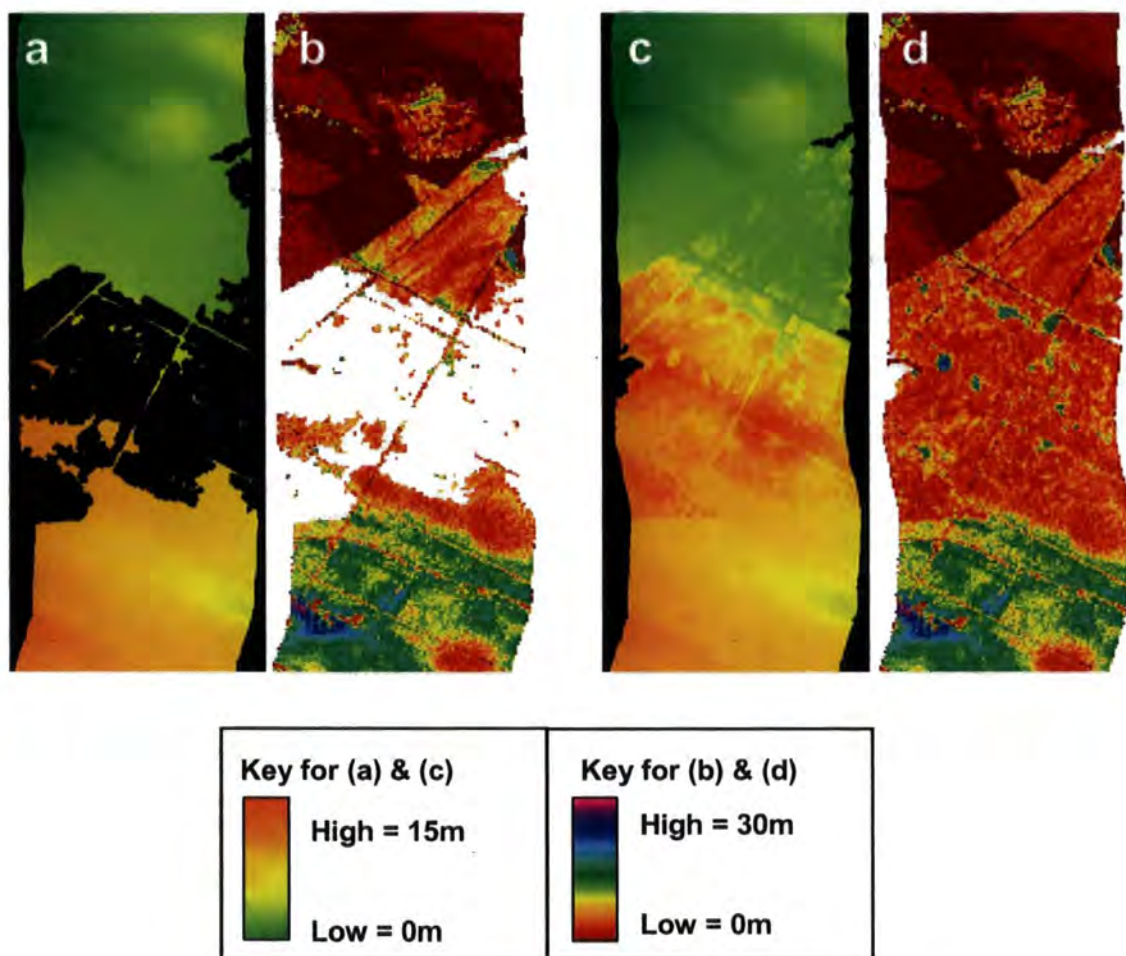
Figure 4.2 The effects of changing window size on a subsection of the 2006 data. Images A (DEM 2006) and B (CHM 2006) have been created with a 60m x 60m window size. Images C (DEM 2006) and D (CHM 2006) have been created using a 200m x 200m window size.

A final window size of 60m x 60m and an iteration distance of 0.5m produced the DEM and canopy height map very close to those shown in Figure 4.2a and 4.2b. Using these ground classification parameters some gaps do remain. However, this is necessary in order to make the DEM as accurate as possible. It also helps highlight the problem of creating DEMs in areas of very dense canopies.

4.1.1.2   2003 and 2006 DEMs

The DEMs displayed in Figure 4.3 have been created by outputting all 'ground' classified points from TerraScan into ArcMap as XY points. These were then used to create a TIN which was next converted into a raster image. This acts to interpolate over the DEM holes observed in Figure 4.2a and 4.2b and allows easier comparison of the dual time series datasets. The holes remain in the data used to create the canopy height models however and can be seen in Figure 4.11. The scale on the DEMs in Figure 4.3 ranges from the lowest areas in black to the highest in white. However, note that the block-like white patches represent areas of no data due to gaps between the data strips.
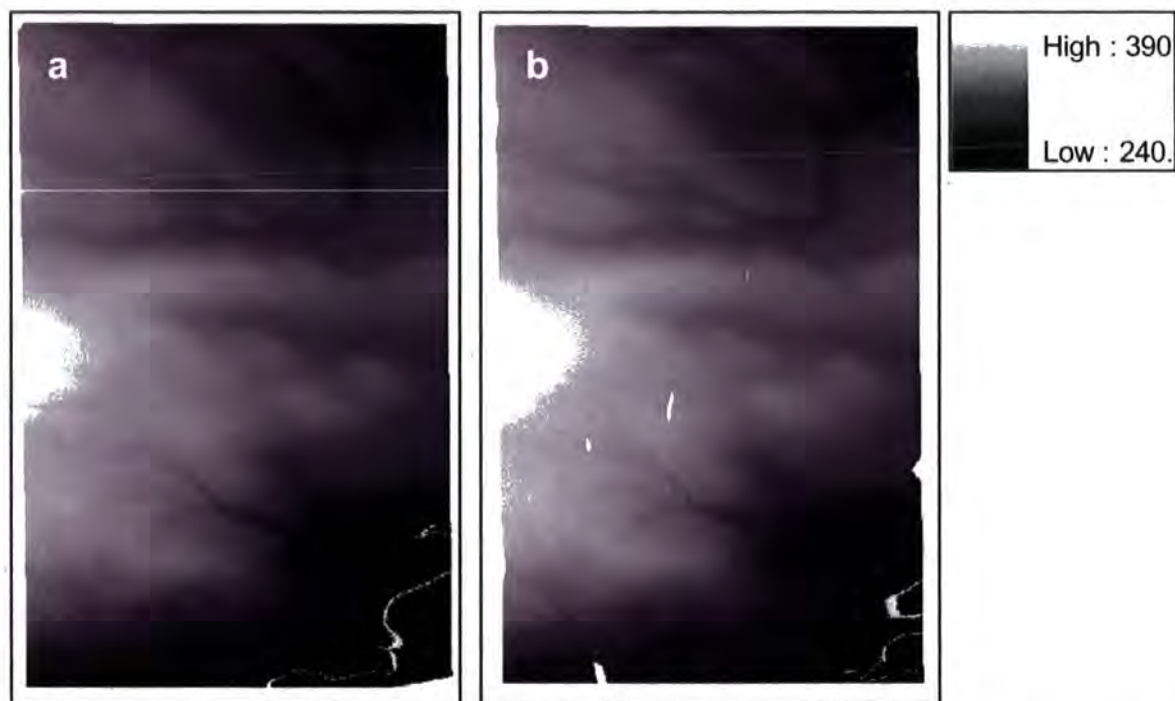
Figure 4.3 DEMs for a) 2003 and b) 2006 (Units are meters). The white areas represent gaps in the data. Each image is roughly 2km across by 3km high.

4.1.1.3 Comparison of DEMs

A subtle difference in tone is visible between the two DEMs in Figure 4.3. Spatial subtraction of the 2003 DEM from the 2006 DEM allowed further assessment of their similarity, as shown by Figure 4.4. The separate 2003 horizontal and 2006 vertical flight lines have become evident on this image. The differences between the two DEMs range from 1.14m to 16.00m. It would be expected that the two DEMs should be very similar, however, this range of difference values suggests otherwise. The histogram for this image (Fig.4.5) gives a mean difference of 7.17m. Given that the standard deviation for this mean difference is only 0.6m it is suggested that this mean difference represents a systematic offset of 7.17m. Consequently 7.17m was subtracted from all 2006 DEM values to shift the histogram to a mean difference of 0.00m.

This 7.17m offset is also evident in Figure 4.7 where the differences between the DEMs have been plotted against 2003 DEM values. Furthermore, the differences between the DEMs seem to have a greater spread at lower 2003 DEM elevations (Fig 4.6). Figure 4.7 shows the before and after adjustment scatter graphs for 2006 DEM values plotted against 2003 DEM values.
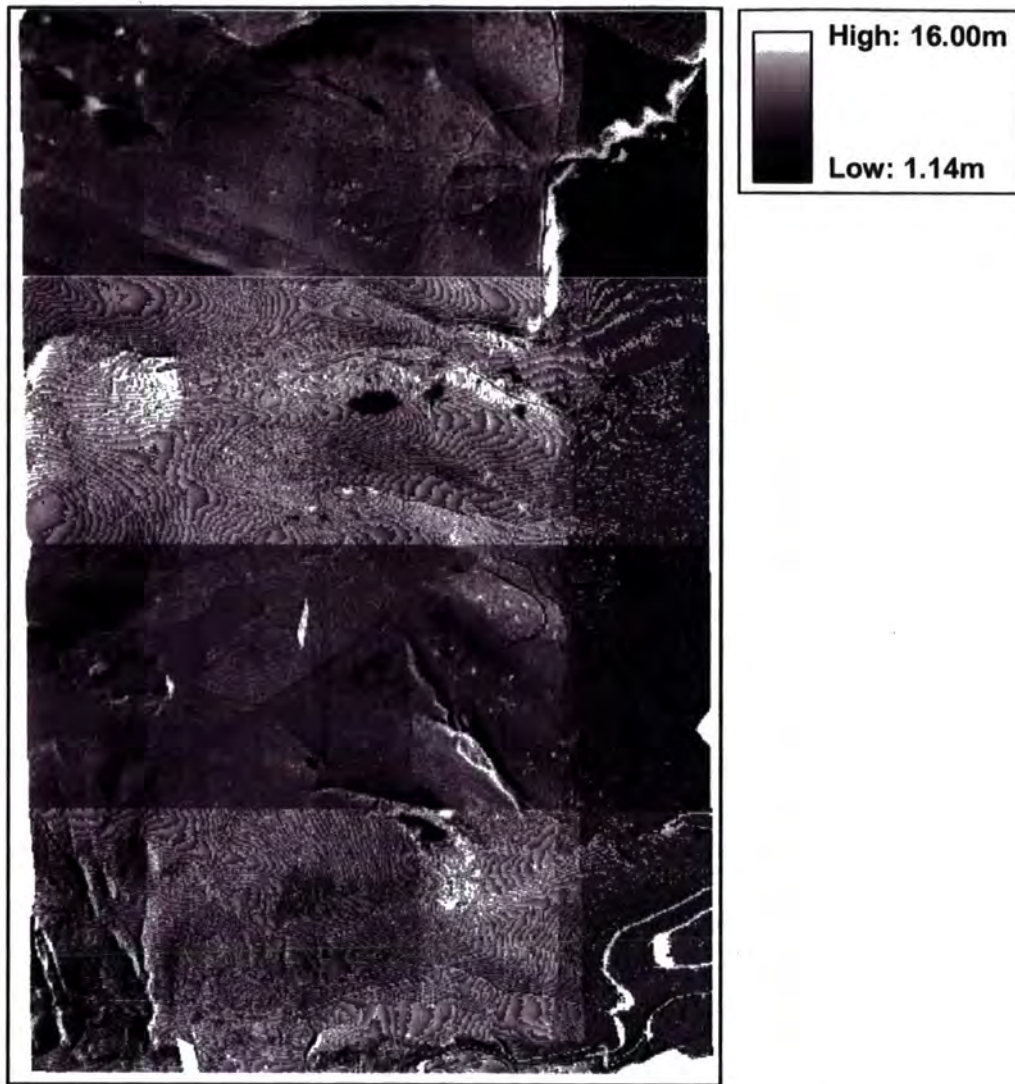
Figure 4.4 DEM difference image (2006 DEM minus 2003 DEM). The image covers an area roughly 2km across by 3km high.
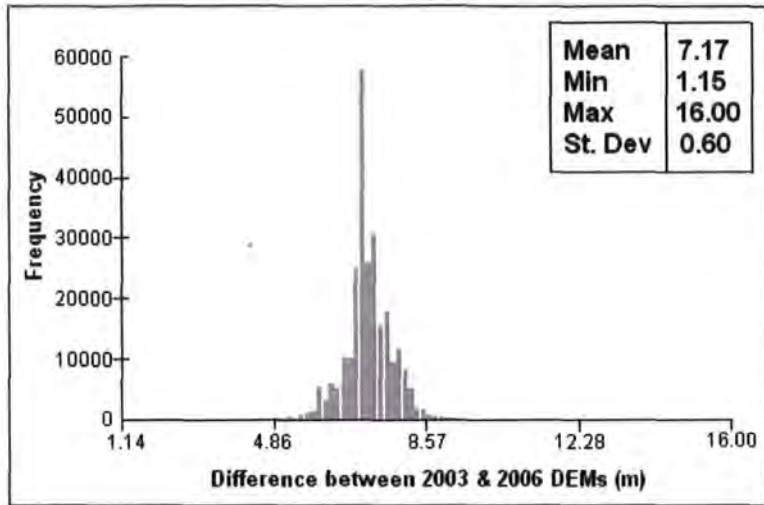
Figure 4.5 Histogram of DEM differences before 2006 DEM adjustment.
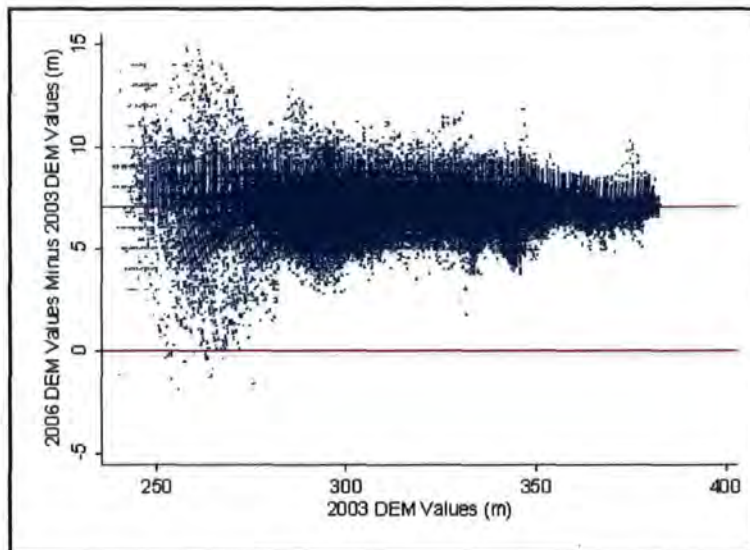
Figure 4.6 Scatter graph showing difference between 2006 and 2003 DEM values plotted against 2003 DEM values.
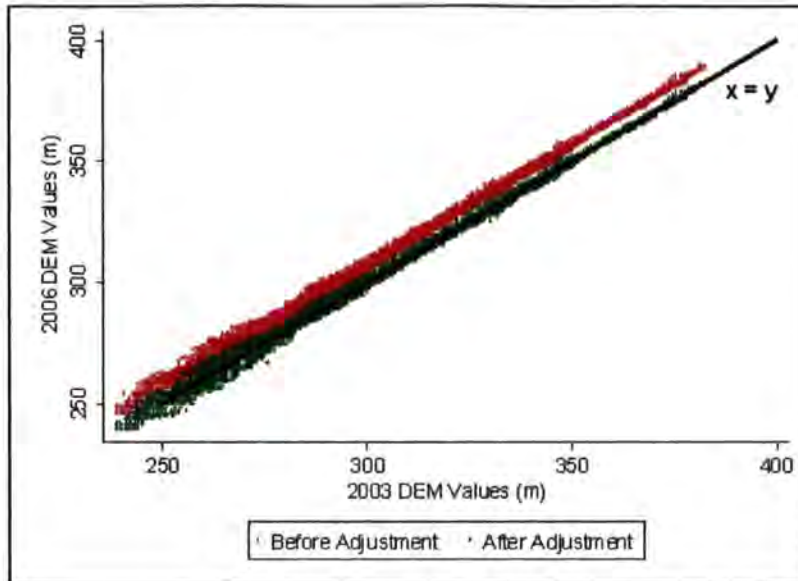
Figure 4.7 Scatter graph showing 2006 DEM values plotted against 2003 DEM values before and after adjustment of the 2006 DEM.

4.1.1.4 Flight line Comparisons (2006 data)

The DEMs for ALS flight lines acquired in 2006 were also compared in areas of overlap. The results are displayed in Figure 4.8. Height differences between the flight lines range from 0m to 6.75m. Some areas of high difference appear to be situated in areas of steep terrain, such a river channels. This is also evident in Figure 4.9 where the 2006 DEM is shown in 3D.
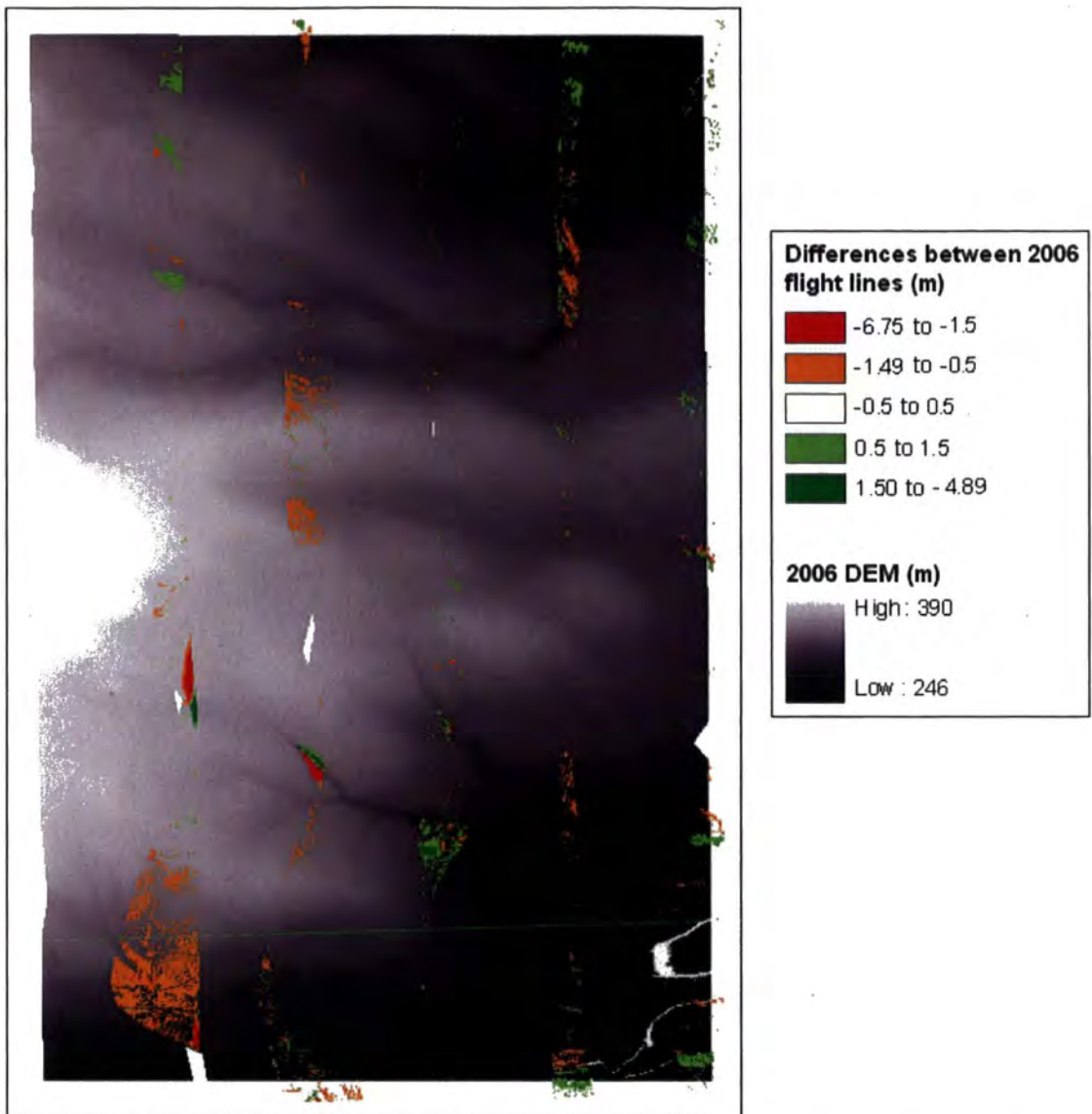
Figure 4.8 Difference betweens 2006 DEM flight lines overlain on the 2006 DEM. (Note: the values between -0.5 and 0.5 for the differences between the DEM flight lines has been set to transparent).
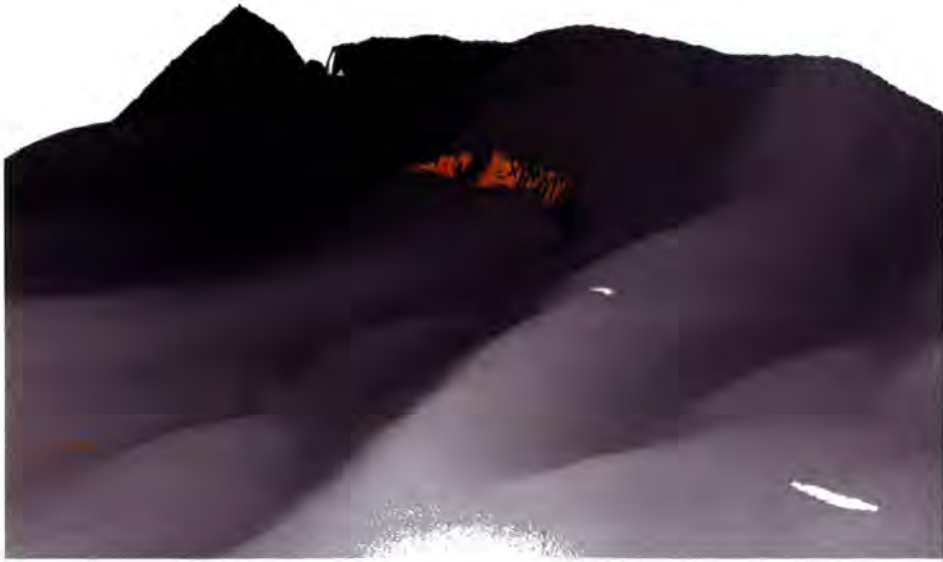
Figure 4.9 3D representation of the 2006 DEM (height exaggerated by a factor of 5) overlain with differences between individual flight lines. See Figure 4.8 for legend. White patches represent areas of no data.

4.1.2 Height Maps

Figures 4.10 and 4.11 display the 2003 and 2006 mean LiDAR height data which has been gridded into 5m by 5m pixels. The very dark blue areas represent bare earth. The gradient of colour from blue through green and up to orange indicates different canopy heights. The 2003 canopy heights are as great as 33.55m, whereas the 2006 heights reach as great as 34.00m. On both images, there are sometimes differences in canopy height within single stands. Furthermore, rides and forest planting compartments can also be picked out. Areas which have been clear-felled within the three year period are present on the 2003 image, but not on the 2006. Such areas are easily identifiable on the growth maps presented in the following section. Height maps were also available for all other height metrics, though they are not displayed here.
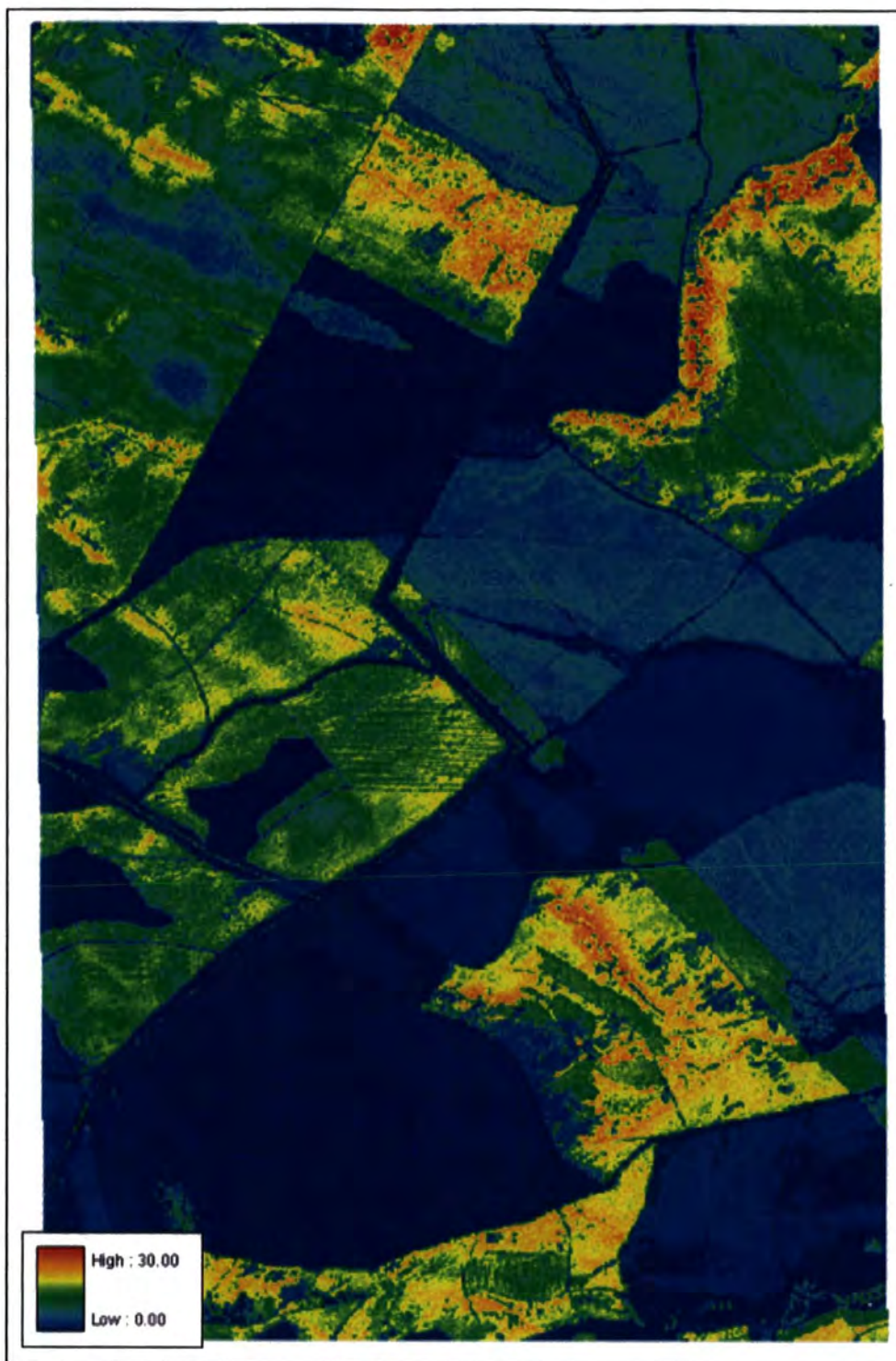
Figure 4.10 Mean Height 2003 derived from LiDAR data, gridded into 5m x 5m pixels.
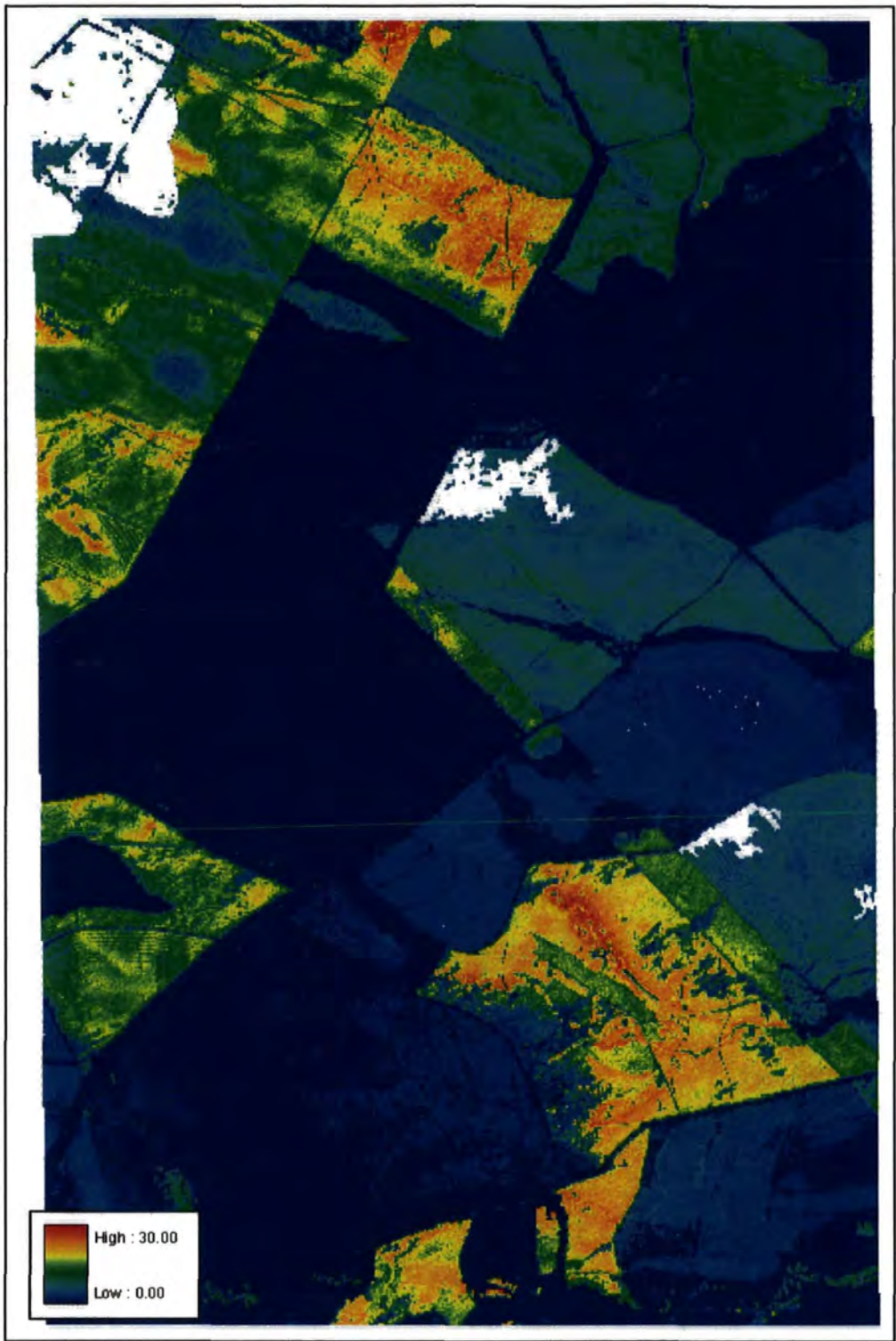
Figure 4.11 Mean Height 2006 derived from LiDAR data, gridded into 5m x 5m pixels.

4.1.3 Growth Maps

Difference imaging allowed the creation of growth maps from the canopy height data. Before correction of the position of the 2006 imagery, the offset between the datasets caused edge effects on the resulting growth map (Fig.4.12a). These were removed by realigning the datasets to give the growth map displayed in Figure 4.12b. The white patches on this image indicate those problem areas from the 2006 DEMs which were left in to illustrate the problems caused by areas of dense canopy. The dark areas have exhibited negative growth over the three year period and correspond to areas of clear-fell and windblow.

Figure 4.13 shows the 2003 canopy heights data plotted against 2006 canopy height data (each point represents one pixel). It is evident that most points have experienced positive change. However, a significant number of points fall below the red line, indicating negative change. When investigated where these pixels fell on the image they included those areas which have been clear-felled, subject to windblow and some along forest planting boundaries. Whilst negative change is to be expected in areas of felling and windblow, it is not so expected along stand boundaries. This suggests that some minor edge effects remain and that the offset has not quite been completely corrected.
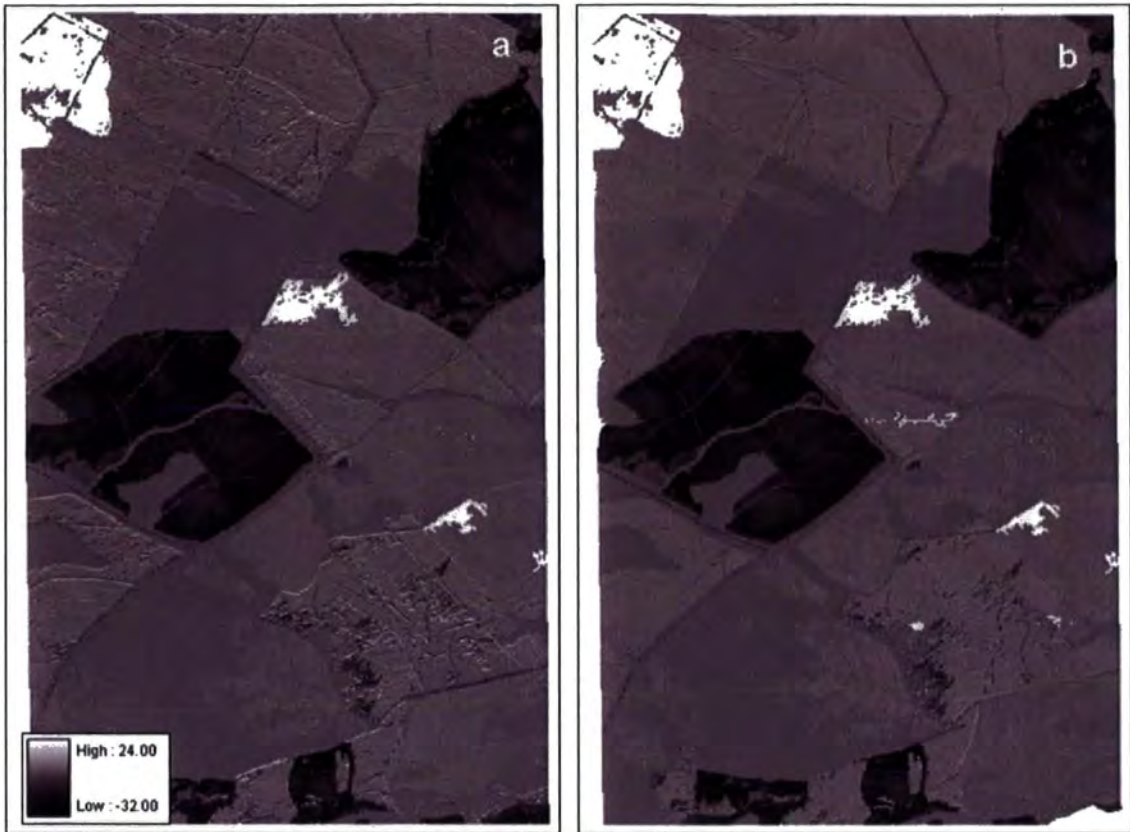
Figure 4.12 Before (a) and after (b) correction of the offset, difference images for mean height. Large white patches indicate problem zones due to DEM gaps. Darker areas exhibiting negative growth are areas of clearfell and windblow. The grayscale bar is the same for both images. Each image is roughly 2km across by 3km high.
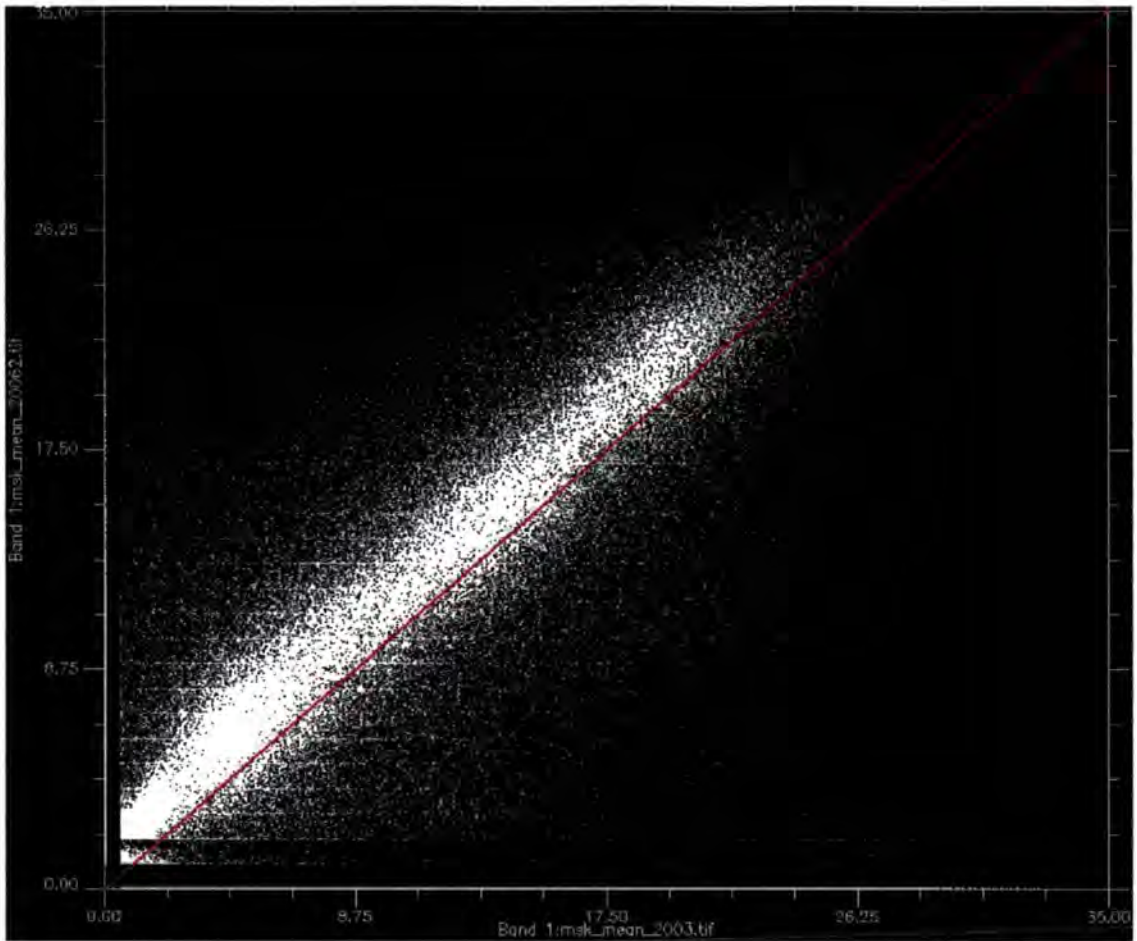
Figure 4.13 Mean LiDAR height 2003 (x axis) plotted against mean LiDAR height 2006 (y axis). The red line represents x = y.

4.1.4 Height and Growth at Plot Locations

A key part of this study is to compare LiDAR with ground truth data collected at specific locations. Thus, this section presents the LiDAR results at the locations of the ground truth plots. Table 4.1 details the average weighted and unweighted LiDAR results for each of the 22 ground validation plots. Growth is evident for all plots, using both the weighted and unweighted LiDAR plot height averages[7]. However, the weighted measure appears to make

---

[7] The weighted average is a LiDAR plot average where pixels have been weighted by the number of trees which fall within them. See section 2.3.9 for details.

little difference when compared to the unweighted measure of average LiDAR height at plot locations.

Plot ID	Tree Count	Weighted LiDAR Heights (m)			Unweighted LiDAR Heights (m)		
		2003	2006	Growth	2003	2006	Growth
2	49	9.33	12.55	3.22	9.29	12.50	3.22
3	29	12.97	15.52	2.55	12.97	15.52	2.55
4	32	12.66	15.05	2.39	12.66	15.05	2.40
5	69	19.86	21.88	2.02	19.44	21.88	2.44
10	41	5.74	7.84	2.10	5.16	7.84	2.67
12	31	2.00	2.82	0.82	2.00	2.83	0.83
13	34	2.00	2.83	0.83	2.00	2.83	0.83
15.	34	2.00	2.83	0.83	2.00	2.83	0.83
16	24	2.00	2.92	0.92	2.00	2.91	0.91
28	244	1.13	2.22	1.09	1.13	2.23	1.10
29	58	0.93	2.60	1.67	0.93	2.60	1.67
30	45	0.87	2.56	1.69	0.89	2.57	1.68
52	34	13.91	16.50	2.59	13.94	16.60	2.66
53	45	13.20	15.68	2.48	13.22	15.70	2.48
54	48	4.73	8.48	3.75	4.73	6.61	1.89
55	37	4.62	6.44	1.82	4.62	6.44	1.82
59	75	2.49	2.93	0.44	1.89	2.93	1.04
60	48	2.66	3.36	0.70	2.00	3.36	1.36
61	49	2.24	2.67	0.43	1.88	2.67	0.78
62	61	12.38	14.14	1.76	12.39	14.15	1.75
63	72	14.89	16.87	1.98	14.86	16.87	2.01
64	65	13.87	15.55	1.68	13.88	15.58	1.70

Table 4.1 LiDAR plot averages.

The data contained in Table 4.2, subdivided according to age class, show the means and standard deviations of some key LiDAR height growth metrics. The following age classes were used:

- **Mature:** planted in or before 1970.

- **Middle-Aged:** planted between 1971 and 1989.

- **Young**: planted in 1990 or after.

Unweighted averages were first calculated for each metric of every plot. Then the age-class average was computed for each metric using the average plot values for all plots falling within that age class. Similarly, the standard deviation of all values for each metric per plot was calculated and then an age-class average computed for each metric.

Growth Metric	Mature		Middle-Aged		Young	
	Mean	St. Dev.	Mean	St. Dev.	Mean	St. Dev.
mean	2.10	0.65	2.33	0.48	0.94	0.54
max	0.86	0.91	1.28	0.65	1.21	0.77
p10	1.91	0.95	2.53	0.86	0.38	0.54
p50	1.90	0.58	2.20	0.58	0.73	0.59
p90	1.54	0.79	2.50	0.70	1.49	0.73

Table 4.2 Mean and standard deviations of growth metrics ordered by plot age class. The mean is an average of all plot means for any given height metric within a single age class. The standard deviation is an average of all mean plot standard deviations for any given height metric within a single age class. The unit for all figures is metres (m).

It is evident that middle-aged plots always exhibit the greatest amount of growth in all the metrics considered here. This growth is as great as 2.53m for the 10th height percentile and as small as 1.28m for maximum height growth. The young plots always show the least amount of growth, except for the maximum height metric for which the mature plots have experienced least growth. For the young plots this growth ranges from as little as 0.38m for the 10th percentile to 1.21m for the maximum height metric. For the mature plots, growth ranges from 0.86m for maximum height growth to 2.10m for mean height growth.

The mature plots always exhibit the greatest standard deviation of these growth measures, with the exception of the 50th height growth percentile for which the standard deviation for

the young plots is greater by 0.01m. The lowest standard deviations are mostly observed for the middle-aged plots, however it is lowest for young plots for the 10th percentile and joint lowest between middle-aged and mature for the 50th height growth percentile. The precision and accuracy of these results are discussed in Chapters 5 and 6, alongside the ground truth data which is presented in the next section of this Chapter.

4.2 GROUND TRUTH DATA

This section presents the plot based ground validation data in Tables 4.3 and 4.4 and Figures 4.14 to 4.17. This data is compared with the plot based results from the LiDAR processing in Chapter 5.

Plot ID	Tree Count	Stems per hectare	Planting Year	Lorey's Mean Height (m)			Unweighted Mean Height			Maximum Height			Minimum Height		
				2003	2006	Growth	2003	2006	Growth	2003	2006	Growth	2003	2006	Growth
2	49	2450	1982	14.03	13.77	-0.26	13.10	12.80	-0.30	16.50	16.00	-0.50	7.80	7.60	-0.20
3	29	1450	1975	16.43	17.92	1.49	15.40	16.60	1.20	18.50	19.80	1.30	5.90	5.10	-0.80
4	32	1600	1975	16.17	17.33	1.16	14.70	15.60	0.90	17.90	19.90	2.00	5.70	6.10	0.40
5	71	3550	1955	20.59	20.12	-0.47	16.04	15.63	-0.41	25.90	26.40	0.50	4.00	4.10	0.10
10	43	2150	1987	9.41	10.31	0.91	7.70	8.54	0.84	13.70	11.6	-2.10	2.70	3.00	0.30
12	33	1650	1994	3.34	5.19	1.85	2.91	4.57	1.65	4.10	7.40	3.30	0.70	1.30	0.60
13	36	1800	1994	3.23	4.71	1.48	2.86	4.31	1.45	4.20	6.00	1.80	0.90	1.80	0.90
15	36	1800	1994	3.41	4.78	1.37	2.82	4.16	1.35	4.50	6.50	2.00	0.50	1.40	0.90
16	26	1300	1994	3.44	5.61	2.17	3.16	5.13	1.97	4.00	7.30	3.30	1.50	2.60	1.10
28	246	12300	1994	0.00	3.19	3.19	1.81	2.19	0.39	4.60	5.50	0.90	0.40	0.50	0.10
29	58	2900	1995	0.00	4.58	4.58	2.80	4.00	1.20	5.00	6.30	1.30	0.60	1.40	0.80
30	45	2250	1995	0.00	4.81	4.81	2.70	4.30	1.60	4.00	6.20	2.20	1.00	2.00	1.00
52	34	1700	1956	18.66	18.35	-0.31	14.88	14.53	-0.35	23.80	25.60	1.80	5.20	3.80	-1.40
53	45	2250	1956	15.64	15.89	0.25	13.07	13.21	0.14	19.80	20.60	0.80	3.50	3.40	-0.10
54	48	2400	1983	7.60	7.98	0.38	5.40	5.80	0.40	9.20	9.80	0.60	0.50	0.50	0.00
55	37	1850	1983	8.03	8.31	0.28	7.10	7.30	0.20	10.70	12.30	1.60	0.90	0.60	-0.30
59	77	3850	1992	0.00	5.31	5.31	3.51	4.18	0.67	6.00	7.70	1.70	0.80	0.33	-0.47
60	50	2500	1992	0.00	6.79	6.79	4.16	5.35	1.18	6.60	9.20	2.60	0.35	0.50	0.15
61	51	2550	1992	0.00	5.48	5.48	3.25	4.22	0.97	5.90	6.90	1.00	0.50	0.40	-0.10
62	61	3050	1944	15.23	15.11	-0.12	12.20	12.10	-0.10	19.40	20.70	1.30	2.70	0.70	-2.00
63	72	3600	1944	16.41	16.29	-0.12	13.30	13.00	-0.30	20.70	20.60	-0.10	3.00	2.30	-0.70
64	65	3250	1944	16.01	15.73	-0.27	14.50	14.20	-0.30	19.30	19.60	0.30	6.30	6.10	-0.20

Table 4.3 Ground validation data from 22 plots.

Note: Lorey's Mean Height and Unweighted Mean Height are plot averages.

Plot ID	Planting Year	Percent of Dominant Trees	Tree Spacing	Yield Class	Yield Model Expected Values		
					2003	2006	Growth
2	1982	67.3	2.0	12	7.8	9.5	1.7
3	1975	44.8	2.0	14	13.0	14.7	1.7
4	1975	62.5	2.0	14	13.0	14.7	1.7
5	1955	29.6	1.7	14	22.5	23.6	1.1
10	1987	62.8	2.0	12	5.0	7.3	2.3
12	1994	78.1	2.0	14	3.0	4.0	1.0
13	1994	83.3	2.0	14	3.0	4.0	1.0
15	1994	*	2.0	14	3.0	4.0	1.0
16	1994	*	2.0	14	3.0	4.0	1.0
28	1994	28.5	2.0	14	3.0	4.0	1.0
29	1995	70.7	2.0	12	2.0	3.0	1.0
30	1995	82.2	2.0	12	2.0	3.0	1.0
52	1956	44.1	1.7	10	17.8	18.8	1.0
53	1956	28.9	1.7	10	17.8	18.8	1.0
54	1983	58.3	2.0	12	7.3	8.9	1.6
55	1983	75.7	2.0	12	7.3	8.9	1.6
59	1992	27.0	2.0	12	3.0	4.5	1.5
60	1992	64.0	2.0	12	3.0	4.5	1.5
61	1992	60.8	*	*	*	*	*
62	1944	37.7	1.7	6	15.6	16.5	0.9
63	1944	29.2	1.7	6	15.6	16.5	0.9
64	1944	40.0	1.7	6	15.6	16.5	0.9

Table 4.4 Further ground validation plot data, including information concerning yield classes and yield modelled growth. * = No data available.
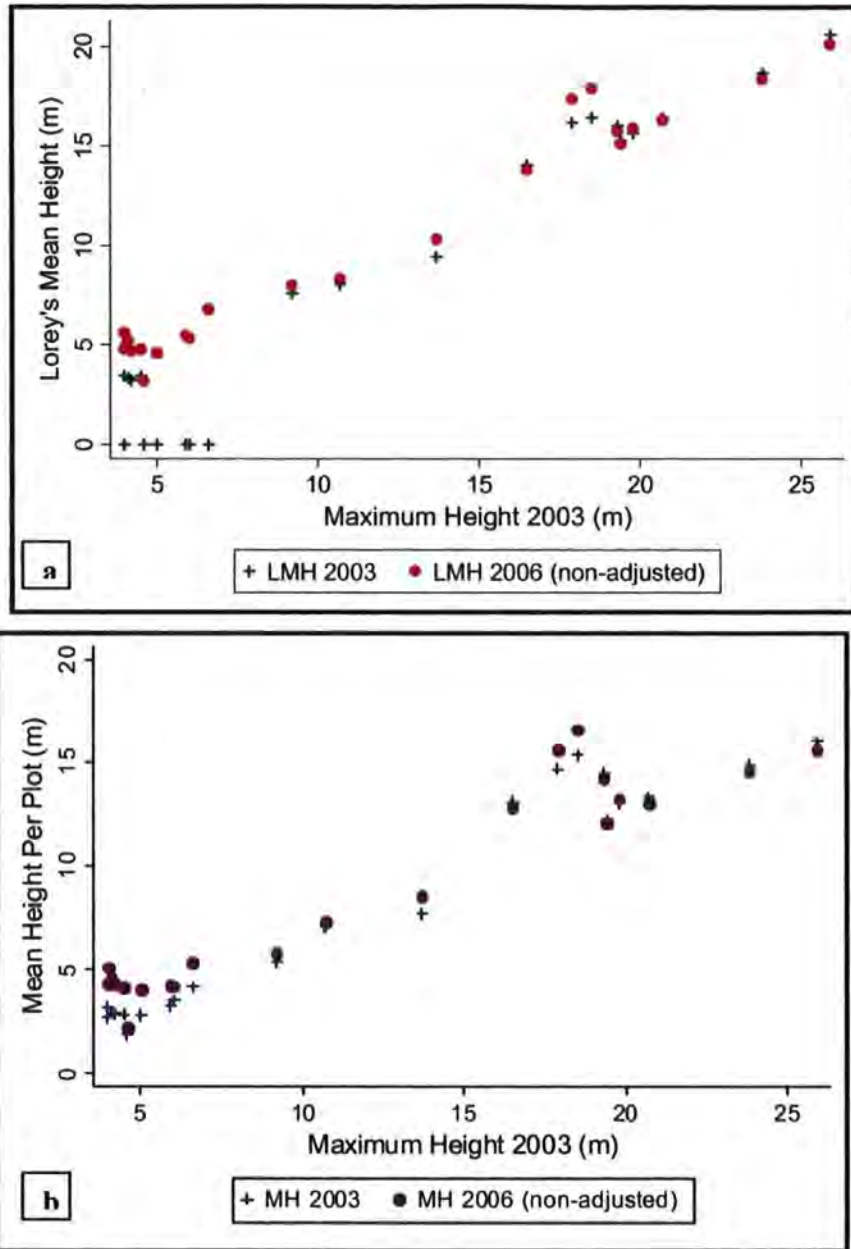
Figure 4.14 a) Lorey's Mean Height data and b) Mean Height data per plot from 2003 and 2006 (non-adjusted data) plotted against Maximum Height data from 2003.

The graphs presented within this chapter are intended as a means of exploring the ground truth data, before it is analysed in comparison with the LiDAR data in the following chapter.

Figures 4.14a and b use the data displayed in Table 4.3 to investigate the relationship of maximum plot heights from 2003 with Lorey's Mean Heights and Mean Heights from the two years. In Figure 4.14a the majority of LMH 2006 data points fall above the equivalent values for 2003, thereby indicating average plot growth. The only exceptions are a few plots which lie in the area of 17-20m of maximum height 2003. The magnitude of the difference between equivalent 2003 and 2006 values gives a measure of growth per plot. Sometimes this is large, as shown by the plot sitting at approximately 7m maximum height for 2003 (Fig 4.14a). Conversely, some plots show little difference between 2003 and 2006 LMH, as shown by those plots sitting around the 20m maximum height 2003 mark. Both the 2003 and 2006 LMH data are strongly correlated with maximum heights from 2003, producing co-efficients of 0.94 and 0.96 respectively.

The 2003 and 2006 mean heights, as displayed in Figure 4.14b show a similar pattern to LMHs. They too show a strong correlation to maximum height 2003 with co-efficients of 0.95 for 2003 and 0.91 for 2006. Again, the majority of 2006 data points fall above those for 2003 indicating average plot growth. The few exceptions, like for LMH, occur only for those plots which had a maximum height greater than 20m in 2003. The differences between the 2003 and 2006 data points are more consistent for mean height than they are more LMH. This is due to the cluster of 2003 data points sitting at less than 8m maximum height (2003) for which the mean height average is significantly greater than the equivalent LMH measures for the same plots. This is clearly shown in Figure 4.16 where the mean height data points all sit below 2m, whereas the LMH data points stretch up to and above 6m.

Figure 4.15 indicates how maximum height varies with plot age. It is possible to apply a linear fit to this data with a resulting correlation co-efficient of 0.8. However, it is also possibly to identify more of a curve. The data seems to show a decline in maximum height between those stands planted in the mid-1950s and the mid-1940s, however it is likely that this is a function of fewer sampling of older plots and/or the lower yield class of the older plots.
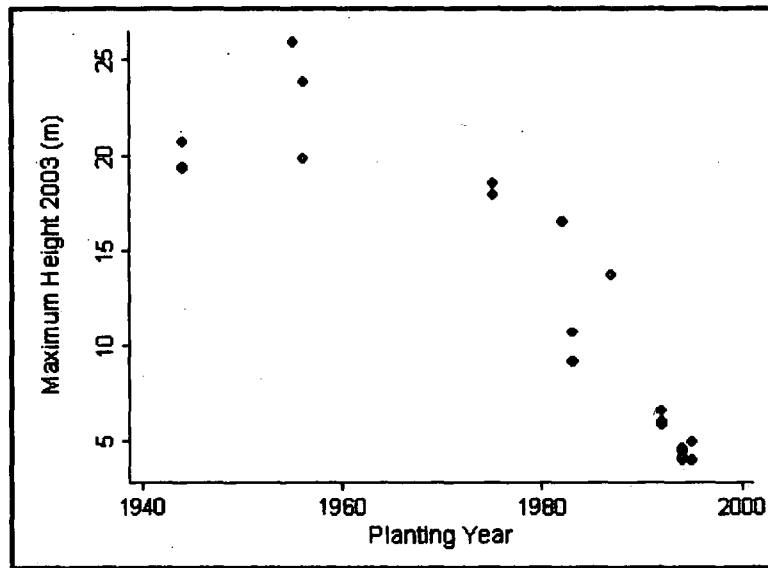
Figure 4.15 Maximum Height 2003 per plot, plotted against Planting Year.
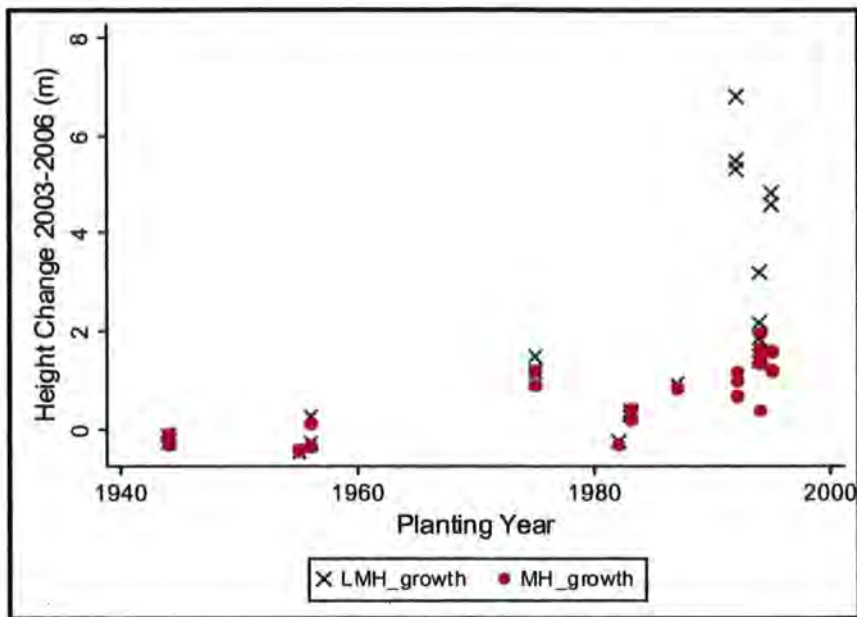
Figure 4.16 Change in height between 2003 and 2006 for plot LMH and MH values, by planting year.

Figure 4.16 uses the differences between 2003 and 2006 plot averages (LMH and MH) and compares them with plot planting year. Given the strong correlations between LMH and MH and maximum height 2003, and between maximum height 2003 and planting year, we might expect a similarly strong relationship here. However, they are not so strong. The correlation between LMH height change 2003-2006 and planting year is weak at $R^2 = 0.45$. The relationship is stronger between MH difference between 2003 and 2006 with an R^2 of 0.61. It is evident from Figure 4.16 that the height change values for LMH and MH are very similar for those plots planted before 1990. However, large differences seem to occur for younger plots planted in the 1990s where the values for LMH change are much greater. A number of negative growth points exist for both LMH and MH change. The majority of these points are for plots planted earlier than 1960, however negative average plot growth is recorded for one plot planted in 1982.

Figure 4.17 displays the same LMH and MH height change values as Figure 4.16, however this time they have been plotted against maximum plot heights from 2006. Here, the large differences between LMH and MH change are again observed for the younger plots which sit at less than 9m on the max height 2006 scale. All other data points show very little or no difference between LMH and MH change. Again the relationship between MH change with max height 2006 is stronger at $R^2 = 0.54$ than for LMH change which is $R^2 = 0.46$. Note that the relationship between MH change with max height 2006 is weaker than that with planting year, however it is slightly higher for LMH. The negative growth points can again be seen for both LMH and MH change. However, here the 1982 anomaly is not so obvious. Instead it can be seen that such negative change only occurs for plots with a maximum height of greater than 15m in 2006.
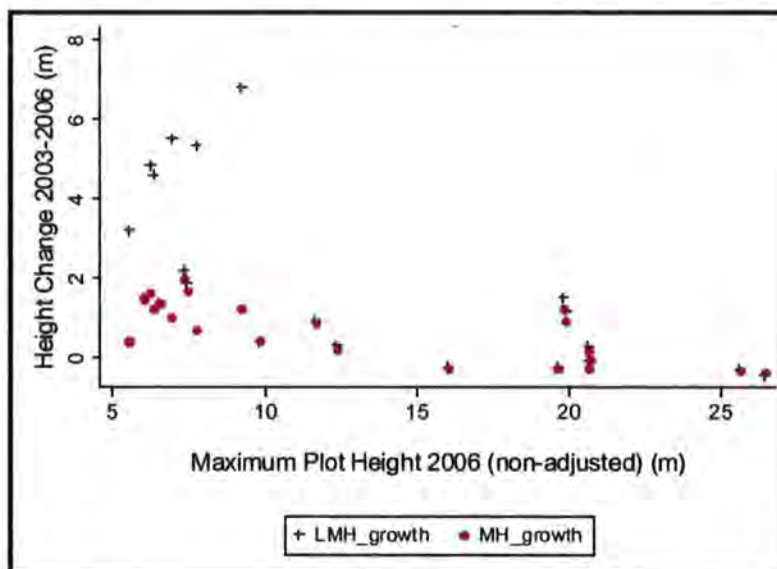
Figure 4.17 Height change between 2003 and 2006 for LMH and MH, plotted against Maximum Plot Height (not adjusted) from 2006.

94

Having explored the nature of the ground truth data collected in 2003 and 2006, this data will be analysed in line with the aims and research questions of this study in Chapter 5: Data Analysis.

4.3 SUMMARY

This section has presented results in the form of data tables, graphs and images. Firstly, from the LiDAR processing, including the presentation and comparison of DEMs, height maps and growth maps. Secondly, from the ground validation including data collected in 2003 and 2006 and plot based averages. The data from this section will next be subject to analysis in Chapter 5 and further interpretation and discussion in Chapter 6.

5 DATA ANALYSIS

This chapter aims to provide a bridge between the results and discussion chapters. In doing so, the data presented in Chapters 3 and 4 will be analysed and interpreted in four key sections. Firstly, the detection of growth using LiDAR will be looked into. Secondly, the LiDAR height and growth estimates will be compared with that obtained by ground truthing at both the plot and individual tree level. Following this, the ground truth error assessment data will be studied with a view to anticipating its effects on the relationship between LiDAR and ground truth growth. Lastly, a number of interactions between the LiDAR system and the field will be addressed with a specific aim to assess the impact these interactions may have on the relationship between LiDAR and ground truth data at different spatial scales. Chapter 6 will then bring together these elements to discuss the estimation of forest growth at Kielder using airborne LiDAR.

5.1 DETECTING FOREST GROWTH USING LiDAR

The first research question of this project asked whether forest growth could be detected at Kielder using airborne laser data collected three years apart. The results presented in Chapter 4.1 and in Figure 5.1 suggest that growth has been detected at the locations of all 22 validation plots. Furthermore, the growth map (Fig.4.12b) demonstrates how areas of positive stand level growth and of negative growth in the form of clear-felling and windblow can be detected.
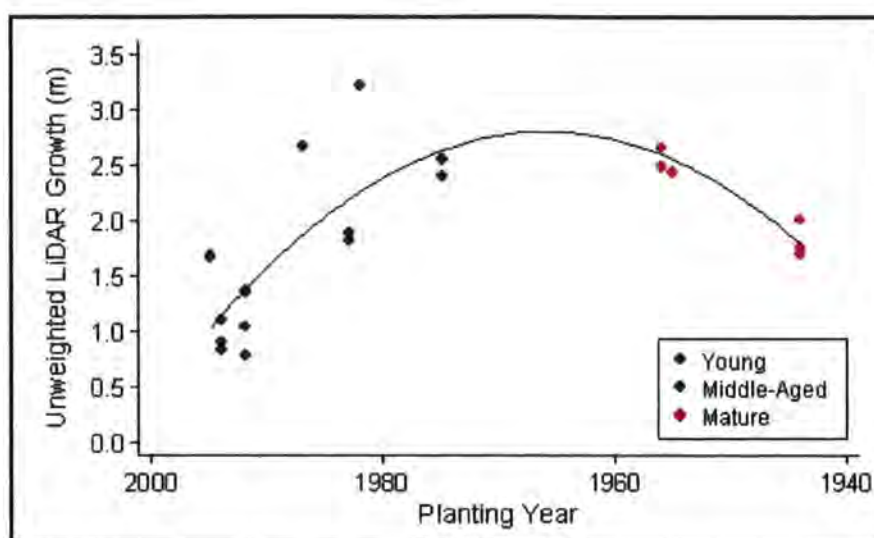
Figure 5.1 Unweighted LiDAR growth plotted against planting year, by plot and age class.

When subdivided into age classes it becomes evident that middle-aged plots exhibit the greatest amount of growth, in terms of both an unweighted average (Fig.5.1) and across a range of height growth metrics; mean, max, p10, p50 and p90. This growth is greatest for the lowest height growth percentile at 2.53m, and lowest for the maximum height metric at 1.28m. Growth is lowest for those plots categorised as young and in between for those classified as mature. This trend, as shown by the black line added onto Figure 5.1 matches that anticipated by the pattern of volume increment for an even-aged stand (Fig.5.2). Here it is evident that younger plots must be a decade or so old before they are featured on this graph. From 10-20 years old, they gain volume rapidly. Many of the plots within the young age class were planted in the early to mid 1990's and so, by this model, between 2003 and 2006 were just beginning to gain volume. However, those in the middle-age category lie well within the region of rapid volume increase and therefore too seem to show the most rapid growth. The volume increment for the mature plots levels off and then declines

thereby supporting a lesser growth rate than middle-aged plots, yet greater than the young plots.
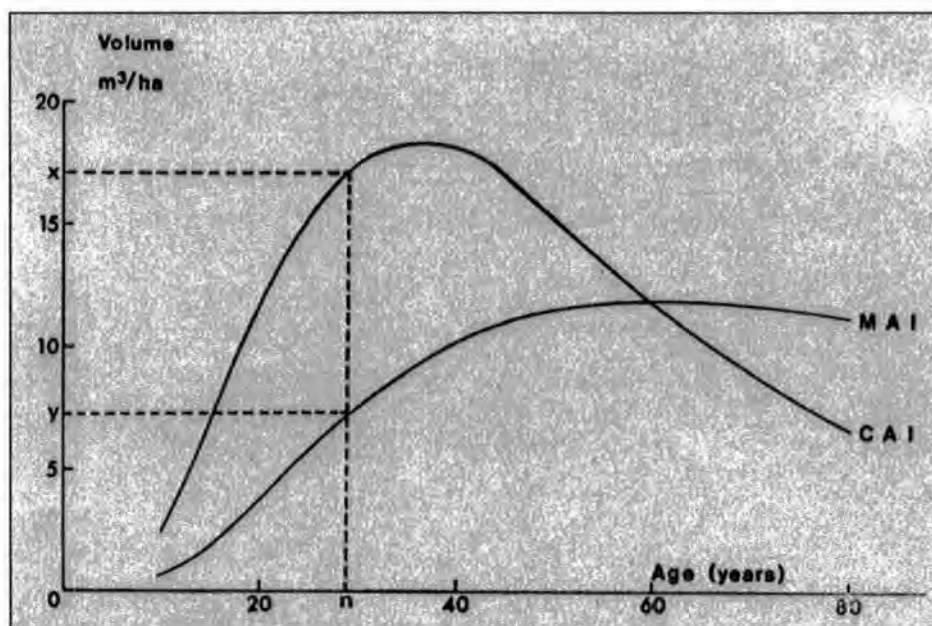
Figure 5.2 Patterns of volume increment in an even-aged stand. CAI = Current annual increment and MAI = Mean annual increment.

It is also observed that the mature class of plots exhibit the greatest standard deviations of growth measures; the greatest of these being for the 10th height percentile and the least for the 50th height percentile. This may result from the wide range of yield classes within this category. The lowest standard deviations were observed for the middle aged plots. Thus it may be inferred that the precision of LiDAR growth estimates in this case is better for middle-aged plots than it is for young and for mature plots. It is likely that this results from the specific conditions present within plots of this age. They are sufficiently old as to have reduced understorey vegetation, yet sufficiently young as to not have such dense canopies which act to reduce the penetration rate of laser pulses. Furthermore, unlike more mature plots they do not feature so many dead trees with broken stems which appear to be experiencing negative growth, thereby increasing the measure of standard deviation and

reducing precision. They also feature a tighter range of yield classes than the mature plots (Table 4.4). Younger plots are affected by understorey vegetation and an open canopy, both of which can act to increase error within height (and therefore growth) measurements. Uneven presence of understorey vegetation makes the terrain surface seem higher than it actually is in certain places. The very top of trees are more often missed by the laser pulse in an open canopy, thus causing an uneven and unpredictable underestimation of tree height by the LiDAR within the plot. The range of yield classes remains the same as for the middle-aged plots however (Table 4.4). Overall, the inequitable distribution of such effects causes an increase in the standard deviation of growth metrics and reduction of precision for younger plots (this is discussed further in section 5.4).

In summary, it is evident that the multitemporal LiDAR data is capable of detecting growth over a variety of Sitka spruce plantation plots within a 3 year period. Furthermore, the age specific nature of this growth reflects that anticipated by volume models.

5.2 COMPARING LiDAR AND GROUND TRUTH

Having established that growth can be observed in the multitemporal LiDAR datasets and that some inferences can be made about the precision of such measurements, it is next necessary to assess their accuracy. Traditionally this is done by validating the LiDAR height and growth estimates to those obtained by ground truthing, making the assumption that the ground truth data represents what is 'true'. However, this project also aims to assess the error associated with ground validation measurements and as a consequence will not assume the ground truth to be true. Instead, it will assess the similarity and agreement between ground truth and LiDAR height and growth data.

5.2.1 Comparing Height Estimates

5.2.1.1 Plot Level

Table 5.1 details the co-efficients of determination for the correlations between ground truth and LiDAR derived height variables. All ground truth and LiDAR derived metrics used here represent plot averages. The majority of the co-efficients lie above 0.9 thereby indicating that relationships between a variety of ground truth and LiDAR height variables are strong and positive. The only cases where the correlation co-efficient is significantly less strong is where minimum height is used as the ground truth variable. Here, the R^2 values range from 0.422 when minimum height 2006 is paired with maximum LiDAR height 2006, to 0.616 when minimum height 2003 is paired with maximum LiDAR height 2003.

		W. Mean 03	W. Mean 06	UnW. Mean 03	UnW. Mean 06	Max 03	Max 06	p90 03	p90 06	p50 03	p50 06	p10 03	p10 06
						LiDAR Derived Height Measures							
Ground Truth Height Measures	LMH 03	0.933		0.942		0.965		0.947		0.937		0.882	
	LMH 06		0.970		0.977		0.984		0.984		0.975		0.968
	MH 03	0.939		0.941		0.959		0.951		0.942		0.894	
	MH 06		0.925		0.935		0.942		0.944		0.933		0.929
	Max 03	0.961		0.958		0.978		0.970		0.957		0.909	
	Max 06		0.959		0.968		0.973		0.971		0.966		0.957
	Min 03	0.597		0.604		0.616		0.606		0.609		0.560	
	Min 06		0.426		0.439		0.422		0.435		0.435		0.453

Table 5.1 Co-efficients of determination for height correlations between ground truth and LiDAR derived variables from 2003 and 2006. (LMH = Lorey's Mean Height, MH = Mean Height, W. = Weighted, UnW. = Unweighted, p90 = 90th height percentile, p50 = 50th height percentile, p10 = 10th height percentile).

The strongest correlation for height data collected in 2003 is that between maximum ground truth height and maximum LiDAR height (Fig.5.3a). Indeed, across the board the maximum ground truth heights are best correlated with the LiDAR metrics. Given that airborne LiDAR systems primarily survey those most dominant trees which form the main canopy it seems logical that maximum ground truth heights should be best correlated with all LiDAR height metrics.
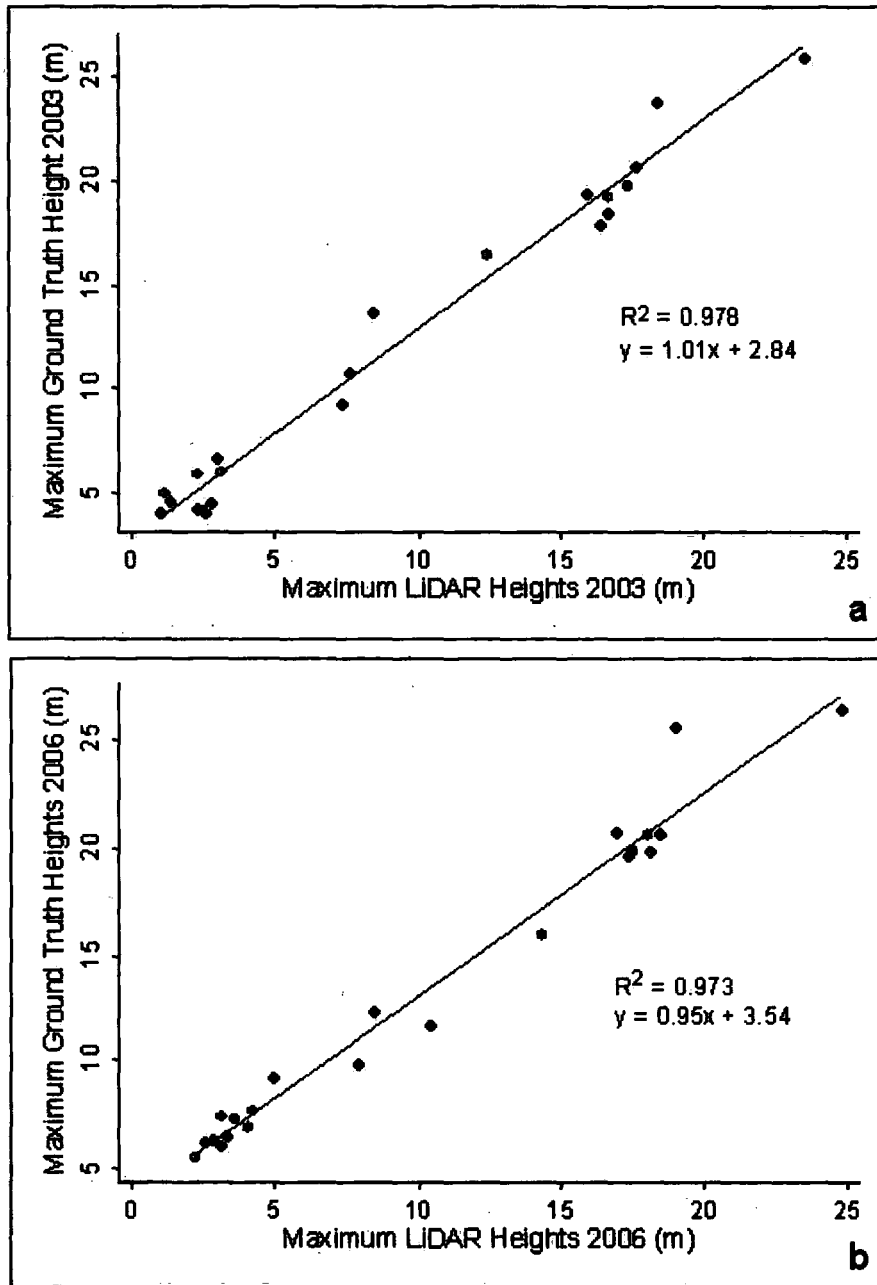
Figure 5.3 Scatter graphs showing the regressions between maximum ground truth heights and maximum LiDAR heights for a) 2003 and b) 2006.

The trend is different however for the data collected in 2006. Here, Lorey's Mean Height (LMH) is the ground truth measure which is best correlated with all LiDAR metrics.

However, ground truth maximum heights remain strongly correlated with all LiDAR variables (especially with maximum LiDAR heights as shown in Figure 5.3b) but not quite as strongly as for LMHs. It is possible that the reason for this lies in the definition of these ground truth height variables. Basal area weighting is applied to all tree heights in the calculation of LMH. In 2003, the diameters of large numbers of trees from the youngest plots were recorded as zero. This caused the average plot LMH to also be recorded as zero. Of course this was not actually the case and as a consequence the 2003 values of LMH are biased and therefore less well correlated with LiDAR height variables. By 2006, the trees of the younger plots had grown sufficiently for their diameters to be measured and for less biased values of LMH to be calculated. Furthermore, LMH gives more weight to those trees with larger basal areas. Such trees also tend to be taller and thus LMH measures from 2006 are better correlated with the 2006 LiDAR height metrics.

Overall it seems that those ground truth measures best able to represent the tallest or largest trees of the plot are best correlated with LiDAR height variables. Indeed it is likely that for these same reasons the minimum ground truth measures are least well correlated with LiDAR variables.

Despite such strong correlations for the majority of the data presented in Table 5.1 and that displayed in Figure 5.3, it is also necessary to quantify the differences between the variables as well as the spread of these differences. For this purpose, mean differences and standard deviations were calculated for those variables best correlated. The mean difference between 2003 variables (Fig.5.3a) was calculated at -2.92m. The standard deviation of these differences is 1.13m. That is, the LiDAR heights are on average 2.92m lower than the

equivalent ground truth heights. Furthermore, this indicates that the LiDAR height measures are consistently lower. LiDAR height underestimation is well documented in studies such as this and is widely accepted to be due to laser pulses over sampling the shoulders rather than the peaks of dominant trees (Aldred and Bonner 1985; Nelson 1988; Nilsson 1996; Næsset 1997; Næsset 2002; Popescu et al., 2002; Yu et al., 2004). This is discussed further in Chapter 5.4.1.

The mean difference between 2006 variables, maximum ground truth and maximum LiDAR height, was calculated at -3.04m. The standard deviation of these differences is 1.21m. This shows that both the systematic error and the random error are greater for the 2006 data, than for the 2003. Again, this indicates that the LiDAR data is on average 3.04m lower than the ground truth data. This further suggests that LiDAR heights underestimate those obtained by ground truthing. However, whether this also means that LiDAR is underestimating true tree heights is unclear at this stage. This will be discussed further in Chapter 5.4.

5.2.1.2 Individual Tree Level

A comparison of ground truth and LiDAR derived heights was also carried out at the individual tree level, the results of which are presented in Table 5.2. Here it is evident that of all the LiDAR variables it is the maximum heights which are best correlated with the ground truth heights for 2003, 2006 and 2006 adjusted (see Chapter 3 for details on adjusted measurements). This reflects the findings from the plot-wise study and reinforces the idea that the LiDAR system is best able to estimate the heights of the tallest trees. The

strongest relationship is for 2003 ground truth and maximum LiDAR heights with an R^2 of 0.7492 (Fig.5.4). The mean difference between these two variables is 0.99m and the standard deviation is 3.82m. This indicates that the maximum LiDAR heights are greater than the ground truth heights by an average of nearly 1m. This does not mirror previous findings that the LiDAR underestimates ground truth heights. Perhaps, however, it results from the nature of the ALS system only detecting and recording the tallest trees and because the maximum height variable is being used here. Indeed this is evident in Figure 5.4. The different age classes are fairly easily separable using LiDAR maximum height (x axis), particularly the definition between young and middle aged plots. However, they are not so easily separable using the ground truth height data (y axis). For example, between 3m and 7m on the y axis there are large number of data points from all three age classes which would be indistinguishable if it were not for the maximum LiDAR height scale or the colour coding. This is due to small trees being present in all plots regardless of age. In the middle-aged and mature plots these are likely to be suppressed or dead trees which are not easily detected by the ALS system or perhaps just not representing the maximum plot heights. Consequently a similar trend is not observed for maximum LiDAR heights and it appears to overestimate in comparison with the ground truth data.

It can also be noted in Table 5.2 that there is a marginally better correlation between 2003 ground truth heights and all the equivalent LiDAR height variables than for the 2006 data. With the exception of the LMH data (discussed previously) this too reflects the findings from the plot-wise study.

		LiDAR derived height variables									
		Mean		Max		p90		p50		p10	
		2003	2006	2003	2006	2003	2006	2003	2006	2003	2006
Ground Truth Height Variables	2003	0.7362		0.7492		0.7430		0.7362		0.7004	
	2006 (not adjusted)		0.7006		0.7055		0.7050		0.6976		0.6894
	2006 (adjusted)		0.4677		0.4659		0.4760		0.4613		0.4658

Table 5.2 Co-efficients of determination for height correlations between ground truth and LiDAR derived variables from 2003 and 2006, at the individual tree level.
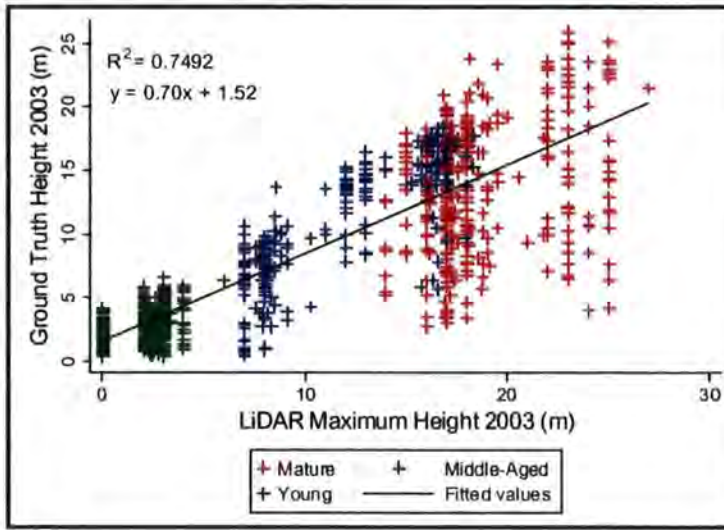
Figure 5.4 Scatter graph showing the relationship between 2003 ground truth height and maximum LiDAR height, colour coded according to age class.

It can also be seen that those correlations which make use of the adjusted 2006 ground truth height data are less strong than the equivalent unadjusted measures. This initially seems strange given that the adjusted measurements are supposedly more accurate, having been carefully assessed during the 2007 revisits (see Chapter 3). However, it should also be noted that the number of observations for the adjusted data is 536, significantly lower than the 1236 observations used in the non-adjusted 2006 data correlations. It is possible that this is causing a drop in the strength of the correlation. It should also be noted that only 44 of these 536 trees were adjusted for inaccuracies. Therefore the somewhat improved

accuracy[8] of the adjusted measurements is unlikely to outweigh the significantly reduced number of observations and thus a reduced correlation co-efficient is observed.

Overall, compared to the plot level co-efficients presented in Table 5.1 the correlations presented here, at the individual tree level, are less strong. The non-adjusted data ranges between 0.69 and 0.75, yet does not begin to approach the R^2 values of 0.9 as calculated for the data at plot level. This suggests that despite the fact that exactly the same data is being used in both regressions, there is something in the rounding or organising of the data into plot groupings which helps to improve the strength of the relationship. This indicates that the spatial resolution or scale at which the LiDAR data is analysed effects the relationship with the ground validation data. As a consequence, if the ground truth is assumed to be 'true' this also affects our perception of how accurate and precise the LiDAR height estimates are. This issue was highlighted in the plot 3 data presented in Chapter 3 and is further discussed in section 6.1.4.

5.2.2 Comparing Growth Estimates

5.2.2.1 Plot Level

Table 5.3 details the correlation co-efficients for the relationships between ground truth and LiDAR growth variables at the plot level. It is immediately evident that these co-efficients of determination are significantly lower than those calculated for height variables. The majority of values fall below 0.4 indicating a very weak correlation. The LiDAR variable

---

[8] Note: An improved accuracy of the adjusted data is an assumption. It cannot definitely be known if accuracy has been improved until felled tree height data is available for comparison.

best correlated with ground truth variables is growth in the 10th percentile. The LiDAR growth variable least well correlated with ground truth growth variables is the 90th percentile, with correlation co-efficients no greater than 0.21. Maximum LiDAR growth is also not at all well correlated with ground truth growth variables with co-efficients in range 0.0144 to 0.2369.

		LiDAR Growth Variables					
		Weighted Mean	Unweighted Mean	Max	p90	p50	p10
Ground *Truth* *Growth* *Variables*	LMH	0.3992	0.3044	0.2369	0.0108	0.4066	0.4122
	MH	0.2625	0.3441	0.0284	0.0065	0.3539	0.3942
	Max	0.2313	0.3456	0.0849	0.2073	0.4052	0.5029
	Min	0.1036	0.1638	0.0144	0.0081	0.1794	0.1694

Table 5.3 Co-efficients of determination for growth correlations between ground truth and LiDAR derived variables, at plot level. (LMH = Lorey's Mean Height, MH = Mean Height, W. = Weighted, UnW. = Unweighted, p90 = 90th height percentile, p50 = 50th height percentile, p10 = 10th height percentile).

The strongest correlation between LiDAR and ground truth growth variables exists between the 10th percentile variable and maximum growth (Fig.5.5). The scatter graph and equation for the linear fit line indicates that this relationship is negative. It shows that ground truth maximum growth is recorded as decreasing with increasing growth in the 10th percentile of the LiDAR data. The mean difference between the two variables is 0.13. That is, the LiDAR 10th percentile growth data is on average, 0.13m less than the ground truth maximum growth data. The standard deviation of this difference is 2.15m indicating the spread of the data.
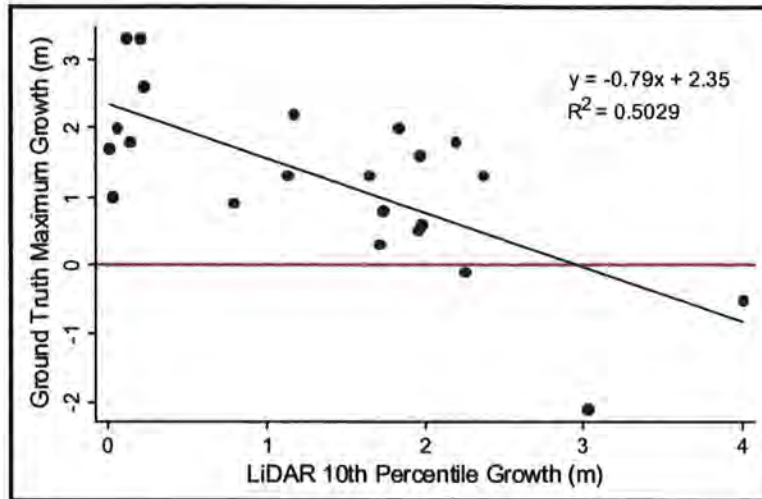
Figure 5.5 Scatter graph showing the regression between maximum ground truth growth and the 10th percentile growth from the LiDAR data.

It was also noticed that an age function existed within this relationship. This is evident in Figure 5.6 where data points have been colour-coded according to their age class. Here it is evident that the young plots are exhibiting the lowest levels of LiDAR 10th percentile growth, yet the highest amounts of maximum height growth as recorded during ground truthing. The middle-aged and mature plots are largely indiscernible, showing similar patterns of maximum ground truth growth as the young plots but higher levels of LiDAR 10th percentile growth. However, two of the middle-aged plots do show much higher LiDAR 10th percentile growth than the main cluster of mature and middle-aged plots. It is unclear at this stage why this trend exists and how it is related to plot age, however this pattern and other age-related trends are also present in Figure 5.7.
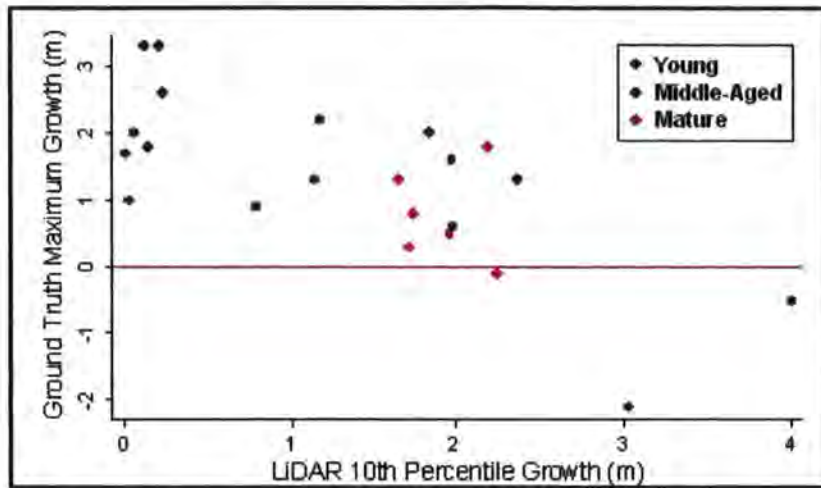
Figure 5.6 Scatter graph showing the regression between maximum ground truth growth and the 10th percentile growth from the LiDAR data, colour coded according to plot age.

Figure 5.7 displays a variety of plot based LiDAR derived growth variables ordered by plot age. The oldest plots are represented by the lowest values on the x axis and the youngest plots by the highest values. The 10th percentile growth values are represented by the blue circles and display the trend observed in Figure 5.6- lowest for younger plots, higher for mature and middle-aged plots and highest for two middle-aged plots. There is not such a clear overall trend with plot age for the other variables, the 90th percentile and maximum growth. Similar growth values are obtained for mature, middle-aged and young plots. However, a pattern does become evident when these growth values are studied in relation to the p10 growth values. For the older plots, the p90 and maximum growth values generally record smaller amounts of growth than for the p10 values. The younger plots however exhibit the complete opposite. Here the p90 and maximum growth values show consistently higher levels of growth than the p10 growth values. This might suggest that younger plots are experiencing greater growth at the treetops, however as observed in section 5.1 and in Figure 5.7 it is the middle-aged plots which show the greatest levels of

growth overall. It is only in relation to the p10 growth values that the p90 and maximum growth values of the younger plots are high.
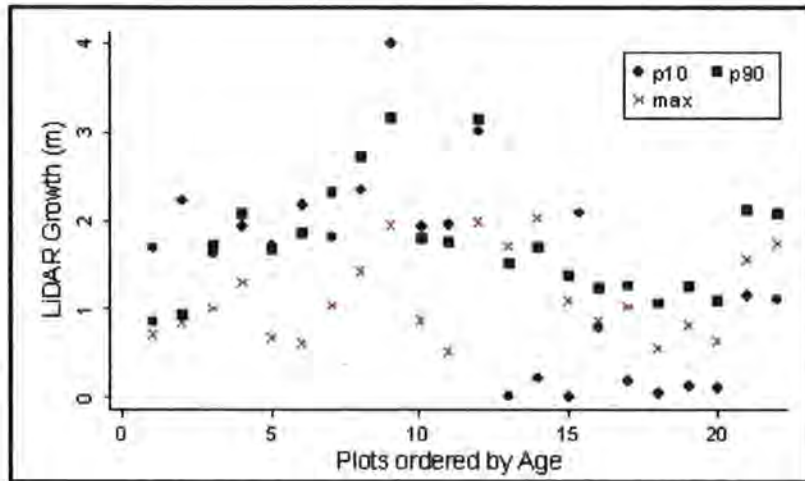
Figure 5.7 Scatter graph showing LiDAR growth variables p10, p90 and max plotted in order of plot age. The smallest values on the x axis represent the oldest plots and the highest, the youngest.

Observations such as this are of interest, and suggest that plot age plays a significant role in the relationship between ground truth and LiDAR estimates of forest growth. This will be discussed further in section 5.4.2. Despite such observations however, overall there remains a weak and negative relationship between all ground truth and LiDAR growth variables, as seen in Table 5.3. This seems curious given the strong and positive relationships observed in the regression of ground truth and LiDAR height variables. A tree by tree (rather than plot by plot) assessment of growth correlations is next performed before the potential reasons for such weak and negative relationships are discussed in Chapter 6.

5.2.2.2 *Individual Tree Level*

Table 5.4 details the co-efficients of determination for the growth correlations between ground truth and LiDAR derived variables at the individual tree level for all of the 22 validation plots. Here the ground measured height and diameter of each tree has been used in the correlation with the equivalent LiDAR derived variable extracted from the exact location of each tree. It is clear that the relationships between all variables are very weak. Furthermore, with the exception of the two co-efficients for maximum LiDAR derived growth, all relationships are also negative. In general, the correlation of LiDAR variables is stronger with ground truth measured diameter growth rather than height growth. The 10th percentile variable is best correlated with height growth, however this remains an extremely weak relationship as observed in Figure 4.8. Here it is evident that there is no discernable relationship. Data points were colour coded in an attempt to highlight any age-related trends, however very little is revealed. Much negative growth is recorded in the ground truthing for mature plots in particular, with some also recorded for the middle-aged plots. Some negative growth of young trees is displayed in the LiDAR 10th percentile data.

Ground Truth Growth Variables		*LiDAR derived growth variables*				
		Mean	Max	p90	p50	p10
	Height	0.0549	0.0035	0.0003	0.0576	0.0688
	Diameter	0.1128	0.0298	0.0001	0.1074	0.1245

Table 5.4 The correlation co-efficients for the regression relationships between ground truth and LiDAR growth variables using data from each individual tree.
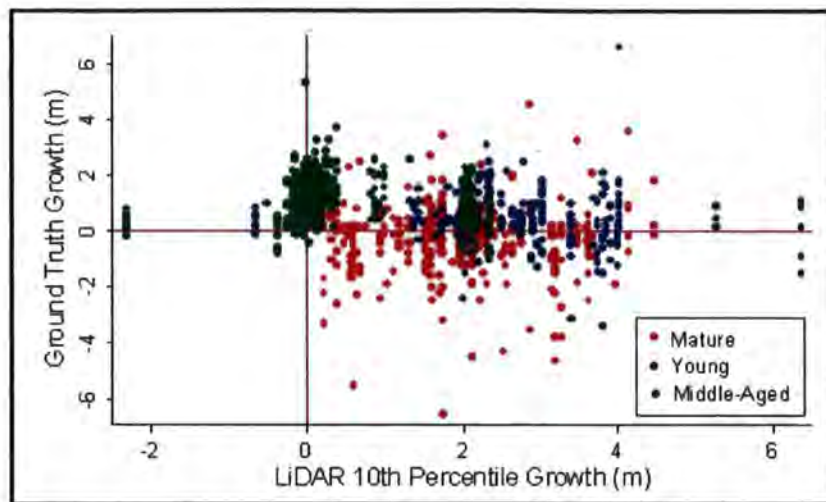
Figure 5.8 Ground truth height growth plotted against growth in the 10th percentile LiDAR data. Data points are colour coded according to the age-class of the tree.

In summary, it is obvious that there is a lack of relationship between ground truth and LiDAR derived growth variables despite the high levels of correlation for height variables. At both the plot and individual tree level correlation co-efficients for growth are low and usually negative. Relationships are stronger when data is analysed at the plot level. However the strongest relationship reaches an R^2 of only 0.5, is negative and seems a strange alliance between maximum ground truth growth and 10th percentile LiDAR derived growth. It also appears to be conditioned somewhat by plot age. If the assumption were to be made that the ground truth data is an accurate reflection of the true tree heights then it might be concluded at this stage that although capable of detecting forest growth, the accuracy and precision of LiDAR growth estimates are poor. However that assumption is not being made here and thus the investigation into the estimation of growth at Kielder Forest using ALS continues.

5.3 GROUND TRUTH DATA ERROR

A specific aim of this project was to assess the accuracy and precision of ground truth equipment and data with a view to gauging the reliability of this as a method for checking LiDAR height and growth estimates. To this end, this section discusses results presented from the assessment of ground truth error and the 2007 revisits in Chapter 3.

Results from Chapter 3 indicate that from both the road and forest viewing angles, the Vertex instrument produces height measures closer to the felled tree heights than those produced by the clinometer and LaserAce. This is further demonstrated by the box plots displayed in Figure 5.9 where average values sit much closer to the zero line and where ranges and interquartile ranges are smaller for the Vertex. This serves to support the use of the Vertex for ground truth measurements within this project, for similar studies and for forest inventorying in general. However, it is the magnitude of the error associated with the Vertex measurements which have a bearing on the use of ground truth data as a check on the LiDAR. As a consequence, it is the Vertex measurements which shall be the focus of the remainder of this section. Furthermore, only those results obtained from the forest viewing angle will be studied, given that they better simulate real plot working conditions.
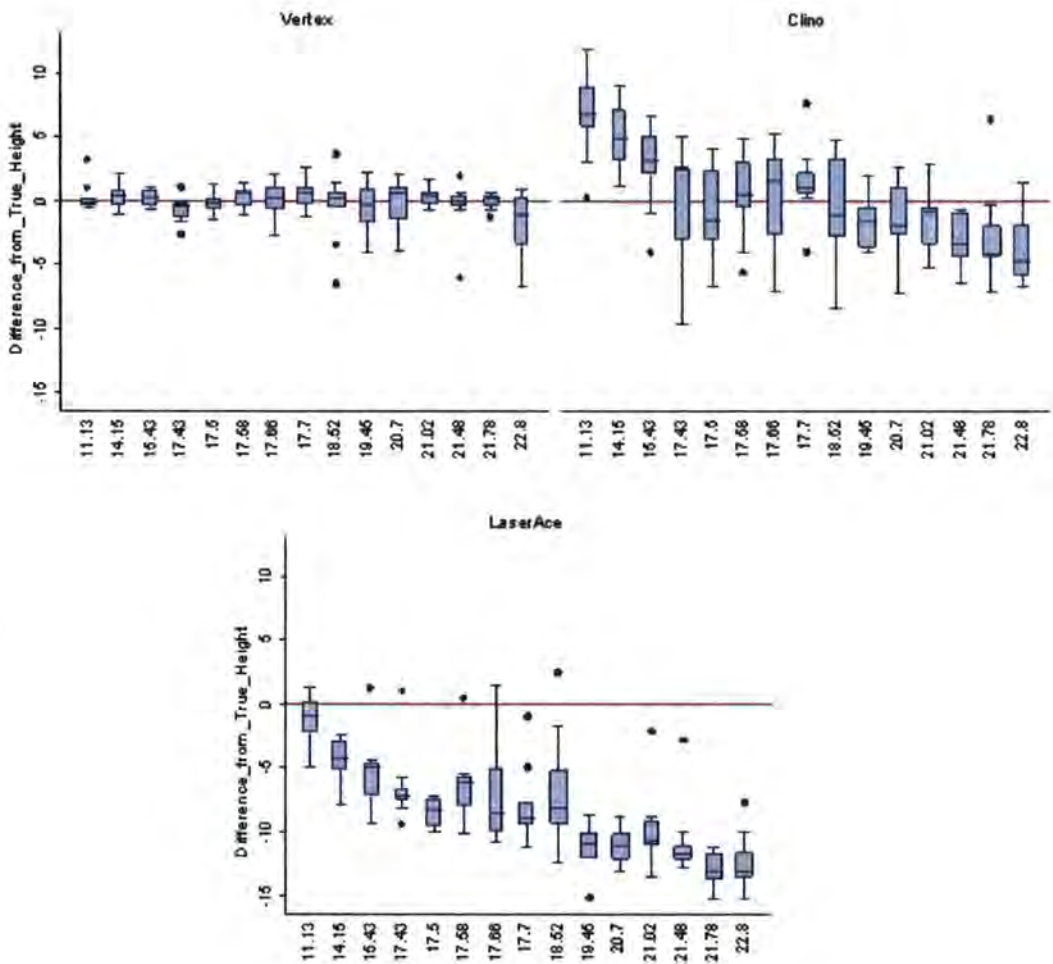
Figure 5.9 Box plots by instrument showing difference from true height for each tree in height order. The middle line of the box represents the mean, the top and bottom of the box the interquartile range and the top and bottom of the extended lines the minimum and maximum values. The points represent outliers.

Considering users of all levels of experience, the mean difference (height error) between measured vertex height and felled height is -0.10m. That is, vertex measured heights are on average 0.10m less than the true tree heights. This seems highly encouraging, however, the standard deviation of this measure is high at 1.68m, with values ranging between +3.7m and -6.8m. This suggests high accuracy but low precision. Perhaps somewhat surprisingly, height error worsens to 0.29m if only experienced users are considered- a drop in the level of accuracy. However, the standard deviation is improved to 0.73m and thus an increase in

precision is observed. The range of values is also improved for experienced users and runs from -1.1m to +2.0m. As would be expected, height error and standard deviation values worsen with decreasing levels of experience as displayed in Table 5.5. This indicates a drop in both accuracy and precision.

Experience Level	Mean	St. Dev.	Max	Min
All	-0.10	1.68	3.70	-6.80
Experienced	0.29	0.73	2.00	-1.10
Some Experience	0.33	1.23	3.10	-3.50
Inexperienced	-0.61	2.12	3.70	-6.80
Data Collectors	0.31	1.05	3.10	-3.50

Table 5.5 Average difference from true tree height (height error) with associated standard deviation and range values, by level of experience using the Vertex III hypsometer. The unit for all figures is metres.

The ground truth data used in this study was collected by users who fit into the 'Experienced' and 'Some Experience' categories. Therefore a new row for 'Data Collectors' was added to Table 5.5 and mean, standard deviation and range values computed. It seems appropriate then to use the ground truth statistics for data collectors for assessment of the ground truth and LiDAR correlations. Despite reduced levels of accuracy and precision compared to the experienced users alone, the data collector category is likely to give a truer representation of the accuracy (or bias) and precision of ground truth tree height measurements undertaken by this project.

For data collectors, the height error is 0.31m with a standard deviation of 1.05m. This suggests that the ground truth data collected as part of this project is on average, 0.31m

greater than the true heights of the trees. The following paragraphs will explore what this means for the assessment of LiDAR data accuracy.

Plot level height correlations between ground truth and LiDAR data were strong and positive for both 2003 and 2006. However, despite strong levels of association, mean differences between the best correlated variables was high at -2.92m for 2003 data with a standard deviation of 1.13m. Bias was higher for the 2006 correlation at -3.04m as was precision with a standard deviation of 1.21m (Fig.5.3). If the bias of ground truth measures is then taken into consideration and figures altered to reflect a 0.31m bias, standard deviation and the strength of the associations remains unchanged but the mean difference between variables for 2003 is increased to -3.23m and for 2006 increased to -3.35m. Furthermore, the mean difference between growth variables (LMH growth and maximum LiDAR growth) is increased to -0.99m. This suggests that error within the ground truth data is not responsible for poor growth correlations. However, this approach only takes into account the mean difference between ground truth and felled data obtained during the trial. It takes no account of the variation in this mean difference as a function of tree height (Fig.5.10).
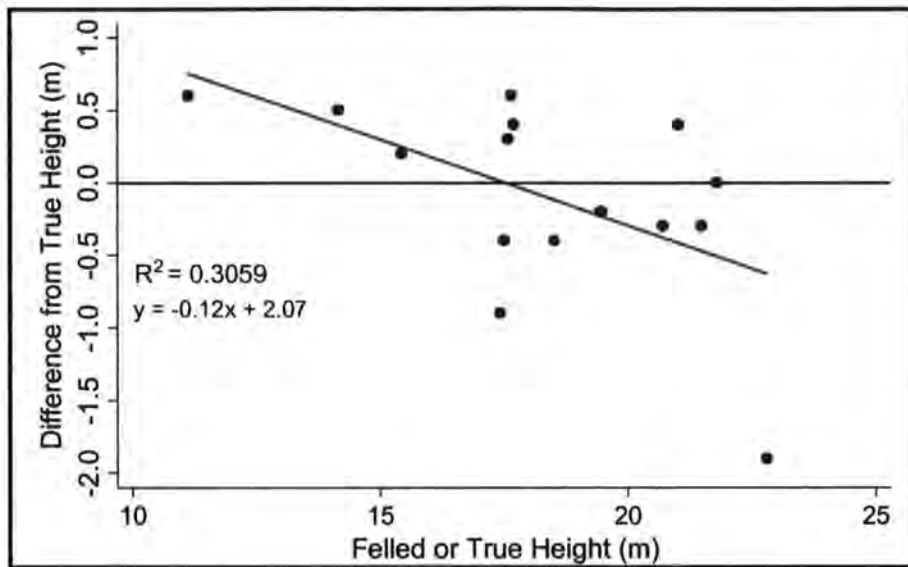
Figure 5.10 Scatter graph showing the relationship between the difference from felled height observed by all users using the Vertex during the trial, and felled or true height. Linear fit line added and correlation co-efficient and equation of the line shown.

Figure 5.10 shows a clear trend of increasing under prediction of heights with increasing true tree height. Greater amounts of scatter are also observed at greater felled heights, as demonstrated in Table 5.6 by the standard deviation measures. If the effects of the ground truth error observed during the trial are to be tested on the ground truth-LiDAR correlations, then the error must be subdivided according to tree height. Table 5.6 demonstrates the three height classes that the data was divided into and the associated errors of each height category.

Tree Height Category	Mean difference from true height (m)	Standard Deviation (m)	Maximum Difference (m)	Minimum Difference (m)
>20m	-0.44	1.96	2.00	-6.80
≥17.5 and ≤20m	0.04	1.68	3.73	-6.50
<17.5m	0.12	1.19	3.10	-2.60

Table 5.6 Tree height categories with associated ground truth accuracy, precision and range measurements (the 'Data Collector' category errors only).

Ground truth plot and individual tree level data were then adjusted to reflect these mean differences from felled height. For example, an average plot height of 21m was increased to 21.44m to compensate for the height under prediction within this height category; a tree height of 17m was reduced to 16.88m to compensate for the height over prediction in this height category and so on. Given that the true heights used during the trial fell between the values of 11.13m and 22.80m, it was anticipated that the error associated with ground truth measurements under 10m could not accurately be predicted by the <17.5m category. As a consequence, it was initially decided that all those plots average heights and individual tree heights which fell below 10m would be excluded from the new correlations (which are taking into account ground truth error). However, given that many of the validation plots used within this study are young, excluding all those plots and trees below 10m left too few observations for the correlations to be meaningful. Therefore all observations were used in the new correlations, all values less than 10m remained in the <17.5m category and were treated accordingly. The before and after results are displayed in Table 5.7.

Growth Correlations	Plot Level		Tree Level	
	Before	After	Before	After
Ground Truth Variable	Lorey's Mean Height Growth		Non-Adjusted Tree Growth[9]	
LiDAR Variable	LiDAR Maximum Growth		LiDAR Maximum Growth	
R^2	0.2369	0.2370	0.0035	0.0035
Line Equation	y = 2.15x - 0.64	y = 2.10x -0.61	y = 0.06x + 0.43	y = 0.06x + 0.43
Mean difference (m)	-0.680	-0.640	0.616	0.617
Standard Deviation (m)	2.02	1.98	1.47	1.49

Table 5.7 Growth correlations at plot and tree level both before and after trial adjustments.

---

[9] 'Non-adjusted' refers to the fact that the 2006 tree height data used in this regression was not adjusted under the 2007 revisits.

119

It is evident from the values presented in Table 5.7 that the tree height adjustments made based on the trial data have had very little effect and there is certainly no significant improvement in the strength of the correlation. The mean difference between growth variables is slightly lower at the plot level following trial adjustments, but is higher at the tree level. The standard deviation is also slightly lower at the plot level following adjustments, indicating a higher level of precision, but again the opposite is true at tree level. The co-efficient of determination for plot level growth is very slightly greater following tree height adjustments, but not enough to make any reliable conclusion that ground truth error is responsible for poor growth correlations. The possible explanations for this are discussed further in Chapter 6.

5.4 INTERACTION BETWEEN LiDAR AND THE FIELD

This section deals with those inaccuracies and biases which may have been incurred due to the nature of the interaction between the laser pulse and the forest. Errors of this kind may be summarised by the scale of their effects. For instance, some consistently affect the entire study area and thus have been classified as 'global'. Others affect specific areas or plots and have been classified as 'regional' effects. Finally, some only influence estimates at the subplot level and thus have been categorised as 'local' effects. Each of these shall be examined in turn which respect to their likely impact on height and growth correlations. For these purposes the ground truth shall be assumed to represent 'true' tree height.

5.4.1 Global Effects

This section considers the nature of the interaction between the LiDAR system and the forest which may affect height and growth correlations at the global scale. This will focus on two areas; firstly, how the LiDAR system predominantly samples the tallest or dominant trees; and secondly, the common issue of LiDAR height underestimation resulting from the majority of laser pulses falling on the shoulders of the tree rather than the crown.

Airborne laser scanning is only able to measure the heights of those trees which are detectable from the air. As a consequence, dominant trees which sit within or above the main canopy stand a greater chance of being measured than smaller trees which lower in the canopy or well below it. Thus it was considered that in height and growth correlations we may not be comparing like with like. That is, whilst the ground truthing measures the heights of all trees within the plot regardless of dominance level, the LiDAR is measuring

121

only the tallest trees. Indeed, this could be the reason why the strongest positive height and growth correlations are observed for maximum ground truth variables or, in the case of the 2006 data, Lorey's Mean Height which also weights larger (and therefore probably taller) trees more heavily. Furthermore the relationships at the individual tree level indicate that the LiDAR is over predicting tree height, contrary to the well documented under estimation which is observed at the plot level. In order to test this further, regressions between ground truth and LiDAR heights and correlations were re-run to consider only those trees classified as 'dominant'. The before and after results for correlations at the individual tree level are presented in Table 5.8.

Individual Tree Level		Correlation Co-efficient	Line Equation	Mean Difference (m)	Standard Deviation (m)
Height 2003	All trees	0.7942	y = 0.70x + 1.52	0.99	3.82
	Dominant trees only	0.9602	y = 0.92x + 1.70	-1.08	1.43
Height 2006	All trees	0.7055	y = 0.65x + 1.72	1.62	4.22
	Dominant trees only	0.9483	y = 0.85x + 1.80	-0.51	1.72
Growth	All trees	0.0035	y = 0.06x + 0.43	0.62	1.47
	Dominant trees only	0.0086	y = 0.09x + 0.53	0.57	1.45

Table 5.8 Correlation co-efficients and associated mean difference and standard deviation values for tree level height and growth regressions, considering all trees and only those classified as 'dominant'. 2003 variables: ground truth height and maximum LiDAR height. 2006 variables: ground truth height and maximum LiDAR height. Growth variables: ground truth height growth and maximum LiDAR growth.

The results show that correlation co-efficients are all stronger when only 'dominant' trees are considered. This is particularly true for the height correlations. The growth co-efficient is not much greater and certainly has not become a significant relationship. For both height correlations, the mean difference between variables has been lowered by just over 2m so that the LiDAR now appears to underestimating 'true' (ground truth) heights. This indicates that once the overestimating effects of LiDAR on the smaller, less dominant trees (due to

greater sampling of taller, dominant trees) has been eliminated, the well documented pattern of underestimation becomes apparent. This underestimation is discussed further on in this section. The mean differences between growth variables has also been reduced, but not to the same extent as for the height correlations. It still sits above zero thereby still indicating an overestimation of growth by LiDAR in comparison with the ground truth. Standard deviation measures are lower in all cases, though are reduced more substantially for the height correlations. This indicates that greater precision is achieved by considering 'dominant' trees only.

These results only give the effects of considering dominant trees for tree level correlations. However, it is likely that similar effects would be observed at the plot level. In conclusion here, it is evident that the growth correlation has not been improved significantly by considering dominant trees only. This suggests that it is not the bias of LiDAR height measuring towards taller (more dominant) trees which is responsible for the poor growth correlations.

The second effect to note which has a global effect is that of LiDAR underestimation of ground truth tree heights. As discussed in the Introduction, it is widely acknowledged that this results from an over sampling of the shoulders of dominant trees, rather than their tips (Nilsson 1996; Næsset 1997; St-Onge 1999; Dubayah et al., 2000; Næsset 2002; Popescu et al., 2002; Suarez et al., 2005; Yu et al., 2004). That is, the very top of the tree does not constitute a good interceptor of the laser pulse compared to the denser shoulder area (St-Onge 1999). Thus it is more likely that the first return is reflected from the tree shoulders leading to an underestimation of the height obtained by ground truthing.

This underestimation is not noted at the tree level until only dominant trees are considered, as shown in Table 5.8. However, it is observed at the plot level. For 2003, the maximum LiDAR heights underestimate maximum ground truth height by 2.92m. This is a significant underestimation, but mirrors that found elsewhere (St-Onge 1999). For 2006, the maximum LiDAR heights too show underestimation of maximum ground truth heights, by 3.04m. Overall, it is evident that this study provides further evidence of LiDAR tree height underestimation at the global scale.

5.4.2   Regional Effects

This section discusses two issues which seem to affect LiDAR height and growth estimation at a more regional scale. That is, these issues tend to be more location specific than those discussed previously. The first issue is that of very dense canopies and the second of plot age.

It has already been seen that areas of very dense canopy cause problems for accurate DEM generation. However, it was suggested by Nelson *et al.,* (1988) that fewer returns from the ground produce better correlations between ground truth and LiDAR derived height measures. Their reasoning for this is that a lower count of returns from the ground indicates a denser canopy. This, in turn, results in fewer pulses hitting the shoulders of the trees and more hitting the very tops, giving a more accurate measure of tree height. Indeed, this may well be so, yet Nelson *et al.,*'s theory takes no account of the fact that a lower count of ground returns results in a lower level of confidence in the DEM and therefore also in the

height estimation. As a consequence, it could also be argued that fewer returns from the ground may result in weaker correlations between LiDAR and ground truth height and therefore also growth estimates. In order to investigate these two lines of argument, height and growth correlations were studied in relation to ground count. The results are shown in Table 5.9.

Variables	Ground Count Conditions Imposed (hits per pixel)	Correlation Co-efficient
Ground truth height 2003 and Mean LiDAR height 2003	None	0.7362
	<12	0.7111
	>12	0.5256
	>6 and <15	**0.7727**
	<1	0.6754
Ground truth height 2006 and Mean LiDAR height 2006	None	0.7006
	<8	0.7090
	>8	0.3840
	>3 and <7	0.7401
	<2	**0.7743**
Ground truth height growth and Maximum LiDAR Growth	None	0.0035
	count 2006 <2	0.0032
	count 2003 >6 and <15	0.0004
	Both of the above	**0.0155**

Table 5.9 The effects of changing ground count on correlation co-efficients for 2003 and 2006 heights and growth. The range of ground hits per pixel was 0-24 for 2004 and 0-15 for 2006.

The table shows mixed results with no clear answer to the investigation. The 2003 height correlation co-efficient was most improved when the number of ground hits per pixel was limited to between greater than 6 and less than 15. It was not significantly improved when assessing only low or high numbers of ground hits. Perhaps this represents a middle-ground or balance between DEM accuracy (high number of ground hits) and true representation of the canopy surface (low number of ground hits). However, the same is not true for the 2006 data. The greatest improvement in correlation co-efficient is achieved when only LiDAR pixels with a ground hit of less than 2 are considered. This seems to support Nelson *et al.*,'s

theory. Yet it remains unclear why there is no consistency between datasets. In terms of the growth correlation though, it is unsurprisingly the combination of the 2003 and 2006 ground count conditions which have the greatest improvement on the strength of the correlation. However the correlation co-efficient remains very weak. This suggests that regional issues of ground count are not responsible for the poor growth correlation.

The second regional issue is that of plot age. It has become evident throughout this study that plot (or tree) age plays a significant part in how accurately the average plot (or tree) height may be estimated. This has already been studied in relation to ground truthing, however this section aims to investigate the effects of plot age on LiDAR height estimation. It might be argued that this is a global issue, yet because different forest stands are of different ages and therefore are affected differently, it is being discussed as a regional issue.

The issue of plot age links into many of the themes already discussed in this paper, including DEM accuracy, CHM accuracy and dominance levels. Here the three previously defined plot age classes will be examined separately (for definitions see section 4.1.4). Here, the ground truth values must be assumed to be true. The results of the individual tree level investigation are presented in Table 5.10.

Tree Level Variables	Condition	Correlation Co-efficient	Line Equation	Mean Difference (m)	Standard Deviation (m)
Ground truth height 03 and Max LiDAR 03	All ages	0.7492	y = 0.70x + 1.52	0.99	3.82
	Young	0.1187	y = 0.37x + 1.96	-0.74	1.39
	Middle-Aged	0.6542	y = 0.99x - 0.70	0.83	2.73
	Mature	0.0464	y = 0.36x + 7.31	4.37	5.09
Ground truth height 06 and Max LiDAR 06	All ages	0.7055	y = 0.65x + 1.72	1.62	4.21
	Young	0.2247	y = 0.70x + 1.42	-0.56	1.48
	Middle-Aged	0.6701	y = 0.98x - 1.44	1.66	2.78
	Mature	0.0395	y = 0.32x + 7.63	5.60	5.41
Ground truth growth and Max LiDAR growth	All ages	0.0035	y = 0.06x + 0.43	0.62	1.47
	Young	0.0002	y = 0.01x + 0.90	0.19	1.40
	Middle-Aged	0.0003	y = 0.02x +0.44	0.83	1.31
	Mature	0.0001	y = 0.02x - 0.30	1.18	1.54

Table 5.10 Correlation co-efficients and related information derived from the regression of height and growth variables, subdivided according to tree age.

It can be seen from the results, that young trees are being under predicted by the LiDAR both in 2003 and 2006. It is likely that this results from one or both of the following. Firstly that the open canopy of younger plots means that more laser hits fall on the shoulders of the trees rather than their peaks, leading to underestimation by the canopy height model. Secondly, the open canopy allows larger proportions of understorey vegetation to grow, thereby leading to an overestimation of the DEM. The combination of these, results in an underestimation of height by the LiDAR, as observed in Table 5.10.

Conversely, it is evident that mature trees are grossly over predicted by the LiDAR, for example, by an average of 5.6m in 2006. As discussed previously, the closed canopies of mature plots have mixed effects on the strength of the correlation between ground truth and LiDAR height values. However it is likely that it is the inability of LiDAR to penetrate the canopy sufficiently to measure less dominant trees that is responsible for such an over prediction of heights, and a large corresponding drop in the strength of the correlation. The

mature category also features the greatest standard deviation value thereby indicating the poorest level of precision.

The middle-aged plots seem to represent a half way point between these two extremes, where the LiDAR and ground truth heights and growth are best correlated when compared to the other age classes. Middle-aged plots have a sufficiently closed canopy for more accurate height estimation and reduced understorey vegetation, yet the canopy is not so dense as to prevent detection of lower trees within the plot.

In summary, it is evident that tree or plot age appears to have a significant effect on the relationship between LiDAR and ground truth height data, with increasing amounts of systematic bias and random error observed for older plots. Consequently it might be assumed that this is responsible for the poor growth correlations. However, Table 5.10 also indicates that not only the strength of the growth correlation, but also the systematic bias and random error are not significantly altered by plot age. Therefore it is concluded that the regional effects of both plot age and dense canopies, are not alone responsible for the observed lack of correlation between LiDAR and ground truth growth variables.

5.4.3 Local Effects

This section discusses the nature of the interaction between LiDAR and the field at the local level. This includes investigating the effects of negative values and dead trees on the LiDAR-ground truth growth correlation.

Negative growth values within the ground truth data result partially from recording errors and partly from dead trees where the top of the stem is progressively breaking off. It is less clear why negative growth values are observed within the LiDAR data, unless of course obvious clear-felling or windblow has occurred. They may result from data misalignment which has already been identified as an issue here. In order to investigate the effects of negative values on growth estimates, the correlation was rerun to exclude all negative ground truth and LiDAR values. The results are presented in Table 5.11.

Condition	Correlation Co-efficient	Line Equation	Mean Difference (m)	Standard Deviation (m)
None	0.0035	y = 0.06x + 0.43	0.62	1.47
Negative values excluded	0.0201	y = -0.13x + 1.18	0.58	1.15
All dead trees excluded	0.0025	y = 0.05x + 0.53	0.54	1.47

Table 5.11 Effects on the correlation between ground truth growth and maximum LiDAR growth caused by exclusion of negative values and exclusion of dead trees.

It is evident from the resulting correlation co-efficient that excluding all negative values does slightly improve the strength of the association between ground truth growth and maximum LiDAR growth. It also reduces the mean difference between the variables and the random error (standard deviation). However, it is important to note that this improvement is very slight. As a consequence, the occurrence of negative growth is not sufficient to explain the poor growth correlation.

The correlation was also rerun to exclude all dead trees. If dead trees with breaking stems were the main cause of negative growth it would be expected that the correlation for excluded dead trees would closely match that achieved by excluding negative values.

However, this is not the case. This suggests that dead trees are not the main cause of the observed negative growth values. It is possible that the level of uncertainty associated with ground truth measurements (Chapter 5.3) leads to false negative growth measurements. Furthermore, LiDAR data misalignment could also be responsible. This supports the requirement for further study of ground truth error and accurate LiDAR positioning.

5.5 SUMMARY

This section has explored the results in greater depth. It has been shown that the multi-temporal surveys were capable of detecting growth over the 3 year time period at Kielder Forest. When compared to ground truth data, the LiDAR height data correlates very strongly, although underestimation of ground truth values is high at roughly 3m. Conversely, growth correlations between LiDAR and ground truth data are weak and mostly negative. Consideration of ground truth error and a variety of interactions between LiDAR and the field did little to improve the strength of the growth correlations, although height correlations were further improved by considering only dominant trees. The following chapter discusses further why such a poor growth correlation is being observed and makes some recommendations for future work.

6 DISCUSSION

This research was initiated with the following key research questions:

1. Can multi-temporal ALS detect forest growth over a three year period?

2. If so, how accurately is this growth predicted?

3. Can this tell us anything about:

   a. the robustness of our LiDAR processing and;

   b. the accuracy, precision and reliability of our methods used to test the LiDAR data?

It was shown in Chapter 5 that the multitemporal LiDAR datasets acquired over Kielder Forest are indeed capable of detecting growth over the three year study period. However, despite strong correlations between LiDAR and ground truth height estimates no such agreement was found for growth data. This might suggest that multi-temporal LiDAR surveys are unable to accurately estimate forest growth. However it is first necessary to explore the potential reasons for this lack of association between LiDAR and ground truth growth estimates. This is the focus of this discussion chapter.

In answering research question No.3 a variety of factors are considered, including positioning error, ground truth error, the set-up of the LiDAR systems and the effects of scale and resolution. The chapter is concluded with a discussion of the implications of these findings for the forest management community and other interested parties.

6.1 POTENTIAL SOURCES OF ERROR

This section aims to investigate why such poor levels of correlation are observed between ground truth and LiDAR derived growth variables. This investigation will assess the robustness of the LiDAR processing chain as well as the accuracy, precision and reliability of the ground validation data; firstly, with a view to exploring the ~7m DEM offset in z, the 5m offset in x between the LiDAR datasets; and secondly with a view to gauging the accuracy of the LiDAR growth estimates. In doing so a number of key themes are discussed, including the effects of; spatial positioning and potential data misalignment; the accuracy and precision of ground truth data and its method of collection; the setup of the ALS system; and lastly some consideration will be given to scale and resolution.

6.1.1 Positioning Accuracy

The misalignment of LiDAR datasets with each other and in relation to the location specific ground truth data has huge implications for the estimation of forest growth. Furthermore, if the ground truth data is assumed to be 'true' then the misalignment also effects our assessment of the accuracy and precision of such growth estimates. This study found the LiDAR datasets to be offset in a northerly direction by 5m and in the z axis by 7m. Given the systematic nature of this offset the spatial correction process was fairly straightforward, however it is worrying that the offset only became evident because multiple LiDAR datasets were being used. Other studies too have found positional offsets between LiDAR and field data to be the single most important source of error (Næsset and Økland 2002). This section discusses a range of possible causes of data misalignment and considers how positional errors might be minimised.

6.1.1.1 GPS Error

ALS data is advertised to be accurately georeferenced from the moment of its acquisition and thus is frequently assumed to be an accurate frame of reference for spatial positioning. However, errors in the recorded GPS measurements are possible and translate themselves into laser point error. In this study, errors in the GPS for either or both LiDAR datasets and/or the ground truth tree and plot locations may be causing positioning errors and subsequent data misalignment. If so, it is likely that they result from one or both of two main issues.

The first of these issues is that of poor geometry from the GPS satellite constellation. This occurs when satellites are spread across the sky in such a way as to result in low levels of locational precision. PDOP or 'Position Dilution of Precision' is the name given to this measure of geometric strength which is determined by the number of satellites being tracked and their location in the sky. A PDOP mask may be applied during data collection to define the limits of acceptable accuracy. A PDOP of less than 4 gives the most accurate results resulting in a confidence of positioning of less than 1m. A PDOP of between 4 and 8 is generally regarded to be acceptable and above 8 gives very poor positional accuracy (Brown 2007, *pers. comm.*; University of Montana website accessed 25.10.07). Correspondence with the Environment Agency confirmed that the 2003 LiDAR dataset used here was collected with a PDOP of less than 4. Furthermore, correspondence with the Unit for Landscape Modelling (ULM) confirmed that the 2006 LiDAR was collected with a PDOP of between 2.60 and 1.41. Thus it is likely that this is not the cause of any significant error within the data.

The second issue concerns the length of the baseline during collection of GPS data. Longer baselines mean greater positioning errors. The distance between the base station and rover, whether during LiDAR acquisition or ground truthing, affects the positioning error at a rate of roughly one in one million. This equates to an increase in error of 1mm for every 1km further from the base station the rover is. It is possible that error introduced by a long baseline may result in positioning errors and subsequent data misalignment. Again, the Environment Agency were able to confirm a baseline length of less than 20km for the 2003 LiDAR data acquisition, resulting in a GPS error of 2cm. ULM were also able to confirm an average baseline length of 10.35km, with a range between 1.52km and 27.78km. This results in a GPS error of between 0.1cm and 2.7cm. This amount of error seems somewhat insignificant when dealing with data which has been summarised into 5m by 5m pixels and does not afford an explanation of a 5m or 7m offset in any dimension. Furthermore, the Environment Agency checked the 2003 LiDAR against 1:10,000 Ordnance Survey maps and Nextmap Synthetic Aperture Radar data for Kielder and found no notable offset. This suggests that the data misalignment is not due to GPS errors of the 2003 or 2006 LiDAR data.

In terms of the GPS error associated with the ground truth plot and tree locations, a positional accuracy of 0.5m is anticipated given a clear view of the sky, decreasing to 0.7m if trigonometric principals had to be employed. This suggests some misalignment between ground truth and LiDAR data is to be expected. However, even a maximum offset of 0.7m is unlikely to cause significant problems given the 5m by 5m spatial resolution of the LiDAR data used for comparison with the ground truth data. Furthermore, such an offset would affect height as well as growth correlations. This has not been observed and thus it

seems unlikely that GPS ground truth error is the principle cause of poor growth correlations.

In summary it seems that there are four possible data misalignment scenarios which would result from GPS error, each with varying effects on height and growth correlations. Scenario one involves significant GPS error in one of the LiDAR datasets but not in the other or the ground truth. This would result in reduced height correlations for that particular dataset and low levels of correlation for the growth regression. Scenario two involves significant GPS error in both LiDAR datasets but not in the ground truth data. This would precipitate lower height correlation co-efficients for both LiDAR datasets and lower growth correlations. Scenario three involves significant GPS error in the ground truth data and not either of the LiDAR datasets. This would cause problems for both height and growth correlations. The final scenario involves significant error in all three GPS sources which would result in poor correlations for both height and growth. The confirmation of both the 2003 and 2006 LiDAR data accuracy from the Environment Agency and ULM respectively rules out scenarios one, two and four. The fact that only growth correlations are poor seems also to rule out scenario three. This then perhaps leads to the conclusion that it is possible that the poor growth correlations and data misalignments do not result from GPS error at all. Thus it is the purpose of the remainder of this chapter to investigate other potential sources of error.

6.1.1.2 Post-Processing Error

Some initial processing was performed on the LiDAR datasets by the data providers before the methodology detailed within this study was performed. Any errors introduced at this stage would, like GPS errors, be translated into laser point errors. It could not be established from the data providers exactly what post processing was carried out on either LiDAR dataset. As a consequence this remains somewhat of a black box issue. Yet despite the fact that error here cannot be quantified, nor can it be ruled out. Thus it remains important to recognise this step as a potential source of error, a potential cause of data misalignment and an influencing factor in poor growth correlations. Future work would benefit from a closer study of the post-processing routine.

6.1.1.3 DEM Error

It is important that errors in the DEM are recognised as being different from laser point errors. Indeed, even if the laser point cloud data were error free the creation of a DEM is still likely to introduce some error, or to at least misrepresent the original surface to a certain extent. Indeed the very definition of a DEM as a smoothed representation of a surface means that this is inevitable. The challenge is to keep the error, or the misrepresentation of the surface, to a minimum. In doing so, the errors associated with tree height and growth estimation may also be kept to a minimum. To this end, much research is currently ongoing into the improvement and development of many different ground classification algorithms.

Given its availability and proven ability the progressive TIN densification algorithm embedded in TerraScan (Axelsson 2000) was used for creation of both the 2003 and 2006 DEMs within this study. DEM difference imagery and data indicates a systematic offset between the two DEMs of roughly 7m. This seems very strange and is a positional error which cannot be explained by the DEM generation sequence alone (other potential explanations for this offset are the study of this chapter in general). The same DEM generation routine was employed for both LiDAR datasets. As a consequence, it may be expected that equivalent magnitudes of error would be incorporated into both DEMs. Whilst this may impede an accurate assessment of tree height in both datasets, the two datasets should remain largely comparable thereby having a lesser effect on growth estimates and certainly not incurring an offset of ~7m in z. Fortunately, this offset is easily corrected and tree height and growth estimates not affected by it[10].

Further study of the DEMs indicates the presence of less systematic errors too though. Indeed, differences between the DEMs following correction of the offset still stretch as great as 8.83m, although the standard deviation value of 0.6m is more encouraging. In terms of the effect these differences may have on the ground truth-LiDAR height and growth correlations, only the DEM differences at plot locations need consideration. At the 22 ground truth plot locations the DEM differences are no greater than 0.95m, with 64% of plots falling in an area where DEM differences are smaller than ±0.25m, and 91% where differences are smaller than ±0.5m. Some difference between DEMs is to be expected and may result from genuine changes in the terrain surface or differences in the system setup of the two LiDAR acquisitions. This is discussed further in section 5.1.3. No improvement in

---

[10] The ~7m offset in z exists for all laser points within the 2006 LiDAR dataset, not solely those points classified as 'ground'. Therefore the difference between DEM and CHM (tree height) remains comparable between datasets regardless of the offset.

growth correlations was achieved by including only those trees in areas of smaller than ±0.25m DEM difference. In the future, investigations into the effects of using a single DEM for growth studies may be beneficial.

Besides a comparison of the two DEMs no independent check was performed on the accuracy of the DEMs. However, given the problems experienced in areas of very dense canopy it is likely that some parts of the DEMs were more accurate than others. Indeed, the problems of generating high accuracy DEMs in heavily vegetated terrain is well documented (Zaksek and Pfeifer 2006; Hyyppä *et al.*, 2005; Hollaus *et al.*, 2006; Kobler *et al.*, 2007) and recent literature details a great number of alternative ground classification algorithms to the TerraScan routine. These include block minimum filters, slope based filtering, iterative robust interpolation as well as the more recent segmentation and classification based filtering algorithms (Pfeifer *et al.*, 1999; Sithole and Vosselman 2004; Zaksek and Pfeifer 2006; Kobler *et al.*, 2007; Pfeifer 2007 *pers. comm.*). Indeed, there is much research currently being channelled into developing an algorithm which can provide an accurate and precise representation of the ground surface, especially in areas of heavily vegetated and steep terrain (Hyyppä *et al.*, 2005; Hollaus *et al.*, 2006; Zaksek and Pfeifer 2006; Kobler *et al.*, 2007). It seems that experimentation with a variety of interpolation and point selection techniques is necessary to find the method capable of creating the most accurate DEM possible for a given study area. Indeed, as LiDAR remote sensing of forestry is still very much in the developmental phase, a single approach for accurate processing of laser data is yet to be properly established within the academic literature. However, it is likely that algorithms specially developed to cope with dense forests conditions would

produce a more accurate representation of the ground surface at Kielder. As a consequence such algorithms may also help to improve height and growth estimates.

It is concluded that the ~7m DEM offset cannot be explained by the DEM generation routine, yet in any case it does not affect height and growth estimates. Variation remains between the two DEMs following offset correction however and yet such variation does not appear to affect growth correlations significantly. It is likely that DEM creation could be improved with the use of an algorithm able to cope with dense canopies. However a reliable assessment of the x, y and z error associated with DEM generation requires investigation of a more quantitative nature. This is not within the scope of this paper. Future work however, would benefit from this.

6.1.1.4   CHM Error

In the creation of the canopy height model there exists the opportunity to introduce error or to misrepresent the 'true' canopy surface, as with DEM generation. Such surface smoothing is necessary for estimation of tree heights and growth, yet it remains important to be aware of CHM creation as a potential source of error. Figure 6.1 gives a schematic representation of how misrepresentation of the canopy surface may occur. Sketch (a) illustrates how the canopy height model may look given the positions of the laser hits, but sketch (b) shows the true canopy surface. This diagram is also applicable for demonstrating DEM errors. Again the challenge is to develop techniques and processes which keep this error or misrepresentation to a minimum.
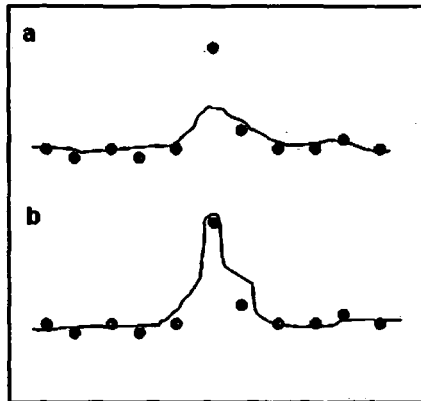
Figure 6.1 A schematic representation of how error may be introduced during creation of a canopy height model. The points represent laser hits, (a) the CHM surface and (b) the true surface.

A quantitative assessment of the accuracy of the CHM created for the Kielder datasets may help to ultimately improve height and growth estimates, however is not within the scope of this project. It has been noted though, that some decisions made concerning canopy classification, prior to CHM generation, may affect the accuracy of the final outcomes. It was decided that all returns falling with 2m of the ground surface would be excluded from canopy height models. Whilst the intention was to remove hits from low lying vegetation and natural debris it was noted during fieldwork that within the youngest plots many trees sit below this height. Whilst height correlations between LiDAR and ground truth data do not seem to have been affected, future studies may benefit from an assessment of the effect on growth correlations.

6.1.1.5 Horizontal Displacement of Tree Crowns

This final section concerning the three dimensional data misalignment concerns the horizontal displacement of tree tops due to strong winds and leaning caused by competition for light and/or damaged stem structure. If a tree is leaning significantly then the ground truth recorded location of the tree base will not be the same as the position at which the

crown is observed by the ALS system (Fig.6.2). This can also occur during strong winds and is an issue which has been previously documented (Popescu *et al.*, 2002; Yu *et al.*, 2005; Yu *et al.*, 2006). If the tree continues to growth in the direction of the initial lean, problems of LiDAR and ground truth misalignment are likely to worsen with age. However, it is likely that the magnitude of the locational error introduced by leaning trees would certainly not exceed a few metres. This links into the consideration of spatial resolution and the scale at which height, growth and error are studied (this is discussed further in section 6.1.4). For ground truth height and growth estimations at the 0.02ha plot level and LiDAR height and growth estimates from 5m by 5m pixels, leaning trees are unlikely to have a significant effect. Some problems may be caused for both height and growth correlations analysed between LiDAR and ground truth data at the individual tree level. However, because both height and growth correlations would be affected, the issue of horizontal displacement of tree crowns cannot be used to explain low R^2 values for growth regressions alone.
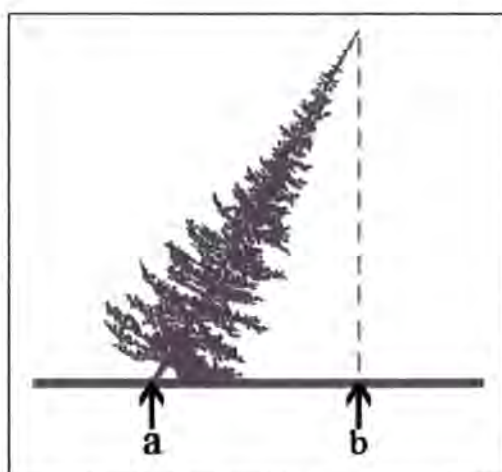
Figure 6.2 The horizontal displacement of the treetop on a leaning tree. Point (a) represents the trees location as recorded by the ground truthing and point (b) represents its location as recorded by the ALS system.

6.1.1.6 Summary

Five potential sources of data error or misalignment have been discussed here. It is possible that the post-processing of the LiDAR data could be responsible for the offsets and poor growth correlations as this currently remains somewhat of a black box issue. LiDAR height and growth estimates, and correlations with ground truth data may benefit from improved DEM and CHM generation routines but neither can confidently be assumed to be responsible for the data misalignment. Further study into the effects of the horizontal displacement of tree crowns may benefit single tree delineation studies, however at the scale of this investigation it is not deemed to be a significant problem. Other possible explanations of the offsets and poor growth correlations are discussed in the following sections of this chapter.

6.1.2   Ground Truth Error

This section aims to discuss the effects of ground truth error on the LiDAR-ground truth relationships. It was found in the previous chapter (Table 5.7) that the tree height adjustments made based on the trial data had very little effect in improving the strength of the LiDAR and ground truth growth correlation. There was also a lack of consistency between plot and tree level results. The co-efficient of determination for plot level growth was very slightly greater following adjustments, but not enough to make any reliable conclusion that ground truth error is responsible for the observed poor growth correlations. This may be as a result of a number of things;

143

1. The trial study was not extensive enough, meaning that only a limited range of trees were studied in terms of height. Given that many ground truth plots were much smaller than those studied by the trial their heights could not accurately be adjusted to reflect the likely errors associated with measuring smaller trees with the Vertex. Further studies would benefit from a more extensive assessment of ground truth error.

2. The tree height categories were not representative enough. Adjusted tree heights only affected the new correlation if the tree had moved into a different height category between 2003 and 2006. Given the wide ranges of the categories (particularly the lower category) which were due to lack of representative trial data, and the distribution of the tree heights, trees rarely moved height category. As a consequence little change was observed in the correlation co-efficients, mean differences or standard deviations. Further studies should consider carefully the height categories used, and perhaps investigate the possibility of estimating ground truth measurement error as a percentage of tree height.

3. The representation of the error associated with Vertex measurements requires a less crude approach. That is, perhaps a better representation of the variation or spread of the error (rather than just an average value) is needed. For example, the trial indicates that the ground truth is on average, over predicting the true tree heights by 0.31m. This figure is based on a range of 'difference from felled height' values taken by experienced and partially experienced users. The mode and median of this range of values both lie at 0.30m. This is very close to the mean value, thus

indicating a fairly normal distribution. Knowing this allows the assumption to be made that 68% of the data lies within one standard deviation of the mean, or in this case between -0.74m and 1.36m difference from true height[11]. If it is assumed that this is a fair range of uncertainty for our average error measurement it can now be applied to the LiDAR growth. The average amount of maximum growth recorded by the LiDAR is only 1.14m. Therefore, when an uncertainty of $\pm$1.05m is assumed for each ground truth height measurement it is easy to see how an agreement between LiDAR and ground truth growth may go undetected or at least, not accurately estimated. The magnitude of the uncertainty associated with the ground truth measurement results in any association or agreement between ground truth and LiDAR growth to be effectively 'lost'. It is unlikely that this magnitude of uncertainty is static, indeed, Table 5.6 in the previous chapter suggests an increase of uncertainty with increasing tree height. Thus, a fuller assessment of ground truth uncertainty in relation to tree height is necessary. Furthermore, the study of growth over a longer timescale may allow the average amount growth measured by the LiDAR to further exceed the ground truth measurement uncertainty, thereby allowing it to be detected. Further work here would greatly benefit LiDAR growth studies.

4.   Error associated with ground truth measurements may not be responsible for the observed poor growth correlations at all. Given the results presented here, a problem of systematic bias seems unlikely. However, it is likely that it is the uncertainty or random error associated with ground truth measurements which causes poor growth

---

[11] This also tells us that 95% of the data lies within 2 standard deviations of the mean and that 99.7% of the data lies within 3 standard deviations of the mean.

correlations. Further inquiry would lead to a better understanding of ground truth error and measurement uncertainty and how that affects the validation of LiDAR data by ground truthing.

Further to the trial study, the 2007 revisits suggest that careful re-measurement of trees seems to produce fairly similar results as previous ground truthing sessions. Of 536 trees assessed, only 44 needed adjusting. Furthermore, there appear to be a greater number of mistakes made for older plots. This supports the findings of the trial as presented in Table 5.6. Whilst this does not help define the level of uncertainty within the measurement, it does suggest that there may be a consistency of uncertainty as a function of tree height or age. However, to reiterate the point from before, the relationship between plot and tree height (or age) and the magnitude of uncertainty deserves further study.

6.1.3 System Set-up

Another potential source of error is the set-up of the LiDAR systems. As detailed in section 2.2, the specifications of the laser scanners used within this study were very different from each other. Other studies have found differences in scan angle, flying altitude and pulse density and distribution to have significant effects on DEM accuracy and therefore tree height estimation. Each of these shall be discussed in turn in relation to this study.

6.1.3.1 Scan Angle

The effects of the size of the scan angle were discussed briefly in section 1.2.1. Many studies have found errors associated with both DEM generation and canopy height estimation to increase with increasing scan angle (Nilsson 1996; Ahokas *et al.*, 2003; Holmgren *et al.*, 2003; Lovell *et al.*, 2005; Goodwin *et al.*, 2006; Friess 2007 *pers. comm.*). It is anticipated that this results from a lower intensity of reflectance at greater scan angles, as dictated by Lambert's Cosine Law.

In his study of forestry in Sweden, Nilsson found that errors caused by the effects of scan angle were responsible for between 2.0m and 2.5m positional error in x and y (Nilsson 1996). Holmgren *et al.*, (2003) found that greater scan angles affected the lower height percentile measures more strongly than it did higher percentiles. They suggest that this results from greater obscuration which acts to increase the underestimation of lower height percentiles. Further to this, Lovell *et al.*, (2005) also found increased errors at scan edges. They attributed the larger errors to a sparser distribution of laser hits which then reduces the accuracy of the DEM.

The 2003 data used within this study was collected with a scan angle of 10°, and the 2006 with a scan angle of 16.5°. Given its wider reach, it might be expected then that the 2006 data would feature greater errors at the edges of its scan lines. Indeed, this may be responsible for the 2006 LiDAR and ground truth correlation co-efficients which are consistently lower than the equivalent results for the 2003 data[12] (Table 5.1). Furthermore,

---

[12] With the exception of Lorey's Mean Height- for reasons discussed in section 4.2.1.1.

it is possible that the errors introduced by the larger scan angle are what is being observed in the discrepancies between the separate 2006 flight lines as shown in Figures 4.8 and 4.9 in the Results Chapter. Here, the areas where the flight-lines overlap are at their very edges where scan angle errors are likely to be greatest. Therefore perhaps it is not surprising that such discrepancies between the DEM lines are observed. This might be analysed further if the flight-line overlap was greater. The recommended amount of overlap is 70% of the scan line width. However, the 2006 data was collected with much smaller amounts of overlap and in some cases with no overlap. This results in a number of 'holes' in the data. Future studies would benefit from ensuring that this does not occur and that flight-line overlap is at the recommended level. The 2003 data was not available in flight-line format and therefore overlaps were not analysed.

It is possible that the increased errors for lower height percentiles, observed by Holmgren *et al.,* (2003) are also being seen here. Lower co-efficients of correlation are observed for virtually all p10 metrics when compared to other height metrics (Table 5.1). However, this is not conclusive proof and may result from a number of factors. Further study is necessary.

The fact that the scan angles are different between the datasets means that different amounts of error will have been introduced into each dataset. Whilst this does not seem to have adversely affected the regressions between ground truth and LiDAR derived heights, it may have made the 2003 and 2006 datasets less comparable thereby affecting the growth correlation. Analysis of a more quantitative nature is needed to establish the precise impact of the different scan angles and to determine whether it is scan angle error alone which is responsible for the observed lack of associated between ground truth and LiDAR growth variables.

6.1.3.2 Flying Altitude

A number of studies have found that greater platform altitudes seem to incur lower density returns (Goodwin *et al.*, 2006; Takahashi *et al.*, 2007). It is thought that the larger distance between sensor and target causes a reduction in the intensity of the return pulse in accordance with Newton's Inverse Distance Law. If this intensity falls below a certain threshold, the pulse becomes indistinguishable from random noise and therefore is not recorded. This is much more likely to happen at greater flying altitudes.

The work of Goodwin *et al.*, (2006) found greater platform altitudes to reduce the proportion of first and last returns. That is that a greater number of last returns were reflected from the same point as the first returns. This indicates a lower canopy penetration rate. Despite this however, Goodwin *et al.*, (2006) concluded that raising the platform from 1000m to 3000m had very little effect on the accuracy of the resulting canopy height model.

Other studies have produced different results though. The work of Takahashi *et al.*, (2007) in Japan found an increase in the percentage of first-return only returns associated with increased platform altitude, which reduced the quality of the DEM. This translated into an increase in both systematic and random errors of mean tree height estimates with increasing altitude. As a consequence, they recommend a flying height of less than 1000m for tree height studies. Furthermore, studies by Ahokas *et al.*, (2003) and Hyyppä *et al.*, (2005) indicate increasing random error with flight altitude. Indeed, Hyyppä *et al.*, (2005) found that increasing the flying height from 400m to 1500m increased the random error within the

DEM by 50% (from 12cm to 18cm). They also found that random errors were greatest in areas of steep terrain.

In light of these studies, it seems possible that the 2006 LiDAR survey flying height of 1750m is incurring a greater amount of random error into the DEM and tree height estimates than the 2003 survey, which was flown at 950m. It may be this which is causing the differences between the 2003 and 2006 DEMs (Fig.4.5) and the slightly lower correlation co-efficients for the 2006 data. Furthermore, the greater altitude is probably resulting in a lower rate of canopy penetration. This would cause most problems in areas of very dense canopy. Indeed, it is quite possible that this is what is being observed in the white data gaps on the 2006 height map in Figure 4.12. The same gaps due to lack of penetration do not occur on the equivalent 2003 height map. This could be simply due to significant growth between 2003 and 2006 resulting in a much denser canopy. However, the difference between the two flying altitudes is so great that it may be unwise to assume no effect on the DEM, CHM and height estimates. In fact, the comparison of 2003 and 2006 regression data (Table 6.1) does show an increase in both random (standard deviation) and systematic (mean difference) errors. Whilst the jump in flight altitude may not be the only cause of this error increase and perhaps resulting poor growth correlation, it is certainly an area which deserves further study for the benefit of forest management.

Year	2003	2006
Flying Altitude (m)	950	1750
Ground Truth Variable	Maximum Height	Maximum Height
LiDAR Variable	Maximum Height	Maximum Height
R^2	0.978	0.973
Equation	y = 1.01x + 2.84	y = 0.95x + 3.54
Mean difference (m)	-2.92	-3.04
Standard Deviation (m)	1.13	1.21

Table 6.1 A comparison of regression results, by year (and flying altitude).

6.1.3.3 Pulse Density and Distribution

Further to differences in flying altitude, there was also a difference in pulse density between the 2003 (2 hits per m^2) and 2006 (4 hits per m^2) datasets. It might be expected that the higher resolution 2006 data would produce better quality height estimates. However, Table 6.1 indicates that this is not so. This may be due to an outweighing effect of flying altitude. That is, greater levels of error have been introduced into the 2006 data by the higher flying altitude than can be masked by a higher point density. Specifically tailored studies are necessary to establish the exact quantitative effects of differences in point density.

Further to the issue of point density, the distribution of points may also influence DEMs, CHMs and therefore height and growth estimates. Næsset (2002) commented that uneven pulse distributions will seriously affect small sample plots in particular, introducing greater levels of both systematic and random error. This is likely to be a larger problem for coniferous forests where the average tree crown area is much narrower than that of a deciduous tree (Yu *et al.*, 2006). And yet, the nature of airborne laser scanning means that pulse distributions will never be perfectly regular, and certainly never repeatable. As a

result the problem of data correspondence remains an issue for all multi-temporal LiDAR studies. In light of this, Næsset (2002) recommends that sample ground truth plots should not be too small. This links into the idea of scale and spatial resolution which seems to be a key consideration for studies of this kind and is discussed further is section 6.1.4.

6.1.4 Scale

Issues of scale and resolution run through most of the potential error sources described within this chapter. Other studies have found the scale at which height and growth are analysed to have a significant impact on results (Woodcock and Strahler 1987). Næsset (2002) recommends the use of coarser spatial resolutions for tree height studies. His reasoning lies in the fact that smaller sample plots experience greater levels of inherent variation of canopy height measures. Gobakken and Næsset (2004) in their study of forest growth also found results improved when looking at larger areas rather than single trees. Indeed, the 'averaging-out' effect of larger plots reduces standard deviations of mean plot values, thereby increasing the precision of height estimates. Given that random error or the precision of ground truth measurements was found to be highly problematic within this project, perhaps a study at coarser spatial resolutions would be helpful. Indeed, analysing height and growth at a larger scale may help to gloss over a multitude of small errors potentially being introduced by the GPS, post processing routine, DEM and CHM generation routines and the horizontal displacement of tree crowns.

For future studies, it may also be advantageous to consider the spatial resolution which results from the LiDAR system setup. Greater pulse densities and lower flying altitudes

will enable greater levels of canopy penetration thereby producing a finer spatial resolution. This would lead to greater levels of accuracy within the DEM and CHM which could then be averaged over a larger area to achieve higher levels of precision.

Finally there is the issue of temporal scale. Currently, within this study the random errors associated with growth estimation are larger than the estimated growth itself, thereby causing the growth to effectively be 'lost'. Studying growth over a longer timescale may allow estimated growth to exceed the random error meaning it could then be successfully detected.

It is evident that the scale at which height and growth is studied using ALS has significant implications for the accuracy, precision and reliability of the results. Future growth studies would benefit enormously from further investigation into the quantitative effects of different spatial and temporal resolutions. However, it is important to keep in mind that there is a balance to be struck between resolution modification and cost. This helps to reiterate the main purpose of this work which was to investigate whether ALS can provide a cost-effective tool for forest management.

6.2 IMPLICATIONS OF THIS STUDY

It is evident that further study is required in a number of areas in order to investigate and minimise the errors associated with LiDAR growth estimation. Despite this though, the multitemporal ALS data has been shown to detect forest growth across a range of different aged plots which matches that predicted by Forestry Commission volume models. Thus, it is anticipated that with some honing, this is a technique which could be reliably employed for production forecasting within forestry.

Furthermore, the results of this study may be valuable to a wider range of users within both science and commerce. For example, the potential exists to use airborne LiDAR for estimating the carbon stocks locked up within forests. In an age where climate change and its effects are becoming so pertinent, LiDAR may offer a valuable tool. In fact, as a signatory nation to the Kyoto Protocol, the New Zealand government are already investigating the potential of airborne laser scanning for this purpose (Donoghue 2007 *pers comm.*; Stephens *et al.*, 2007). LiDAR may also prove to be a useful tool for compliance checking of grant funded planting schemes, which is both time consuming and costly when carried out on the ground.

It is becoming standard procedure to fly other instruments concurrently with airborne laser scanners. Such practice is advocated by a number of studies (Nelson *et al.*, 1988; Baltsavias 1999; Hudak *et al.*, 2002; Suárez *et al.*, 2005). Indeed, the integration of LiDAR data with other forms of remote sensing may help in the classification and filtering of laser points or to help identify particular areas of interest. This concept of data fusion may prove useful for future studies at Kielder Forest. Furthermore, the recent availability of laser scanners with

'multiple pulse in the air' (MPiA) capability may also benefit future work concerning forest growth monitoring (Rohrbach 2007 *pers. comm.*). The Optech ALTM Gemini is the first of this kind to become commercially available and is publicised to provide higher density, more cost effective datasets (www.optech.ca accessed 15.11.07).

It seems evident that there are still many avenues to explore in terms of furthering the study of forest growth using airborne laser scanning. A summary of the results and interpretations of this work are presented in the concluding chapter and recommendations for future studies concerning the use of LiDAR for estimating forest growth are also suggested.

7 CONCLUSIONS AND FUTURE RECOMMENDATIONS

7.1 INITIAL AIMS

Airborne laser scanning is an active remote sensing technique which has been developed rapidly in recent years. It is capable of providing accurate estimates of tree heights and other biophysical variables. This research has investigated the extension of this technology from single time-series tree height estimations to a multi-temporal study of forest growth within a temperate environment. This work aimed to explore whether growth could be detected over three years and across a range of different aged plots. Growth was then compared to estimates obtained by traditional forest inventorying techniques. Lastly the data and methods were examined for potential sources of error with a view to highlighting how this technology may be enhanced in the future.

7.2 RESULTS

Initial results showed the LiDAR data to be capable of detecting growth over a variety of Sitka spruce plantation plots within the three year period. Furthermore, the age related nature of growth reflected that shown in Forestry Commission volume models. As found by many other studies, LiDAR height estimates at the plot and tree level from both years were found to be strongly correlated with height measures obtained by ground truthing. However, despite a change in height (growth) being detected by the LiDAR, little correlation was observed between this LiDAR growth estimate and the growth estimate obtained by ground truthing. Indeed, the correlations obtained on the comparison of LiDAR and ground truth growth measures were weak and mostly negative. The reason(s) for this

156

must be concerned with either some kind of error within the LiDAR data itself or secondly, some kind of error within the ground truth data to which the LiDAR is being compared (or both).

7.3 POTENTIAL ERROR SOURCES

The study of multi-temporal datasets to estimate forest growth relies on the assumption that the two (or more) datasets in question are directly comparable. This means it is important to use the same processing chain on both LiDAR datasets (as done here). However, it also means it is highly important to ensure the specifications and use of the LiDAR systems are as similar as possible. In this study, scan angle, flying altitude and point density were very different between the two LiDAR datasets. Whilst a quantitative assessment of the error sources was not within the scope of this work, it is likely that the use of such different systems introduced different magnitudes of error thereby reducing the comparability of the datasets and the strength of the LiDAR-ground truth growth correlation. Despite the operational constraints of doing so, it is highly recommended that the set up and use of LiDAR systems for multi-temporal studies be as similar as possible.

A study of ground truth error was also undertaken by this research. It was found that the magnitude of uncertainty (random error) associated with ground truth height measurements was so large that any association between LiDAR and ground truth growth estimates was effectively being lost. In other words, the errors associated with ground truth growth estimation were larger than the estimated growth itself thereby allowing it to go undetected. This might be ameliorated in a number of ways. Firstly, by studying growth over a longer

157

timescale. This might allow the amount of growth to exceed the errors of growth estimation, therefore allowing it to be detected. The work of Yu *et al.*, (2005) has already found this to be beneficial for forest growth studies and under normal forest management practices in the UK, forest growth is only analysed at the five year timescale anyway (Woodhouse 2007 *pers. comm.*). Secondly, further study into the magnitude of ground truth measurement uncertainty would be valuable, particularly in relation to tree height and/or age. Thirdly, it may be that growth is better analysed at a coarser spatial scale. The 'averaging-out' effects of summarising data over larger spatial areas may help to increase precision and reduce random error.

A number of other factors at a variety of spatial scales were also considered as the cause of the poor growth correlation. However, none of these factors were found to be significantly influential. The inclusion of only those trees classified as 'dominant' did significantly improve height correlations at the individual tree level, but no such improvement was observed for the relationship between LiDAR and ground truth growth. Different strength correlations were observed when the data was subdivided according to age, indicating that height and growth of middle-aged plots seem to be most accurately predicted by the LiDAR. Thus, it is anticipated that future research would benefit from further study into the age specific accuracy and precision of LiDAR height and growth estimates.

7.4 RECOMMENDATIONS AND FUTURE WORK

In light of this study, a number of recommendations can be made for future research concerning stand level forest growth. Firstly, the LiDAR datasets must be directly

comparable. This means the same system setup; in terms of scan angle, flying altitude and pulse density; similar flying conditions in terms of season and time of day; and the same LiDAR processing routine. Secondly, it is suggested that the timescale studied should be longer than three years to allow the amount of growth to exceed any potential error. Lastly, growth studies may benefit from further study into the magnitude and variability of ground truth errors.

It would also be of interest to extend future LiDAR research into other areas. This might include the study of species other than Sitka spruce or non-monoculture plantations and natural forests and a closer investigation into the effects of yield class on growth. Within this study, LiDAR has also demonstrated the potential for identifying areas of canopy damage. Thus it may be possible to extend the technique for making assessments of stand quality. This might be aided further by the concept of spatial data fusion, by linking LiDAR data with other forms of remote sensing. The monitoring of forest carbon stocks may also benefit from multi-temporal LiDAR surveying. Furthermore, it will be interesting to observe the changes in data quality or cost efficiency introduced by MPiA capability. Lastly, it is suggested that a comparison of LiDAR predicted forest growth at different spatial scales would be valuable for furthering our understanding of this technique.

7.5 FINAL CONCLUSIONS

It is concluded that airborne LiDAR surveys have a great deal to offer the forest management community. LiDAR height estimates are strongly correlated with ground truth data and whilst the technique of using multi-temporal LiDAR surveys for forest growth studies needs some improvement, it is anticipated to be highly valuable in the future.

LiDAR datasets must be directly comparable and the systematic and random errors associated with ground truthing need to be quantified. Once this is achieved, multi-temporal airborne LiDAR surveys have the potential to revolutionise forest management by providing a rapid, cost-effective, non-invasive, repeatable technique of timber production forecasting. Furthermore, multitemporal surveys are capable of providing information concerning carbon stocks and thereby may help facilitate the international decision making process concerning carbon policy and global climate change. Studies of this nature are thus of benefit to foresters, climatologists, researchers and non-academics alike and therefore should not only continue but be enhanced in the future.

8 REFERENCES

Articles:

Ackermann, F. 1999. Airborne laser scanning- present status and future expectations. *ISPRS Journal of Photogrammetry & Remote Sensing* 54(2-3): 64-67.

Ahokas, E. *et al.*, 2002. Accuracy of high-pulse laser scanners for digital target models. In: *Observing our environment from space. New solutions for a new millennium.* Proceedings of the 21st EARSeL Symposium, Paris, 14-16 May 2001. Balkema Publishers.

Ahokas, E. *et al.*, 2003. A quality assessment of airborne laser scanner data. In: *The International Archives of the Photogrammetry, Remote Sensing and Spatial Information Sciences,* Dresden, Germany, XXXIV-3/W13.

Aldred, A.H. and Bonner, G.M. 1985. Application of airborne lasers to forest surveys. Info Rep. PI-X-51, Tech. Info and Dist. Center, Petawawa National Forest Inst., Chalk River, Ontario, 62pp.

Axelsson, P.E. 1999. Processing of laser scanner data- algorithms and applications. *ISPRS Journal of Photogrammetry & Remote Sensing* 54(2-3): 138-147.

Axelsson, P.E. 2000. DEM generation from laser scanner data using adaptive TIN models. In: *The International Archives of Photogrammetry and Remote Sensing,* Amsterdam, The Netherlands, Vol. XXXIII, Part B4/1, pp.110-117.

Baltsavias, E.P. 1999. A comparison of photogrammetry and laser scanning. *Journal of Photogrammetry and Remote Sensing* 54: 83-94

Barron, R.J. 2001. Precision of three tree height measuring devices in forest conditions. *Research Note 1, 2001,* Forest Research Branch, Loughgall, Northern Ireland.

Bechtold, W.A. 2003. Crown position and light exposure classification- an alternative to field-assigned crown class. *Northern Journal of Applied Forestry* 20: 154-160

Blair, J. B., *et al.*, 1999. The Laser Vegetation Imaging Sensor: a medium-altitude, digitisation-only, airborne laser altimeter for mapping vegetation and topography. *ISPRS Journal of Photogrammetry & Remote Sensing.* 54: 115-122.

Blair, B.J., *et al.*, 2001. Wide-swathe imaging LiDAR development for airborne and spaceborne applications. In: *Proceedings of International Archives of Photogrammetry and Remote Sensing*, Volume XXXIV-3/W4 Annapolis, MD, 22-24 Oct. 2001.

Cox, N.J. 2006. Assessing agreement of measurements and predictions in geomorphology. *Geomorphology* 76: 332-346.

Donoghue, D.N.M., *et al.*, 2004. An evaluation of the use of satellite data for monitoring early development of young Sitka spruce plantation forest growth. *Forestry* 77: 383–396.

Donoghue, D.N.M. and Watt, P.J. 2006. Using LiDAR to compare forest height estimates from IKONOS and Landsat ETM+ data in Sitka spruce plantations. *International Journal of Remote Sensing.* 27(11): 2161-2175

Drake, J.B. *et al.*, 2002. Sensitivity of large-footprint LiDAR to canopy structure and biomass in a neotropical rain forest. *Remote Sensing of Environment* 81: 378-392

Flood, M. and Gutelius, B. 1997. Commercial implications of topographic terrain mapping using scanning airborne laser radar. *Photogrammetric Engineering and Remote Sensing* 63: 327-366.

Gobakken, T. and Naesset, E. 2004. Effects of forest growth on laser derived canopy metrics. Proceedings of ISPRS Working Group VIII/2 Vol XXXVI, Part 8/W2, Freiburg, Germany 3-6 Oct. 2004.

Goodwin, N.R. *et al.*, 2006. Assessment of forest structure with airborne LiDAR and the effects of platform altitude. *Remote Sensing of Environment* 103: 140-152

Henning, J.G. and Radtke, P.J. 2006. Ground-based laser imaging for assessing 3D forest canopy structure. *Photogrammetric Engineering and Remote Sensing* 72(12): 1349-1358

Hollaus, M. *et al.*, 2006. Accuracy of large-scale canopy heights derived from LiDAR data under operational constraints in a complex alpine environment. *ISPRS Journal of Photogrammetry and Remote Sensing* 60: 323-338

Holmgren, J. *et al.*, 2003. Estimation of tree height and stem volume on plots using airborne laser scanning. *Forest Science* 49(3): 419-428

Hudak, A.T., *et al.*, 2002. Integration of LiDAR and Landsat ETM+ data for estimating and mapping forest canopy height. *Remote Sensing of Environment* 82: 397–416.

Hyyppä, J. *et al.*, 2000. Accuracy comparison of various remote sensing data sources in the retrieval of forest stand attributes. *Forest Ecology and Management* 128: 109-120

Hyyppä, J. et al., 2001. A segmentation-based method to retrieve stem volume estimates from 3-dimensional tree height models produced by laser scanner. *IEEE Transactions on Geoscience and Remote Sensing* 39: 969-975

Hyyppä, J. *et al.*, 2005. Factors affecting the quality of DTM generation in forested areas. *ISPRS WG III/3, III/4, V/3* Workshop 'Laser Scanning 2005' Enschede, The Netherlands, September 2005.

Kobler, A. *et al.*, 2007. Repetitive interpolation: A robust algorithm for DTM generation from aerial laser scanner data in forested terrain. *Remote Sensing of Environment* 108(1): 9-23.

Kraus, K. 2002. Principles of airborne laser scanning. IPRS Conference, Vienna.

Kraus, K., and Pfeifer, N. 1998. Determination of terrain models in wooded areas with airborne laser scanner data. *ISPRS Journal Photogrammetry and Remote Sensing* 53: 193–203.

Lefsky, M.A. *et al.*, 1999. LiDAR remote sensing of the canopy structure and biophysical properties of Douglas-Fir Western Hemlock Forests. *Remote Sensing of* Environment 70: 339-361.

Lim, K. *et al.*, 2003. LiDAR remote sensing of forest structure. *Progress in Physical Geography* 27: 88–106.

Lohr, U. 1998. Digital Elevation Models by Laser Scanning. *Photogrammetric Record* 16(91): 105-109.

Lovell, J.L. *et al.*, 2005. Simulation study for finding optimal LiDAR acquisition parameters for forest height retrieval. *Forest Ecology and Management* 214: 398-412.

Maltamo, M. *et al.*, 2004. Estimation of timber volume and stem density based on scanning laser altimetry and expected tree size distribution functions. *Remote Sensing of Environment* 90(3): 319-330.

Means, J.E. *et al.*, 1999. Use of large-footprint scanning airborne LiDAR to estimate forest stand characteristics in the Western Cascades of Oregon. *Remote Sensing of Environment* 67(3): 298-308

Means, J.E., *et al.*, 2000. Predicting forest stand characteristics with airborne scanning LiDAR. *Photogrammetric Engineering and Remote Sensing* 66(11): 1367–1371.

Næsset, E. 1997. Determination of mean tree height of forest stands using airborne laser scanner data. *ISPRS Journal of Photogrammetry and Remote Sensing* 52: 49–56.

Næsset, E., and Bjerknes, K.O. 2001. Estimating tree heights and numbers of stems in young forest stands using airborne laser scanner data. *Remote Sensing of Environment* 78: 328-340.

Næsset, E. 2002. Predicting forest stand characteristics with airborne laser using a practical two-stage procedure and field data. *Remote Sensing of Environment* 80: 88–99.

Næsset, E., and Økland, T. 2002. Estimating tree height and tree crown properties using airborne scanning laser in a boreal nature reserve. *Remote Sensing of Environment* 79: 105–115.

Næsset, E. and Gobakken, T. 2005. Estimating forest growth using canopy derived metrics from airborne laser scanner data. *Remote Sensing of Environment* 96: 453-465.

Nelson, R. *et al.*, 1984. Determining forest canopy characteristics using airborne laser data. *Remote Sensing of Environment* 15: 201-212

Nelson, R. *et al.*, 1988. Estimating forest biomass and volume using airborne laser data. *Remote Sensing of Environment* 24: 247-267

Nilsson, M. 1996. Estimation of tree heights and stand volume using an airborne LiDAR system. *Remote Sensing of Environment* 56: 1–7.

Pereira, L.M.G., and Janssen, L.L.F. 1999. Suitability of laser data for DTM generation: a case study in the context of road planning and design. *Photogrammetry and Remote Sensing* 54: 244–253.

Pfeifer, N. 2007. DSM/DTM Filtering. *Presentation given at 'The Theory and Application of Laser Scanning' ISPRS Summer School*, Ljubljana, Slovenia, 1-8 July 2007.

Pfeifer, N. *et al.*, 1999. Interpolation of high quality ground models from laser scanner data in forested areas. In: *The International Archives of the Photogrammetry, Remote Sensing and Spatial Information Sciences*, La Jolla, California, USA. WG III\5 and WG III\2.

Popescu, S.C. *et al.*, 2002. Estimating plot-level tree heights with LiDAR: local filtering with a canopy-height based variable window size. *Computers and Electronics in Agriculture* 31: 71–95.

Rieger, W. *et al.*, 1999. Laser-scanning for the derivation of forest stand parameters. In: *The International Archives of the Photogrammetry, Remote Sensing and Spatial Information Sciences*, La Jolla, California, USA. WG III\5 and WG III\2.

Romano, M.E. *et al.*, 2004. Innovation in LiDAR processing technology. *Photogrammetric Engineering and Remote Sensing* 70(11): 1201-1206

Ruppert, G. et al., 2000. An adaptive multi-resolutional algorithm for high precision forest floor DTM generation. *Proceedings of SPIE, laser radar technology and applications V, 2628 April, Orlando, USA, vol. 4035*

Schreier, H. *et al.*, 1984. Calibrating an airborne laser profiling system. *Photogrammetric Engineering and Remote Sensing* 50(11): 1591-1598

Schreier, H. *et al.*, 1985. Automated measurements of terrain reflection and height variations using an airborne infrared laser system. *International Journal of Remote Sensing* 6(1): 101-113

Sithole, G. and Vosselman, G. 2004. Experimental comparison of filter algorithms for bare-Earth extraction from airborne laser scanning point clouds. *ISPRS Journal of Photogrammetry and Remote Sensing* 59: 85-101.

Stephens, P.R. *et al.,* 2007. Estimation of carbon stocks in New Zealand planted forests using airborne scanning LiDAR. *IAPRS Workshop on Laser Scanning and SilviLaser 2007, Espoo, September 12-14, Finland.* Vol. XXXV1, Part 3 / W52.

St-Onge, B. 1999. Estimating individual tree heights of the boreal forest using airborne laser altimetry and digital videography. In: *The International Archives of the Photogrammetry, Remote Sensing and Spatial Information Sciences,* La Jolla, California, USA. WG III\5 and WG III\2.

St-Onge, B. and Vepakomma, U. 2004. Assessing forest gap dynamics and growth using multi-temporal laser-scanner data. *International Archives of Photogrammetry, Remote Sensing and Spatial Information Sciences,* Vol. XXXVI-8/W2.

Suárez, J.C., *et al.,* 2005. The use of airborne LiDAR and aerial photography in the estimation of individual tree heights in forestry. *Computers and Geosciences* 31: 253 –262.

Takahashi, T. *et al.,* 2007. Assessment of LiDAR-derived tree heights estimated from different flight altitude data in mountainous forests with poor laser penetration rates. *IAPRS* Volume XXXVI, Part 3/W52.

Watt, P.J. 2005. An evaluation of LiDAR and optical satellite data for the measurement of structural attributes in British upland conifer plantation forestry. *PhD Thesis* Durham.

Watt, P.J., and Donoghue, D.N.M. 2005. Measuring forest structure with terrestrial laser scanning. *International Journal of Remote Sensing* 26: 1437–1446.

Woodcock, C.E., and Strahler, A.H. 1987. The factor of scale in remote sensing. *Remote Sensing of Environment* 21: 311– 332.

Wulder, M.A. *et al.*, 2007. Integrating profiling LiDAR with Landsat data for regional boreal forest canopy attribute estimation and change characterization. *Remote Sensing of Environment* 110(1):123-137.

Yu, X. *et al.*, 2004. Automatic detection of harvested trees and determination of forest growth using airborne laser scanning. *Remote Sensing of Environment* 90: 451-462

Yu, X. *et al.*, 2005. Measuring the growth of individual trees using multitemporal airborne laser scanner point clouds. Workshop V/3 'Laser Scanning 2005' ISPRS.

Yu, X *et al.*, 2006. Change detection techniques for canopy height growth measurements using airborne laser scanner data. *Photogrammetric Engineering and Remote Sensing* 72(12): 1339-1348.

Zaksek, K. and Pfeifer, N. 2006. An improved morphological filter for selecting relief points from a LiDAR point cloud in steep areas with dense vegetation. *Technical Report of work performed at TU Delft, The Netherlands.*

Books:

Edwards, P.N. and Christie, J.M. 1981. Yield Models for Forest Management: *Forestry Commission Booklet 48*, Forestry Commission, Farnham, Surry.

Hurn, J. 1993. Differential GPS Explained, Trimble.

Websites:

Dubayah, R.O. *et al.,* 2000. Land surface characterisation using LiDAR remote sensing. VCL website.

Dubayah, R.O. and Drake, J.B. 2000. LiDAR remote sensing for forestry applications. VCL website.

GIS Center Website: www.gis.gov.ae (accessed 15.1.07)

Godin, J. 2000. LVIS looks down from above. VCL website

Haglöf Website: www.haglofsweden.com (accessed 20.9.07)

Kielder Forest Website: www.kielder.org (accessed 18.10.06)

MDL Laser Systems Website: www.laserace.com (accessed 20.9.07)

Multimap Website: www.multimap.com (accessed 15.1.07)

Optech Website: www.optech.ca (accessed 15.11.07)

Riegl Website: www.riegl.com (accessed 15.1.07)

University of Montana website:
www.forestry.umt.edu/academics/courses/X495/planning.htm (accessed 25.10.07)